CBS Domains Regulate CLC Chloride Channel Gating:

Role of the R-Helix Linker

By

Sonya Davé

Dissertation

Submitted to the Faculty of the

Graduate School of Vanderbilt University

in partial fulfillment of the requirements

for the degree of

DOCTOR OF PHILOSOPHY

in

Molecular Physiology and Biophysics

December, 2010

Nashville, Tennessee

Approved:

Dr. Hassane Mchaourab

Dr. Jerod Denton

Dr. Jens Meiler

Dr. Al Beth

Dr. Danny Winder

I dedicate my thesis to the best parents in the world, Gopali and Suresh Dave',

and my loving friend, Vishwas Sinha.

ACKNOWLEDGEMENTS

I am grateful and lucky to have Dr. Kevin Strange as my advisor. He has always been around to guide me and keep my research on track. Kevin has also taught me to communicate science articulately, be it presentations, papers or grants. He has shown me what is important to become an outstanding scientist, both in terms of ideas and performing experiments. His excellent teaching abilities have made me an experienced electrophysiologist. His jokes, friendship and teasing have also made me a better person.

Of course, this project could go nowhere without funding Kevin has secured. This work was supported by NIH grants R01 DK51610 to Kevin Strange and R01 GM080403 to Jens Meiler. I am also grateful to American Heart Association's Predoctoral Training Grant for my stipend.

All current and former members of the Strange Laboratory have been very valuable colleagues and enjoyable friends. Our lab manager Rebecca Morrison has always been there with a thorough answer and solution for many questions arising in experiments. Former lab members Dr. Keith Choe, Dr. Liping He, Dr. Juan Xing and Dr. Xiaohui Yan have been very helpful for teaching me molecular biology and discussing experimental difficulties. Stacey Johnson and Rebecca Wright have been valuable assistants for many of the experiments described, especially molecular biology and cell culture. Dr. Rebecca Falin has been a wonderful colleague to discuss CLC biology, a patch clamp companion, and much more. She has also helped acquire data for electrophysiology experiments involving MTSET.

My project would not have been possible without assistance from the Center for Structural Biology, especially Dr. Jonathan Sheehan and Dr. Jens Meiler. Jens and Jonathon have provided crucial assistance, advice, and ideas for our structural modeling computations. Dr. Jonathan Sheehan and Dr. Eric Dawson have very patiently taught me all I needed to know for modeling computations that formed the basis of this project.

My committee members Dr. Jerod Denton, Dr. Danny Winder, Dr. Jens Meiler, Dr. Al Beth, and Dr. Hassane McHaourab have all provided valuable insights, ideas and possible experiments. Their suggested experiments have helped me carry out a strong and scientifically sound thesis project.

My parents have been the most loving, supportive, and valuable influence in my life. They have always encouraged me to go after my ambitions and supported all my decisions and been beside me in times of difficulties. I am forever grateful to my friend Dr. Carrie Jones for helping me get through the hardest parts of graduate school and never once doubting that I could do very well. There is nothing I can do that could ever pay back for what she has done for me. Finally, I am very happy to have the company and encouragement of my beloved friend, Vish. Talking with him everyday keeps me energetic and happy and ready to tackle the next hurdle.

TABLE OF CONTENTS

LIST OF TABLES

LIST OF FIGURES

CHAPTER 1

INTRODUCTION

CLCs are important chloride channels with poorly understood structure-function relations

Chloride channels and transporters are membrane embedded proteins that permit chloride ions to cross the membrane of cells or intracellular organelles. There are four main classes of chloride channels: the Cystic Fibrosis Transmembrane Receptor (CFTR), ligand gated chloride channels, such as the GABA receptor, Bestrophins, and CLCs. (Suzuki et al., 2006). Mutations in CFTR give rise to Cystic Fibrosis. Compounds that modify GABA receptor function have been used in treatment of many brain disorders (Ticku, 1983). Mutations in Bestrophins are associated with a rare form of macular degeneration, and can lead to blindness (Hartzell et al., 2005). We will focus our attention on the CLC family of chloride channels and transporters, which underlie many important physiological processes to be discussed (Jentsch, 2008).

CLCs are found in organisms ranging from bacteria to humans, and expressed throughout the organism (Thiemann et al., 1992; Jentsch et al., 1995; Brandt and Jentsch, 1995; Steinmeyer et al., 1991; Sasaki et al., 1994). In mammals, there are nine CLCs:

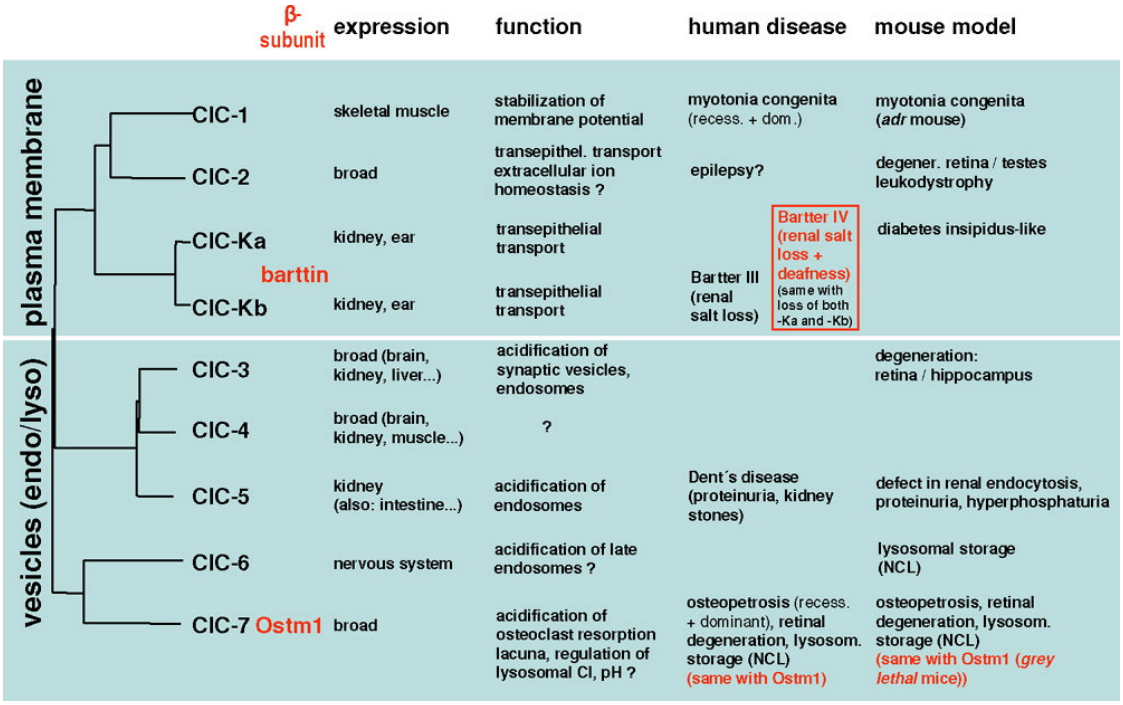

Figure 1: Summary of, for mammalian CLCs, (from right to left) vesicular vs. plasma membrane localization, CLC name, auxiliary β subunit, expression pattern in mammals, function, human diseases caused by mutation, and available mouse models. CLC-1 to 2, Ka and Kb are plasma membrane channels, while CLC-3 to 7 are vesicular. β-subunit indicates auxiliary subunits that interact with CLC-Ka, CLC-Kb, or CLC-7. Mouse model indicates the phenotype due to knockout of the channel, or beta subunit (indicated in red). Figure taken from Jentsch TJ. Crit Rev Biochem Mol Biol. 2008

CLC 1-7, CLC-Ka, and CLC-Kb. Mammalian CLCs have important physiological roles such as controlling cell excitability (Wang et al., 2006), transporting chloride through epithelial tissue (Uchida, 2000), trafficking of receptors necessary for endocytosis (Christensen et al., 2003), and acidification of intracellular vesicles (Stobrawa et al., 2001; Hara-Chikuma et al., 2005). Additionally, mutations in human CLC encoding genes give rise to muscle (Koch et al., 1992), kidney (Lloyd et al., 1997), and bone disorders (Kornak et al., 2001). In fact, mutations in CLC-1 are the primary cause of a

muscle disease called myotonia (Koch et al., 1992). Figure 1 summarizes the function of and diseases caused by mutation of mammalian CLCs. These observations underscore the essential roles of CLCs in normal and pathological physiology.

Many of the aforementioned human disease associated mutations have been found in the intracellular portion of CLCs (Pangrazio et al., 2010; Tosetto et al., 2009). A central question in the CLC field is, thus, how do intracellular processes regulate channel or transporter function. My research has addressed this question by furthering an understanding of structural mechanisms by which the intracellular domain of CLCs regulate CLC gating. I have approached this question using electrophysiology and model-driven mutagenesis in the *C. elegans* CLCs, CLH-3a and CLH-3b. These two *C. elegans* CLCs offer clear advantages for deciphering structure-function relationships. Additionally, many such structural and physiological characteristics of CLCs have been conserved over hundreds of millions of years of evolution, making my *C. elegans* studies relevant to mammalian CLCs (Dutzler et al., 2003; Estevez et al., 2003; Meyer and Dutzler, 2006; Markovic and Dutzler, 2007; Meyer et al., 2007; Engh and Maduke, 2005; Lin and Chen, 2003; Rutledge et al., 2001; Dutzler et al., 2002).

In this introduction, I will provide an overview of CLCs' essential physiological roles as channels and transporters, the *C. elegans* model system we use, namely CLH-3a and CLH-3b, and CLC structure function. The last item includes pore structure and associated gating mechanisms as well as Cystathionine-β-Synthase domain structure and physiological roles.

CLCs comprise a family of channels and transporters with essential physiological roles

CLCs are anion conducting channels and transporters

The CLC family of proteins include both voltage gated channels and transporters (Zifarelli and Pusch, 2007). Transporters carry multiple ion species across the membrane, while channels only carry one type of ion. Initially, all CLCs were assumed to be channels. However, electrophysiological experiments showed that, for some CLC channels, gating is dependent on pH in a manner that could be explained by CLCs also transporting H^+ (Accardi and Miller, 2004). Local pH changes within the cell also suggested that some CLCs transport H^+ (Picollo and Pusch, 2005). Of the nine mammalian CLCs, CLC-1, 2, Ka, and Kb are Cl^- ion channels, while CLC-4 and 5, and possibly 3 are H^+/Cl^- antiporters (Zifarelli and Pusch, 2007) with a $2Cl^-/1H^+$ stochiometry (Zifarelli and Pusch, 2009a). CLC-3 to CLC-7 are largely expressed intracellularly, while the other CLCs, which are channels, are largely expressed on the plasma membrane (Zifarelli and Pusch, 2007)(Figure 1). The similarity of CLC channels and transporters is underscored by the fact that a point mutation of a single residue in a prokaryotic CLC transporter, CLC-ec1, can make it function as a constitutively active channel (Accardi and Miller, 2004).

CLCs are anion channels or transporters that are more permeable to Cl^- than other anions. Certain anions can either permeate the CLC channel or block it, depending on the CLC family member. These anions, which include: F^-, Br^-, I^-, SCN^-, NO_3^-, and $CH_3SO_3^-$, permeate or block by binding to anion specific binding sites in the pore (Fahlke, 2001). These sites have a stronger binding affinity for larger or multi-atom ions (e.g. I^-, SCN^-, NO_3^-) as opposed to small single-atom ions (e.g. F^-, Cl^-). Usually, the ions with stronger

binding affinity, which is to say larger ions, are less permeable. Nonetheless, CLCs vary in terms of the most permeable anion. This lack of consistency in terms of permeation preference is generally not seen in cation channels. This difference has been suggested to be due to there being more types of single ion cations than anions in the body, and thus selectivity could be more critical in cation channels (Fahlke, 2001).

CLC mutations lead to myotonia, osteopetrosis, and renal disorders

CLC mutations lead to myotonia (Koch et al., 1992), osteopetrosis (Kornak et al., 2001), and renal disorders (Jeck et al., 2000; Wolf et al., 2003; Konrad et al., 2000; Simon et al., 1997; Lloyd et al., 1996; Barlassina et al., 2007). Myotonia is characterized by delayed muscle relaxation and is due to impaired function of CLC-1, the "muscle" CLC. CLC-1 conduction represents ~70% of plasma membrane conductivity in muscle cells. CLC-1 steady state current is an outward rectifier, meaning Cl^- only enters the cell at steady state, and this results in hyperpolarization of the cell. Cl^- entering the cell is considered outward current because of the negative charge of Cl^-, and thus the inward flow of positive charge. It is estimated that an 80% reduction in muscle chloride conductance will lead to myotonia by increasing excitability of muscle cells. Over 120 mutations in CLC-1 have been identified to be associated with either dominant congenital myotonia (Thompsen's Disease) or recessive generalized myotonia (Becker myotonia). (Lossin and George, Jr., 2008).

Osteopetrosis is a disease of bone hardening that can result from disruption of CLC-7 function (Kornak et al., 2001). It characterized by dense, fragile bones lacking

bone marrow, and leads to blood cell formation outside the bones (Zhao et al., 2009). An acidic pH is necessary between the bones and osteoclasts (cells that decrease bone mass) for proper dissolving of inorganic bone material and enzymatic breakdown of bone matrix. CLC-7's function as an H^+/Cl^- antiporter is necessary for maintaining acidic pH in this space (Zhao et al., 2009).

The renal disorders Bartter's syndrome and Dent's disease are associated with mutations to CLC-Kb (Jeck et al., 2000; Wolf et al., 2003; Konrad et al., 2000; Simon et al., 1997) and CLC-5 (Grand et al., 2009; Brakemeier et al., 2004; Yamamoto et al., 2000; Cox et al., 1999; Igarashi et al., 1998), respectively. Three CLC proteins, CLC-Ka, CLC-Kb and ClC-5, and an accessory subunit, Barttin, are mainly expressed in the kidney (Sasaki et al., 1994; Steinmeyer et al., 1995). These CLCs function in concentration of urine, salt transport through epithelia, and acidification of endosomes (Plans et al., 2009).

Dent's disease is characterized by the presence of low molecular weight proteins in the urine. Normally, such proteins are reabsorbed by receptor-mediated endocytosis in the proximal tubule. However, CLC-5 function disruption in Dent's disorder leads to defects in endocytosis, which can lead to the proteins not being reabsorbed. CLC-5's role in endocytosis comes from the fact that endocytosis require proper vesicle acidification in order for receptor proteins to bind ligands. Such acidification could be mediated by CLC-5's function as a H^+/Cl^- antiporter (Plans et al., 2009).

Bartter's syndrome is characterized by dehydration and improper salt concentrations in urine. CLC-Ka's chloride transporting ability is necessary for

maintaining the concentration gradient along the Loop of Henle, which allows for concentration of urine. Thus, CLC-Ka dysfunction leads to excessively dilute urine and, thus, diabetes insipidous, as reported in mice (Matsumura et al., 1999). Such fluid loss could contribute to dehydration. CLC-Kb, on the other hand, is necessary for tubular reabsorption of Cl^- and other ions along the distal tubule. CLC-Kb dysfunction, therefore would lead to the excessive salt loss associated with Bartter's syndrome (Wolf et al., 2003).

C. elegans **and their CLCs are an ideal model system with physiological relevance to mammals**

C. elegans**, with six CLC encoding genes, is a useful model system**

We use the *C. elegans* CLCs, CLH-3a and CLH-3b, as a model system for our structure-function studies. The *C. elegans* genome contains six CLC-encoding genes, *clh*-1 to *clh*-6, (for Cl^- channel homolog) (Schriever et al., 1999) which have homologs of the members of the three subfamilies of mammalian CLCs (Waldegger and Jentsch, 2000). These subfamilies are the CLC channels (CLC-0 to CLC-2, CLC-Ka and CLC-Kb), the CLC transporters (CLC-3 to CLC-5) and the third subfamily containing CLC-6 and CLC-7.

The *C. elegans* genes encode chloride channels that are expressed throughout the *C. elegans,* as delineated here (Nehrke et al., 2000). *clh-1* is expressed in neurons, epithelia, intestinal, reproductive cells, and cells involved with cuticle formation called seam cells. *Clh-2* is expressed in neurons, body wall muscles, and intestines. C*lh-3* is expressed in excretory cells, intestinal epithelia, defecation muscles, and the

hermaphrodite-specific neurons (*C. elegans* are almost always hermaphrodites) (Schriever et al., 1999). *Clh-4* is expressed in the excretory cells alone. *Clh-5* and *clh-6* are expressed in many cells, though *clh-6* is mostly in non neuronal cells (Nehrke et al., 2000). Of these genes, only *clh-1* and *clh-3* encode proteins of known function. Specifically, c*lh-1* disruption results in a nematode with increased body width (Petalcorin et al., 1999). *Clh-3*, our focus, is activated during meiosis and is sensitive to cell volume (Rutledge et al., 2001).

Our lab first started understanding CLCs through the *C. elegans* channels in part because of the ease of RNAi in *C. elegans* (Timmons et al., 2003). For whole animal knockdown, *C. elegans* can simply be fed or, in a more controlled manner, injected double stranded RNA, and this leads to loss of function of the corresponding protein throughout the worm (Timmons et al., 2003). Injection in mammals can be quite complicated (Lieberman et al., 2003) and was not an established method (Kawakami and Hashida, 2007) at the time of our initial study (Rutledge et al., 2001). *C. elegans* injection, on the other hand, is a relatively straightforward procedure, when compared with mammalian injection (Dudley and Goldstein, 2005).

CLH-3b is volume sensitive and activated during meiotic maturation in the oocyte

In an effort to understand cell volume regulation, local injection of RNAi was used to identify the molecular basis of an inwardly rectifying volume sensitive chloride current. This current, in the *C. elegans* oocyte, was determined to be carried through a CLC protein encoded by *clh-3* (Rutledge et al., 2001). *Clh-3* has two splice variants:

CLH-3a and CLH-3b (Denton et al., 2004). The pH and volume sensitivity of CLH-3b are consistent with that of the volume sensitive oocyte current (Rutledge et al., 2001; Rutledge et al., 2001; Denton et al., 2004). Additionally, the CLH-3b protein was found to be expressed in the *C. elegans* oocyte (Denton et al., 2004). Thus, the volume-sensitive oocyte current is carried through CLH-3b.

The physiological signal for CLH-3b activation, however, is not volume regulation, but rather a process called meiotic maturation in the oocyte (Rutledge et al., 2001). In reproduction, oocytes arrest during prophase of meiosis. Meiotic maturation is the process by which oocytes continue onto metaphase after this temporal arrest, and is triggered by a hormonal signal from the sperm. During the time of meiotic maturation, the nuclear envelope breaks down, the cytoskeleton rearranges, and the meiotic spindle forms. Meiotic maturation leads immediately to ovulation, fertilization, and zygote formation. Ovulation requires repetitive contraction of muscles in the *C. elegans* called gonadal sheath cells (Greenstein, 2005). C*lh-3* knockdown via RNAi leads to these contractions initiating sooner (Rutledge et al., 2001).

Cell cycle processes, such as meiotic maturation, are regulated by the same class of enzymes as those that confer CLH-3b's volume sensitivity. Specifically, the cell cycle phosphatases CeGLC-7 α and CeGLC-7 β activate CLH-3b during cell swelling (Rutledge et al., 2002; Dan et al., 2001), while Germinal Center Kinase (GCK)-3 of the Ste20 family deactivates CLH-3b and inhibits such activation. Besides deactivation, GCK-3 affects biophysical properties of CLH-3b (Denton et al., 2005). Ste20 kinases are involved in cell cycle processes such as cell growth, differentiation, and death (Pombo et

al., 2007). Similar regulation is found in mammals: a Ste-20 kinase, PASK, regulates the volume sensitive Na-K-Cl cotransporter, NKCC1 (Dowd and Forbush, 2003; Gagnon et al., 2006).

This link between cell volume regulation and cell cycle progression is certainly not limited to CLH-3b. Indeed, periodic cell cycle events, such as S-phase DNA replication and mitosis are triggered by the cell reaching a critical size (Mitchison, 2003). Similarly, apoptotic cell death is preceded by a type of cell shrinkage termed Apoptotic Volume Decrease. This volume decrease, and the subsequent apoptosis, is prevented by blocking volume-regulatory K^+ or Cl^- channels (Maeno et al., 2000).

Regulatory volume decrease is a type of volume regulation where swelling diminishes after hypotonicity is maintained for extended time periods. Proteins encoded by *clh-3* do not play a role in such volume regulation. That is, they do not affect the magnitude of volume increase or regulatory decrease due to hypotonicity (Rutledge et al., 2001).

Additionally, based upon their voltage sensitivity and expression patterns, it is possible that CLH-3a functions during electrical activity in muscles and hermaphrodite specific neurons, while CLH-3b functions during Cl^- transport in non-excitable cells (Denton et al., 2004). This is because CLH-3a activates at more negative voltages than CLH-3b. Additionally, this activation in CLH-3a is potentiated by prior positive holding voltages. Such potentiation could be physiologically relevant during action potentials or periods of depolarization followed by hyperpolarization. *C. elegans* neurons generally lack action potentials (Goodman et al., 1998), although recent reports suggest that some

C. elegans neurons may use action potentials (Lockery et al., 2009; Mellem et al., 2008). Nonetheless, *C. elegans* neurons do show a wide range of membrane voltages and a relatively large, though graded, change in potential due to small electrical stimulus. Specifically, the membrane potential of *C. elegans* neurons varies in the range of –30 to –90 mV, a range where CLH-3a's potentiation could start to become physiological (Goodman et al., 1998; Denton et al., 2004). *C. elegans* enteric muscles, which express *clh* –3, do exhibit action potentials (Lee et al., 1997; Davis et al., 1995). These action potentials have relatively long Ca^{++} channel dependent depolarizations (Lee et al., 1997), which could be affected by CLH-3a's potentiation.

Electrophysiology Basics: Current represents the number of open cell-surface channels

We use electrophysiology, specifically the whole cell configuration, to assess channel function. We patch onto green fluorescent HEK 293 cells that have been transfected with channel plasmids and GFP. In the whole cell electrophysiology setup, the inside of the cell is electrically connected to a voltage-clamp amplifier. This amplifier injects current into the cell, as necessary, to maintain constant voltage across the cell membrane. The magnitude of this current relates to the number of open channels, as I will explain.

The injected current necessary to maintain constant voltage can be determined from a form of ohms law:

Current injected = Membrane voltage * Conductance across cell membrane

As this shows, with voltage maintained constant, current injected is proportional to conductance across the membrane. Conductance, and thus current, is a measure of the number of channels that are on the cell surface and open. Conductance is also affected by the unit conductivity of each channel. However, this rarely changes and, for CLH-3b, is believed to be too small to measure.

The following terms are often used in electrophysiology. "Membrane potential" or "membrane voltage" refers to the voltage difference between the inside and outside of the cell. "Hyperpolarization", often caused by a "hyperpolarizing current", is a decrease in membrane voltage, making the voltage across the membrane more negative or less positive. "Depolarization", often caused by a "depolarizing current", is an increase in membrane voltage, making the voltage less negative or more positive.

With clear gating & sequence differences, CLH-3a and CLH-3b are an excellent model system for structure-function studies

My studies use CLH-3a and CLH-3b as a model system to understand structure-function relationships in CLCs. As splice variants, CLH-3a and CLH-3b have localized differences in sequence of the N- and C- termini, shown in Figure 2 (Denton et al., 2006; He et al., 2006). The intramembrane domains of CLH-3a and CLH-3b are completely identical. The major differences in sequence of the channels are a 71 amino acid

extension at the N-terminus of CLH-3a, a 160 amino acid extension at the C-terminus of CLH-3b and an insertion of 101 amino acids in CLH-3b between two structural domains called Cystathionine–β-Synthase domains (Bateman, 1997) (CBS1 and CBS2) (Denton et al., 2006; He et al., 2006). In addition, eight of the last nine amino acids of CLH-3a are distinct from their corresponding amino acids in CLH-3b (Denton et al., 2004). These localized differences in sequence are one of three reasons that the splice variants make excellent model systems for structure-function studies.

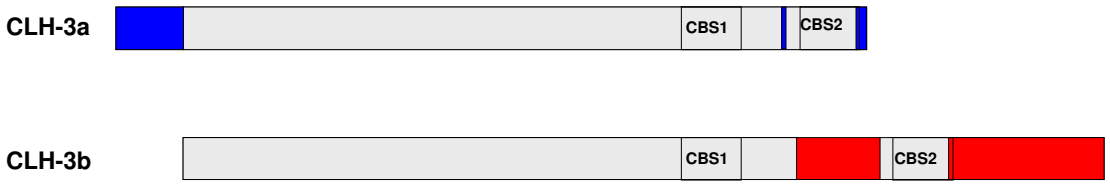

Figure 2: Diagram illustrating sequence difference between the *clh-3* splice variants CLH-3a and CLH-3b. Grey regions are identical; blue regions are unique to CLH-3a; red regions are unique to CLH-3b. CBS refers to the structural domain called Cystathionine-β-Synthase domains. The figure shows sequence differences between the splice variants are localized and at the N- and C- termini. The major differences in sequence are a 71 amino acid extension at the N-terminus of CLH-3a, a 160 amino acid extension at the C-terminus of CLH-3b and an insertion of a 101 amino acid motif in CLH-3b between CBS1 and CBS2. In addition, eight of the last nine amino acids of CLH-3a are distinct from their corresponding amino acids in CLH-3b and there is one distinct residue, besides the 101, between CBS1 and CBS2.

Another reason for using the splice variants is their striking differences in channel gating. While both CLH-3a and CLH-3b activate in response to hyperpolarizing negative voltages, CLH-3a has a more negative activation voltage (Figure 3A) and shows increased sensitivity to extracellular Cl^- (Figure 3B) and pH (Figure 3C) (He et al., 2006; Denton et al., 2004). Specifically, lowering the external [Cl^-] deactivates CLH-3a, while

it has virtually no effect on CLH-3b activation. Additionally, acidic pH of 5.9, as compared to pH 7.4, activates CLH-3a by ~3-fold, while it activates CLH-3b by only ~ 1.6-fold. Most strikingly, CLH-3a exhibits sensitivity to prior depolarizing voltages, termed "prepotentiation", mentioned earlier. That is, holding resting membrane potential at positive voltages prior to hyperpolarizing activation increases channel current induced by the subsequent hyperpolarized voltages (Denton et al., 2004; He et al., 2006) (Figure 3D). Moreover, previous studies have shown that mutations to CLH-3a or CLH-3b always had gating that closely resembled one of the two splice variants (Denton et al., 2006; He et al., 2006). In other words, novel or intermediate gating was not seen.

Finally, CLH-3b's close functional and sequence homology to the mammalian CLC-2 (Rutledge et al., 2001), along with the general conservation of CLC structure (Dutzler et al., 2003; Dutzler et al., 2002; Estevez et al., 2003; Engh and Maduke, 2005; Lin and Chen, 2003; Meyer and Dutzler, 2006; Markovic and Dutzler, 2007; Meyer et al., 2007), make CLH-3b structure-function likely to be applicable to mammals. Much like CLC-2, CLH-3a and CLH-3b are inward rectifiers, only allowing Cl^- to leave the cell (Cl^- is negative; thus the flow of charge is inward) (Rutledge et al., 2001; Denton et al., 2004). CLH-3a, CLH-3b, and CLC-2 all activate in response to hyperpolarizing stimulus (Rutledge et al., 2001; Denton et al., 2004), and CLH-3b and CLC-2 both activate by cell swelling (Rutledge et al., 2001). In short, gating of CLH-3b closely resembles that of CLC-2.

To summarize, the localized sequence differences, strikingly distinct and discrete gating, and relevance to mammalian physiology make CLH-3a and CLH-3b useful tools for elucidating relationships of CLC structure and function.

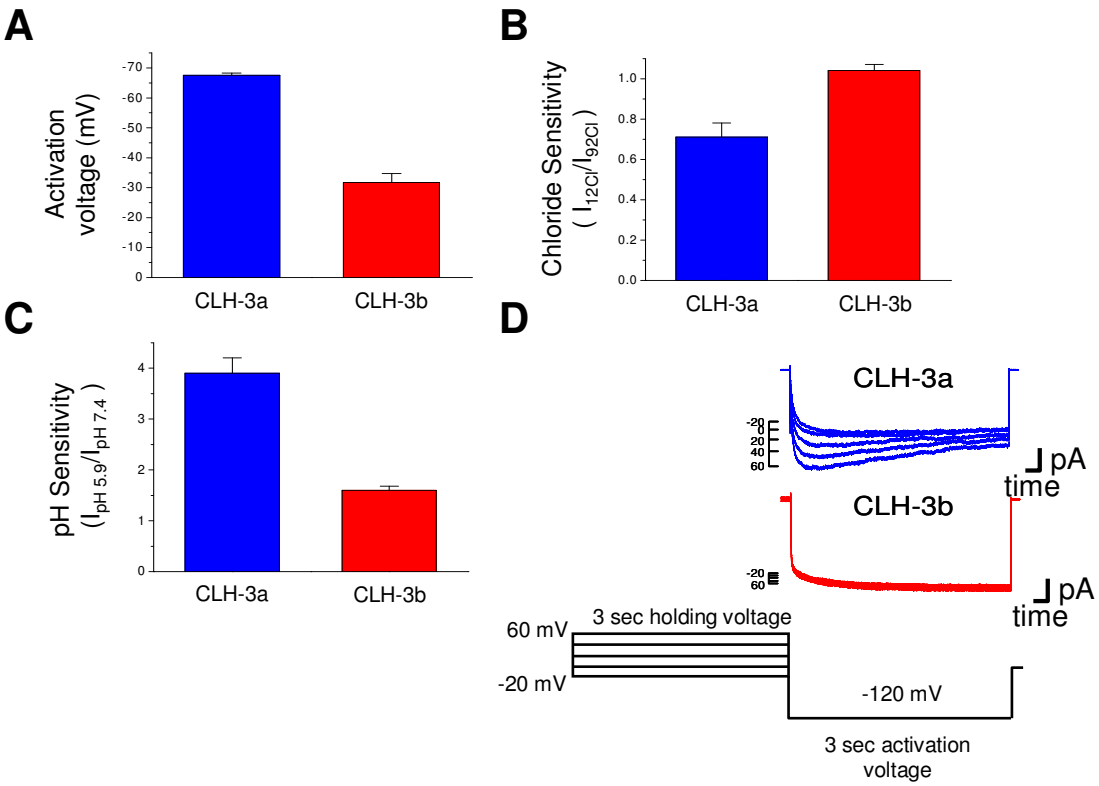

Figure 3: CLH-3a and CLH-3b exhibit clear differences in channel gating. A. CLH-3a requires hyperpolarization to more negative voltages to activate. B. CLH-3a is more sensitive to external [Cl^-]. Plot show ratio of current at -100mV with 12mM external [Cl^-] to current at -100mV with 92 mM external [Cl^-]. Deviation from one indicates increased sensitivity. C. CLH-3a has increased sensitivity to external pH. Plot shows ratio of current with external pH 5.9 to current with external pH 7.4 D. CLH-3a is sensitive to positive holding voltages (i.e. exhibits prepotentiation), while CLH-3b is insensitive. First, a three second depolarized holding voltage between -20 and + 60 was applied, during which channels were closed. Next, for three seconds, voltage was dropped to -120 mV and sample recorded currents are shown. Five traces indicate five different holding voltages. For CLH-3b all five traces coincide, thus CLH-3b is insensitive to positive holding voltages. For CLH-3a more positive holding voltage potentiates channel current.

CLC structure-function relations are known in the pore, but not cytoplasmic, region

CLCs are homodimers with a conserved alpha-helical membrane region

Crystal structures have been solved for bacterial CLCs (Dutzler et al., 2002; Dutzler et al., 2003) and the cytoplasmic region of eukaryotic CLCs (Meyer and Dutzler, 2006; Markovic and Dutzler, 2007; Meyer et al., 2007). All CLCs are homodimers with a single pore per monomer (Figure 4A). Each monomer consists of 18 alpha helices, A-R, 17 of which are intramembrane (Figure 4B). In eukaryotic and some prokaryotic CLCs, each monomer also has a large cytoplasmic region containing two Cystathionine-β-Synthase (CBS) domains (Bateman, 1997) per monomer (Meyer and Dutzler, 2006; Markovic and Dutzler, 2007; Meyer et al., 2007) (Figure 4B). CLC membrane structure is likely to be conserved in organisms ranging from bacteria to humans (Dutzler et al., 2003; Dutzler et al., 2002; Estevez et al., 2003);(Engh and Maduke, 2005; Lin and Chen, 2003), and CLC cytoplasmic structure is likely conserved among eukaryotes (Meyer and Dutzler, 2006; Markovic and Dutzler, 2007; Meyer et al., 2007). Thus, *C. elegans* CLC structure function studies are highly applicable to mammalian CLCs.

CLCs have a "slow" gate common for both subunits and two individual "fast" gates

The crystal structures of the membrane region of bacterial CLCs have provided insights into channel gating mechanisms. CLCs have a "slow" gate and two "fast" gates (Dutzler et al., 2002; Dutzler et al., 2003; Ludewig et al., 1996), named after their opening kinetics. The slow gate acts on both pores simultaneously and is also called a "common" gate. The fast gates are individual to each pore (Figure 4A).

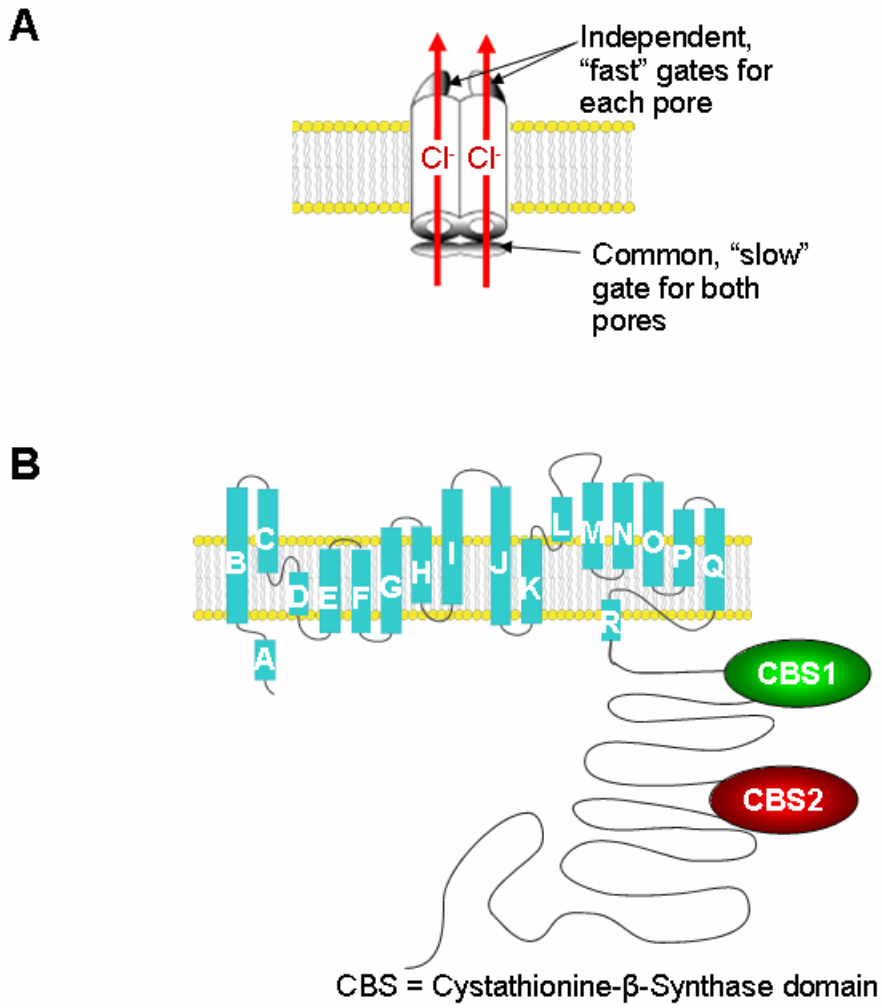

Figure 4: Structure of CLCs. A. CLCs are homo dimers with one pore per monomer. There are two fast gates, individual to each pore and one slow gate, common for both pores. B. Structure of a CLC monomer. There are 18 helices, A-R, 17 of which are intramembrane. The cytoplasmic region contains two Cystathionine-β-Synthase domains per monomer in all eukaryotes.

The currents through fast vs. slow gates can usually be distinguished by analyzing opening kinetics of CLCs electrophysiological traces. We will take the trace of CLH-3b as an example. CLH-3b opens in the millisecond time range in response to negative voltages and does not deactivate (Denton et al., 2004; He et al., 2006). The opening kinetics of CLH-3b, as well as many CLCs, can be fitted with two exponential time constants. The current fitting to the faster time constant (~ 5 ms for CLH-3b) (Denton et al., 2004) is defined to be through the fast gate, while the current fitting the slower time constant (~ 20 ms for CLH-3b) (Denton et al., 2004) is defined to be controlled by the slow gate. In the case that exponential fits cannot resolve the separate current components, one can measure the component due to slow gating by blocking slow gating with Zn^{++} (Chen, 1998) or using special voltage protocols (Yusef et al., 2006). In some (de Santiago et al., 2005; Yusef et al., 2006), but not all (Miller, 1982), CLCs the fast and slow gate are believed to be coupled.

Fast gating is controlled by the glutamate gate, while slow mechanisms are not understood

The fast gate structure can be understood in detail from the membrane structure of bacterial CLCs. Four of the seventeen membrane helices, D, F, N, and R, converge to form the fast gate, channel pore, and selectivity filter in CLCs (Dutzler et al., 2002; Dutzler et al., 2003). The fast gate, itself, is an extracellular glutamate residue located on helix F, and is also called a "glutamate gate" (Dutzler et al., 2003; Dutzler et al., 2002). Mutation of the fast gate in various CLCs is known to abolish all sensitivity of the

channel to voltage, external pH, and external [Cl^-] (Traverso et al., 2003; He et al., 2006; Traverso et al., 2006; Dutzler et al., 2003; Yusef et al., 2006).

As such, the fast gates in CLCs underlie their sensitivity to negative membrane voltages, acidic pH, and high external [Cl^-]. In general, opening and closing of the fast gate involves a minor change in orientation of just the negatively charged glutamate gate (Dutzler et al., 2003; Dutzler et al., 2002). In the closed state, the negative oxygens of the glutamate residue displace the chloride ion (Figure 5A). The Cl^- ions are held in place at the pore by polar hydroxyl groups of a serine and a tyrosine, as well as a polar amide nitrogen of the main chain (Dutzler et al., 2003).

Mechanisms have been postulated for how voltage, pH, and external Cl^- regulate the fast gate. CLC channels have a voltage sensor unlike any other family of channels: the permeant chloride ions themselves confer the voltage sensitivity (Pusch et al., 1995). Specifically, it is believed that the permeating chloride ions are repelled by negative internal voltage, and this ion movement displaces the fast gate, which results in further channel opening (Pusch et al., 1995) (Figure 5B). An important part of this gating mechanism is the fact that there are three Cl^- binding sites in the pore (Dutzler et al., 2002; Dutzler et al., 2003), and thus, binding of one Cl^- ion influences binding of other Cl^- ions (Pusch et al., 1995). In the case of activation by acidic pH, electrophysiological studies (Zifarelli et al., 2008; Bisset et al., 2005) suggest that the glutamate gate is protonated by low pH, thereby loosing its negative charge, and is no longer held closed by coordination with residues in helices D, N, and R (Figure 5C). For high external [Cl^-], it has been proposed that the negative external chloride ions may be competing with the

glutamate gate for the pore, thereby holding it in open position (Zifarelli et al., 2008; Bisset et al., 2005) (Figure 5D). Mutation of the glutamate gate to alanine results in loss of the negatively charged oxygen, and thus the gate is not likely to be held closed (Figure 5E). All of these proposed mechanisms involve only the fast gate, although the slow gate is also activated by negative voltage, acidic pH, and high external [Cl^-] (Rychkov et al., 1996).

As of yet very little is known regarding mechanisms of slow gating. Opening the slow gate is believed to require large conformational changes, according to Fluorescence Resonance Energy Transfer (FRET) studies (Bykova et al., 2006) and temperature sensitivity of channel currents (Zuniga et al., 2004; Ludewig et al., 1997; Bennetts et al., 2001). Specifically, FRET studies (Bykova et al., 2006) showed that upon closing the slow gate, the distance between cytoplasmic C-termini increased. The temperature sensitivity studies (Zuniga et al., 2004; Bennetts et al., 2001) show the slow gate function has a high temperature sensitivity, as compared to the fast gate. This high temperature sensitivity points to a large conformational rearrangement during slow gating (Pusch et al., 1997). Slow gate currents in CLCs are also known to be blocked by Zn^{++}(Chen, 1998). Based on this Zn^{++} sensitivity, it is believed that the prepotentiation gating in CLH-3a (discussed earlier) is carried through the slow gate (Denton et al., 2004). Electrophysiological and mutagenesis studies in CLCs have suggested the cytoplasmic region (Fong et al., 1998), including Cystathionine-β-Synthase (CBS) domains (Estevez et al., 2004; Yusef et al., 2006), may be an important structural element involved in slow gating.

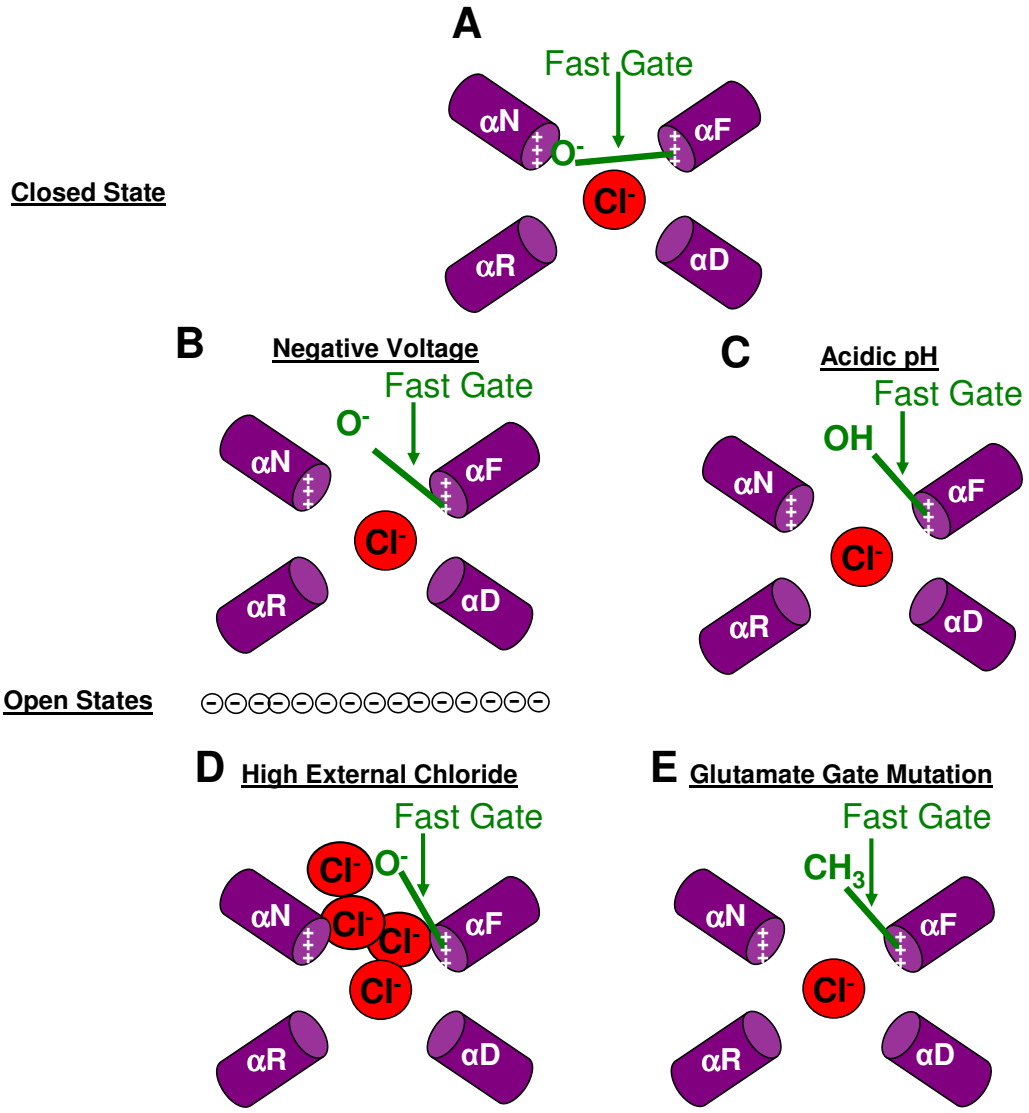

Figure 5: Proposed mechanism for CLC fast gate activation. A. At neutral pH, the oxygen of the glutamate residue in the fast gate is deprotonated. Thus, it can co-ordinate with positive residues in the membrane helices (aD, aN, and aR) and close the channel. B. Negative internal voltage repels the Cl^- ion, causing it to displace the glutamate (fast) gate. C. Acidic pH protonates the oxygen of the glutamate residue, thereby neutralizing its charge and freeing it from coordination with helices. D. External chloride ions compete with the oxygen of the glutamate gate, thereby holding the gate open. E. Mutation of the glutamate gate to alanine (side chain is CH_3) removes the negative charge, prevents coordination with the helices and, thus, makes the channel constitutively open.

CBS domain's tertiary, but not quaternary, structure is conserved

CBS domains are found in over a 1000 different types of proteins (Scott et al., 2004) (predicted by SMART) (Schultz et al., 1998), and have a variety of functions. CBS domains are 50-60 amino acids in length, and they consist of two alpha helices (α1 and α2) and three beta strands (β1-3) in the order β1-α1-β2-β3-α2 (Figure 6A). There are crystal structures for CBS domains in proteins as diverse as AMPK (Jin et al., 2007) (Day et al., 2007), IMPDH (Zhang et al., 1999), a theoretical cystathionine-β-synthase domain containing protein (Miller et al., 2004), a Mg^{2+} transporter (Hattori et al., 2007) and three CLCs (Markovic and Dutzler, 2007; Meyer and Dutzler, 2006; Meyer et al., 2007). In all known CBS domain structures, CBS 1 and 2 exist as pairs that interact at the surfaces of β2 and β3 to form a dimer (Figure 6B and C). These pairs of CBS domains often dimerize with other CBS domain pairs to form quaternary structure. While the structure of the CBS1-CBS2 pair is conserved, the quaternary structures of CBS domains vary (Jin et al., 2007; Meyer and Dutzler, 2006; Markovic and Dutzler, 2007; Meyer et al., 2007; Hattori et al., 2007; Day et al., 2007; Zhang et al., 1999; Miller et al., 2004).

Crystal structures and biochemical data demonstrate that the cytoplasmic regions of CLC-0, CLC-5 and CLC-Ka have a dimeric quaternary structure, with each monomer containing two CBS domains (Meyer and Dutzler, 2006; Markovic and Dutzler, 2007; Meyer et al., 2007) (Figure 6B and C). In CLCs, the cytoplasmic monomers interact at a 90-degree angle. The interface is formed by CBS2 α1 and other regions of CBS2 of each

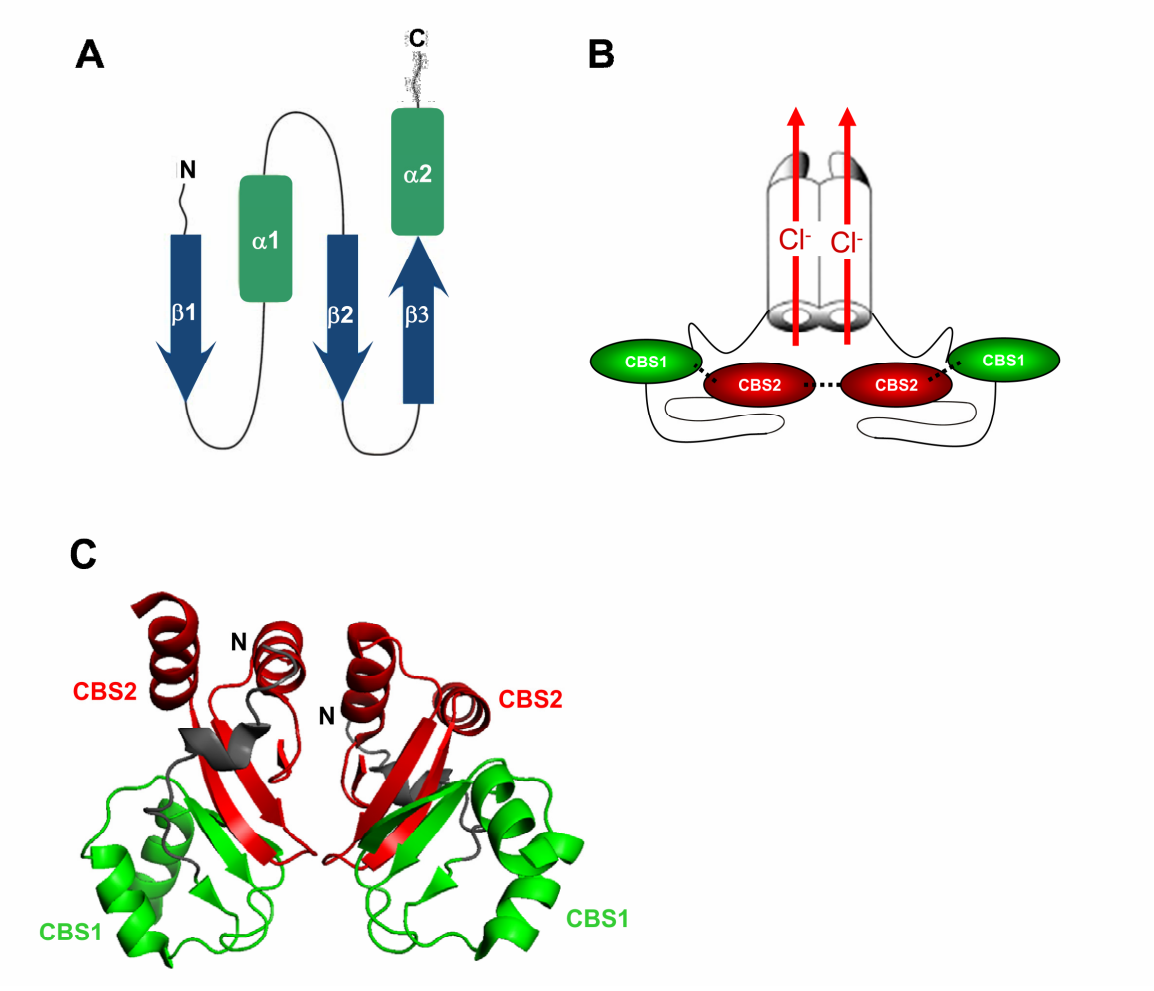

Figure 6: Structure of CBS domains in CLCs. A. CBS domains are defined by the secondary structure pattern: β1-α1-β2-β3-α2. B. Interactions between CBS domains in the cytoplasmic region of CLCs. CBS1 and CBS2 interact to form a pair in each CLC monomer. These pairs then interact with the CBS domain pair of the other monomer, at CBS2, to form quaternary structure. Dashed lines indicate interactions. C. Crystal structure of the cytoplasmic region of CLC-Ka, indicating conserved arrangement of CBS domains. CBS1 and CBS2 of each monomer interact at β2 and β3, and CBS2 of separate monomers interact at α1.

monomer. In non-CLC CBS domain containing proteins, monomers either associate in parallel "head-to-head'" (CBS1 with CBS1 and CBS2 with CBS2) or "head-to-tail" (each CBS1 with the other CBS2) configurations. Thus, the quaternary structure of CBS domains in CLCs is unique among CBS domain containing proteins (Jin et al., 2007;

Meyer and Dutzler, 2006; Markovic and Dutzler, 2007; Meyer et al., 2007; Hattori et al., 2007; Day et al., 2007; Zhang et al., 1999; Miller et al., 2004).

Cystathionine-β-Synthase (CBS) domains have a wide variety of essential functions

CBS domains have many different functions, in accord with the wide variety of proteins in which they are found. Mutations in human CBS domains give rise to cardiac (Oliveira et al., 2003), metabolic (Shan and Kruger, 1998), retinal (Kennan et al., 2002), and muscle disorders (de Diego et al., 1999; Sasaki et al., 1999). Mutations in CBS domains also alter protein trafficking (Pena-Munzenmayer et al., 2005; Bateman and Kickhoefer, 2003; Carr et al., 2003), energy metabolism (Scott et al., 2004; Janosik et al., 2001), protein multimerization (Jhee et al., 2000), binding of ligands (Scott et al., 2004; Jin et al., 2007; Day et al., 2007; Meyer et al., 2007; Tanaka et al., 2007), and ion channel gating (Bennetts et al., 2007; Lin et al., 2006; Denton et al., 2006; Wu et al., 2006; He et al., 2006; Estevez et al., 2004; Bennetts et al., 2005; Yusef et al., 2006).

In particular, CBS domains bind ions and adenosyl compounds. Specifically, CBS domains of the MgtE Mg^{2+} transporter bind Mg^{2+} ions and may sense intracellular Mg^{2+} concentrations (Hattori et al., 2007). CBS domains in a bacterial organic osmolyte transporter called OpuA detect changes in intracellular ionic strength. This likely occurs by non specific association of solute ions with the CBS2 domain and interaction of CBS2 with negatively charged plasma membrane moieties (Mahmood et al., 2009). Additionally, adenosyl compounds such as AMP, ADP, and ATP bind to CBS domain pairs of IMP dehydrogenase-2 (Scott et al., 2004), AMP-activated protein kinase (Scott et

al., 2004; Townley and Shapiro, 2007; Jin et al., 2007; Day et al., 2007), Cystathionine-β-Synthase (Scott et al., 2004), ClC-2 (Scott et al., 2004) and ClC-5 (Meyer et al., 2007). Such binding occurs in a pocket formed by the interface of CBS1 with CBS2. Studies by Bennetts and colleagues show that ATP can regulate gating in CLC-1 (Bennetts et al., 2005; Bennetts et al., 2007), possibly by binding to CBS domains.

CBS domains also regulate trafficking of CLCs. Specifically, normal endosome trafficking of CLC-5 is prevented by disease-associated truncation mutations that disrupt CBS2 domain structure (Carr et al., 2003). Additionally, basolateral, as opposed to apical targeting of CLC-2 in certain epithelial cells is governed by a di-leucine motif in CBS2 (Pena-Munzenmayer et al., 2005). In short, CBS domains have a variety of important cellular functions, yet our understanding of their structure-function relationships is still limited.

Cytoplasmic regions of CLCs regulate gating, likely through the membrane helix R

Given that CBS domain mutations in CLCs regulate gating (Bennetts et al., 2007; Lin et al., 2006; Denton et al., 2006; Wu et al., 2006; He et al., 2006; Estevez et al., 2004; Bennetts et al., 2005; Yusef et al., 2006), the mutations are likely to change the conformation of the channel gate. An important unanswered question in the field is how the cytoplasmic region of CLCs can alter structure at the extracellular gate. There have been numerous studies that show mutations of the cytoplasmic CBS domains in CLCs affect channel gating (Bennetts et al., 2007; Yusef et al., 2006; Lin et al., 2006; Wu et al., 2006; Denton et al., 2006; He et al., 2006; Estevez et al., 2004; Bennetts et al., 2005). Of

significance to our work, studies show that mutations to CBS2 impact gating (Yusef et al., 2006; Estevez et al., 2004; Wu et al., 2006) to a larger extent than do mutations to CBS1 (Estevez et al., 2004). Mutations in the cytoplasmic region outside the CBS domains also affect channel gating (Estevez et al., 2004; Hryciw et al., 1998; Schmidt-Rose and Jentsch, 1997; Wu et al., 2006; Hebeisen et al., 2004; He et al., 2006; Macias et al., 2007). The importance of CBS domain mutations is further underscored by the fact that human CBS mutations associated with myotonia (Lin et al., 2006) and kidney stones (Lloyd et al., 1997) also alter channel gating.

Like in many CLCs, CLH-3a's and CLH-3b's gating are regulated by their cytoplasmic regions. The splice variants have clearly different gating and localized sequence differences, as discussed earlier and in Figures 2 and 3. Of these sequence differences, our lab has found that the ones leading to the difference in gating are either in the CBS domains or in the large 160 amino acid extension following CBS2 in CLH-3b (He et al., 2006). Additionally, changes in the phosphorylation state of CLH-3b due to kinases and cell swelling regulate channel gating through an intracellular domain located between the CBS domains (Falin et al., 2009; Denton et al., 2005). While it is clearly demonstrated in CLCs that the cytoplasmic region, including CBS domains, regulate gating, as of yet there is no experimentally demonstrated mechanism for this regulation.

Dutzler and colleagues (Dutzler et al., 2002) have suggested just such a possible mechanism (Figure 7). The cytoplasmic region is connected to the membrane helix R, which is part of the channel pore and selectivity filter (Dutzler et al., 2002). Thus, the

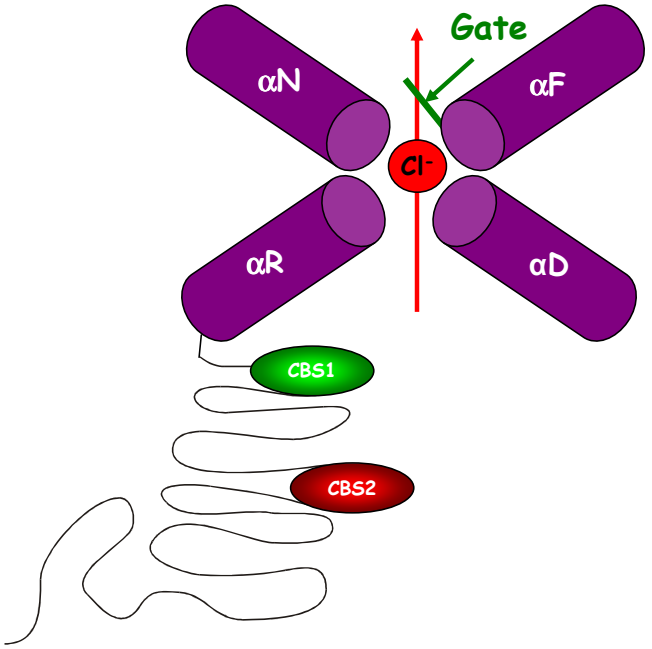

Figure 7: Proposed mechanism for regulation of gating by the cytoplasmic regions. αN, αF, αR, and αD are four membrane helices that make up the fast gate, selectivity filter, and channel pore. The cytoplasmic region, including Cystathionine-β-Synthase domains (CBS1 and CBS2), is connected to the channel pore through the R helix. Thus, the R helix may transmit a conformational change from the cytoplasmic region to the channel gate. As of yet, this hypothesized mechanism lacks direct proof.

mechanism is that Helix R provides a link to transmit a conformational change from the cytoplasmic region to the channel pore.

This hypothesized mechanism and information from crystal structures help explain the strong effect of CBS2 mutations on gating. Specifically, crystal structures show CBS2 is in proximity to the N-terminal portion of the cytoplasmic domain, which connects CBS1 to the R helix (Markovic and Dutzler, 2007; Meyer et al., 2007; Meyer

and Dutzler, 2006). Dutzler and colleagues (Meyer and Dutzler, 2006) proposed that this R helix-CBS1 connector, which we call the "R-Helix linker" may be important for transmitting conformational changes. This suggests a possible structural link between the CBS domains and the R Helix, which my thesis will explore.

Central question of thesis

The goal of my dissertation research is to address an important question in the CLC field: how do the CBS domains regulate CLC channel gating. The *C. elegans* splice variants, CLH-3a and CLH-3b offer unique advantages for understanding structure - function relationships, given their localized sequence differences and discrete differences in channel gating. This gating difference has been found to be due to the cytoplasmic region of the splice variants, which includes CBS domains.

I have tested the hypothesis that splice variation of the CBS domains regulates gating differences between CLH-3a and CLH-3b. My first aim was that this regulation was carried through the R Helix linker. I have approached this question using structural homology modeling, mutagenesis, and electrophysiological methods. My work is one of the first studies supporting the involvement of the R helix linker in regulation of CLC gating by CBS domains.

Mechanisms derived from the *C. elegans* CLCs are pertinent to mammalian CLCs since CLC and CBS domain structure is highly conserved. Thus, these studies shed light onto mechanisms of CBS domain regulation of gating in mammals and an

understanding of many human muscle, kidney, and bone diseases associated with mutations in CBS domains of CLCs (reviewed in: (Ignoul and Eggermont, 2005)). In short, this work has broad significance related to fundamental mechanisms of CLC biology and to human pathology.

CHAPTER II

HOMOLOGY MODEL OF CLH-3b PREDICTS AN INTERACTION OF THE R-HELIX LINKER AND α2 OF CBS2

Summary

Homology models allow one to hypothesize intra-protein interactions and thereby help elucidate mechanisms for regulation of protein function. We use homology modeling in order to understand mechanisms by which CBS domains alter CLC function. We developed homology models for the CBS domains of the splice variants CLH-3a and CLH-3b based upon the high resolution and high homology structure of CLC-Ka. Using Rosetta modeling, we predicted the structural difference between CLH-3a and CLH-3b CBS domains lies in the length of α2 of CBS2. In addition to affecting the length of α2, the splice variation of CLH-3b is predicted to alter interactions with the R-helix linker. The R-helix linker is a set of unstructured amino acids that connects the CBS domains to the pore-forming R-helix. Our model predicts a possible interaction of CLH-3b F559 in the R Helix linker with CLH-3b A836 in α2 of CBS2. A possible functional importance of A836 is consistent with results from calculations on the change in stability due to mutation of the splice variation. Further experimental studies are important to

experimentally test for the functional importance of the hypothesized α2 / R-helix linker interaction.

Introduction

Why use a homology model?

Homology modeling can provide a useful tool for structure function studies in the absence of a crystal structure of the protein of interest. Specifically, homology modeling allows one to develop a putative structure that is based upon the structure of a homologous protein. With this structure, one can postulate possible interactions within the protein that may be functionally important and, then, assess the functional effect of disrupting such interactions through mutagenesis.

Homology models of the cytoplasmic region of other CLCs have successfully identified mutations that affect channel function and shed light on CLC structure function. For instance, Estevez and colleagues used a homology model of CLC-1 CBS domains, based on IMPDH, to identify residues that have substantial impact on channel gating (Estevez et al., 2004). Martinez and colleagues used a homology model of CLC-Kb, based on the extremely closely related CLC-Ka, in order to determine the arrangement of cytoplasmic monomers in CLC-Kb (Martinez and Maduke, 2008). CLC mutations affecting channel ATP sensitivity have been determined using homology modeling combined with electrophysiology (De Angeli et al., 2009) and also modeling alongside computational ligand docking (Bennetts et al., 2005).

In the CLC I study, particularly CLH-3b, previous work in our lab (He et al., 2006) has suggested the CBS domains or the 160 C-terminal amino acids (Figure 2) are critical for normal channel gating. To understand how the CBS domains regulate gating, I have made a homology model of the CBS domains of CLH-3a and CLH-3b.

CLH-3a and CLH-3b are excellent candidates for homology modeling

Homology models are based on the crystal structure of a carefully chosen homologous protein called the template. Accuracy of the model depends upon the template's resolution and its percent homology with the modeled protein.

Three possible template structures for CLH-3b are the cytoplasmic regions of CLC-0 (Meyer and Dutzler, 2006), CLC-5 (Meyer et al., 2007), and CLC-Ka (Markovic and Dutzler, 2007). The percent homology with the modeled region of CLH-3b and the angstrom resolution of these templates are shown in the table below (Meyer and Dutzler, 2006; Meyer et al., 2007; Markovic and Dutzler, 2007). CLC-0 was crystallized as a cytoplasmic monomer (Meyer and Dutzler, 2006), while CLC-Ka and CLC-5 were crystallized in the native cytoplasmic dimeric state (Markovic and Dutzler, 2007; Meyer et al., 2007). CLC-Ka has made an excellent template choice for us, given its high resolution (1.6A) and high homology to CLH-3b (~50 %), and likely physiological dimeric structure (Markovic and Dutzler, 2007). Such high homology and high template resolution tend to yield accurate models.

Template	*% Homology to CLH-3b**	*Resolution (Å)*
CLC-0	57	3.1
CLC-Ka	48	1.6
CLC-5	44	2.3

*Calculated with Vector NTI (Lu and Moriyama, 2004)
Table 1: Percent homologies and resolution of templates. Table shows, for each possible template of homology model, percent homology with CLH-3b of CBS domains and crystal structure resolution.

Homology modeling: overview of procedure and theoretical basis.

Six general steps are used in homology modeling, as I discuss for our CLH-3b model. First, CLC-Ka was chosen as a template for reasons mentioned previously. Next, secondary structure prediction was done on the template and CLH-3b in the region modeled. Third, secondary structure predictions were used to align the sequence of CLH-3b and CLC-Ka. Fourth, the CLH-3b backbone model was predicted by replacing each amino acid in the template with its corresponding one from CLH-3b. Fifth, homology modeling software was used to predict the structure of regions of CLH-3b that did not correspond to any part of CLC-Ka. Finally, the side chain orientations were predicted.

The majority of programs we used to predict structures are based upon bioinformatics knowledge of all experimental structures. BCL::Align (Dong et al., 2008) alignment software incorporates three secondary structure prediction algorithms (Bradley et al., 2003; Meiler and Baker, 2003; Jones, 1999; McGuffin et al., 2000; Karplus et al., 1998). The software Modeller (Sali and Blundell, 1993) develops the backbone using "spatial restraints" from the template. Spatial restraints are limitations on parameters,

such as distances between adjacent atoms and dihedral angles, which are derived from values in the template (Sali and Blundell, 1993). Modeller predicts the structure of regions not aligned to amino acids in the template using theoretical physics principles as well as spatial restraints, this time based on many existing protein structures. The program SCWRL (Canutescu et al., 2003) predicts side chain conformation using knowledge of common conformations in experimental structures.

To test our modeling methods, a homology model of CLC-5 based on CLC-Ka (PDB Code: 2pfi) (Markovic and Dutzler, 2007) was generated and compared with the crystal structure of CLC-5 (PDB Code: 2j9l) (Meyer et al., 2007).

Predicting difference in structure between CLH-3a and CLH-3b: length of the α-helix 2

Using domain recognition software (Finn et al., 2006; Pagni et al., 2004; Quevillon et al., 2005), the CBS domains of CLH-3b were found to span amino acids 561 to 614 and 791 to 838. The homologous regions of CLH-3a are 632 to 685 and 761 to 808. The only difference in CBS domain sequence between CLH-3a and CLH-3b is the last six amino acids of CBS2. Three amino acids C-terminal to CBS2 are also distinct. Preliminary homology modeling suggested that part of these nine amino acids are in α2 of CBS2, and that α2 may be longer in CLH-3b than in CLH-3a. As such, Rosetta modeling software (Bradley et al., 2003) was used to predict fine differences between the length of α2 in the splice variants as well as various CLH-3b mutants. Specifically, we

had Rosetta predict, *de novo*, the structure of the splice variation using the remainder of the homology model as a fixed structural context.

Secondary structure prediction programs were not considered precise enough for such predictions of helix length for two main reasons. For one, the expected difference in helix lengths, based on preliminary modeling, were too fine for the accuracy of secondary structure predictions. Second, secondary structure prediction programs only incorporate sequence information, while the Rosetta modeling uses information about predicted tertiary structure of the surrounding protein for predictions.

Such *de novo* predictions with Rosetta can be used for prediction of entire protein structures, not just fragments. The usefulness of *de novo* predictions is highlighted by the fact that the majority of sequences do not have a homologous template. Additionally, the Protein Data Bank database of existing structures does not represent all theoretically possible conformations. *De novo* predictions can partially compensate for these difficulties.

To calculate structure *de novo*, Rosetta breaks the protein sequence into three or nine amino acid fragments and looks for the structure of the fragment in other existing proteins. The protein structure fragments are selected based upon sequence and secondary structure similarity with the predicted fragment and with amino acid in vicinity of the fragment. Three dimensional fit into the remainder of the protein is also considered. The fragments are assembled in various conformations, and a structure is chosen using three criteria, in this order: 1. Highly unfolded proteins are eliminated 2.

Low energy structures are selected 3. The most representative of the remaining structures is chosen (Rohl et al., 2004).

Predicted effects of mutation of the splice variation on CBS domain stability

We also did a computational screen for amino acids in the splice variation that may be critical for protein stability, and hence possibly protein function. Specifically, we had Rosetta predict the effect on stability of mutating each of the nine spliced amino acids, i.e., LRLAIEYLQ, in CLH-3b to all other amino acids. Such calculations were also done to compare the predicted stability of the CBS domains in CLH-3a vs. CLH-3b.

"Stability" of a protein is predicted by calculating the stored, i.e. potential, energy of the protein. Since potential energies are always relative, in protein biochemistry they are considered to be the energy of the native protein with respect to the unfolded polypeptide chain. This energy is compared for WT and mutant proteins in order to assess the effect of mutations on stability.

Potential energy of folding a protein is equal to the sum of potential energy of component non-covalent interactions and disulfide bonds. These interactions are, from strongest to weakest: disulfide bonds (70-100 kcal/mol), hydrogen bonds (2-5 kcal/mol), electrostatic forces between charges or dipoles (1-3 kcal/mol), and van der Waals, i.e. hydrophobic, forces (<1 kcal/mol) (Dill, 1990). The energies indicated are the energies stored in the interaction. Point mutations will change these interactions, eliminating some of these stored energy components, and forming new interactions which store

energy. Thus, for instance, a point mutation that disrupts just one hydrogen bond would be expected to change protein potential energy by ~2-5 kcal/mol.

The main force contributing to folding of a protein and to its stored energy is hydrophobic or van der Waals forces (Dill, 1990). This is consistent with the dramatic effect of solvents on protein stability. Hydrogen bonds are also essential for folding, since they compose secondary structure. There are two forms of electrostatic forces affecting stability: net charge on the entire protein, which tends to be destabilizing, and local electrostatic interactions, such as salt bridges, which stabilize a protein. Electrostatic forces are not predominant in proteins, and thus they are not believed to make a sizable contribution to protein stability (Dill, 1990).

In our study, estimations of change in stability of proteins were made by providing a structure, which was the CLH-3b homology model. In Rosetta's method, the program replaces amino acids as directed by the mutation and determines the new side chain orientations. For each new side chain, different conformations found in existing structures are tested, and the lowest energy conformation is chosen (Kaufmann et al., 2010).

There are numerous energy functions detailing methods to compute potential energy of folding. Rosetta has two types of energy functions for protein structure prediction, one is for preliminary calculations and the other refined (reviewed in: (Kaufmann et al., 2010)). The preliminary Rosetta function treats side chains as centroids and incorporates several factors: solvation, pairing of beta strands, charge and polar interactions, and steric clashes. Van der Waals repulsive forces are taken into

account by the steric clash term, which penalizes very short atomic distances. Van der Waals attractive forces are taken into account by modeling the protein's radius of gyration and using the premise that more compact proteins have larger attractive forces (Simons et al., 1997a). The refined function incorporates direct calculation of van der Waals forces, solvation, hydrogen bonding, electrostatic interactions, and internal free energy of amino acids. These two functions are used to choose the most favorable structure after mutation. The energy function used for calculating the energetic effects of mutations incorporates "implicit" solvation (solvent represented as a dielectric constant), van der Waals attractions and repulsions, hydrogen bonds, and charge-charge interaction (Kortemme and Baker, 2002). The functions described are largely knowledge based, meaning they derive from experimental information in known structures.

Methods

Homology model

A homology model for the CLH-3b cytoplasmic C-terminus was generated based on the crystal structure of the CLC-Ka C-terminus (PDB code 2pfi). BCL::Align software (Dong et al., 2008) was used to align amino acids 544 – 625 and 783-848 of CLH-3b with amino acids 542-681 of CLC-Ka. BCL::Align is based on a weighted sum of gap penalties, the chemical properties of amino acids, PAM (R.M.Schwartz and M.O.Dayhoff, 1978), BLOSUM (Henikoff and Henikoff, 1992) and PSI-Blast (Altschul et al., 1997) scoring matrices, and three different secondary structure prediction methods (Meiler and Baker, 2003; Jones, 1999; McGuffin et al., 2000; Karplus et al., 1998). The

alignment of the amino acids immediately C-terminal to CBS1 and N-Terminal to CBS2 were adjusted by hand in order to produce the alignment shown in Figure 8. Modeller software (Sali and Blundell, 1993) version 9.3 was used to develop 120 candidate structures for CLH-3b. The structure with the lowest predicted energy (i.e. most stable) was chosen and side chain orientations were determined using SCWRL 3.0 software (Canutescu et al., 2003). The model was refined by a 500 step minimization with AMBER 9 software (Woods and Case, 2005; Ponder and Case, 2003). The software was checked using the structure validation software Procheck (Laskowski et al., 1993), WhatIf (Vriend, 1990), and Harmony (Pugalenthi et al., 2006).

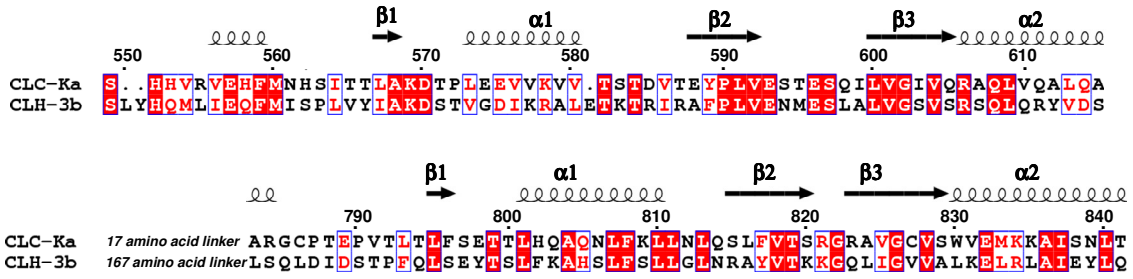

Figure 8: Amino acid alignment of CLC-Ka and CLH-3b used for developing C-terminus homology model. Secondary structure assignments and CBS domain locations are shown for CLC-Ka and are based on its crystal structure (Markovic et al., 2007). CLC-Ka CBS domain secondary structure is denoted β1–α1–β2–β3–α2. Amino acid numbering is based on CLH-3b sequence.

Homology models were made, by the same methods, based upon the crystal structures of ClC-0 and combined template structural information from both CLC-0 and

CLC-Ka. The resulting homology models had similar structure to the model based upon CLC-Ka (RMSD < 2 Å). The model based upon CLC-Ka was used for all future analysis and calculations. Parts of this CLC-Ka based model that were not consistent with the other two models were removed, to yield a model of the amino acids specified earlier (552-615 and 783-841 of CLH-3b). The same method and template was used to build a homology model of CLH-3a, covering amino acids 623-686 and 753-811 and a homology of separate CBS domains of CLC-5 (amino acids 588 to 657 and 678 to 743).

The homology model of CLH-3b was manually docked to CLC-ec1 (PDB code: 1ots) by optimizing 3-dimensional fit and electrostatic interactions.

Predicting difference in structure between CLH-3a and CLH-3b: length of α-helix 2

To estimate how splice variation or mutations affect α2 helical structure, we used Rosetta software (Simons et al., 1997b; Bonneau et al., 2002) and the homology model generated by Modeller and SCWRL. Calculations were done for the cytoplasmic region of CLH-3a (amino acids 623-686 and 753-811) and CLH-3b, CLH-3b A836D, CLH-3b L835DA836D, and CLH-3b L835KA836K (amino acids 549-615 and 783-841) and for the CBS2 domain of CLH-3a (amino acids 753 to 811) and CLH-3b (amino acids 783 to 841). Rosetta was used to develop de novo 3,000 or 20,000 candidate structures of amino acids 803-811 for CLH-3a and 833-841 for WT and mutated CLH-3b. We used a command of the format:

```
rosetta.gcc -series aa -protein CLH3  -chain A -relax -looprlx -s WTstructure.pdb
-loop_file regiontobuild.loops -loop_model -nstruct 3000  -ccd_closure -
loop_farlx -fast_loop_farlx -looprlx_fix_natsc
```

Rosetta calculations were done on proteins that include nine alternatively spliced residues: the six C-terminal residues of CBS2 and the three following residues. The structure of the remainder of the modeled region surrounding these nine amino acids was included for context and held in a fixed conformation. For each predicted structure, a script counted the number out of the nine spliced amino acids that were predicted to be helical. Then, another script counted the number of structures that had a certain number of predicted helical amino acids.

Predicted effects of mutation of the splice variation on CBS domain stability

The mutlist command was used to calculate the predicted change in stability, called $\Delta\Delta G_{mutation}$, due to mutation of the nine amino acid splice variation of CLH-3b (amino acids 833-841: LRLAIEYLQ) to all amino acids. I used a command of the format:

```
rosetta.gcc -interface -s CLH3.pdb -read_all_chains -mutlist
listofmutations.mutlist -intout resultfile.intout -repack_neighbors >& mutlist.log
```

Results

Homology model: Testing modeling methods

The separate homology models of CBS1 and CBS2 of CLC-5 were each structurally aligned to the experimental crystal structure of the corresponding regions of CLC-5 (PDB code: 2j9l). Both alignments produced RMSD < 2.5 Å (calculated with PYMOL, www.pymol.org), which is comparable to the resolution of CLC-5. This result gives an example of the accuracy of our modeling methods.

Homology model: Interactions between domains are conserved

The homology model of CLH-3b shows interfacing surfaces that are consistent with the CLC cytoplasmic region crystal structures. Specifically, in the CLH-3b model, the interface of cytoplasmic monomers is found to be at CBS2, in particular α1. Dutzler and colleagues (Marcovic, 2007) demonstrated that interaction of the two L650 of CLC-Ka monomers form part of the monomer-monomer interface. The homology model of CLH-3a and CLH-3b also suggests there is an interface between the two L780 and two L810, respectively, which are homologs of CLC-Ka L650. Thus, the monomer-monomer interface is likely to be conserved in CLH-3a and CLH-3b.

Interfaces within the cytoplasmic monomer are also maintained in the CLH-3b homology model. First, in many CBS domain containing proteins, CBS1 and CBS2 interact at β2 and β3. Second, Dutzler and colleagues demonstrate, in CLC cytoplasmic region structures, the N-terminus of the cytoplasmic region preceding CBS1 is in proximity to α2 of CBS2. These two arrangements are found in the CLH-3a and CLH-3b models.

Homology model predicts A836 in α2 of CBS2 interfaces with R-helix linker at F559

The homology model manually docked to the membrane region of CLC-ec1 (PDB code 1ots) is shown in Figure 9. The only difference in sequence of the CBS domains in CLH-3a vs. CLH-3b is splice variation of 9 amino acids in and following the C-terminus of CBS2. This homology model predicts that the splice variation is part of

α2 of CBS2 and includes amino acids C-terminal of α2. Since this is the only splice variation of CBS2, it is likely that these amino acids lead to differences in channel gating. Experimental studies to be discussed in chapter III confirm this is the case. Thus, I proceeded to analyze the model for interactions of this splice variation.

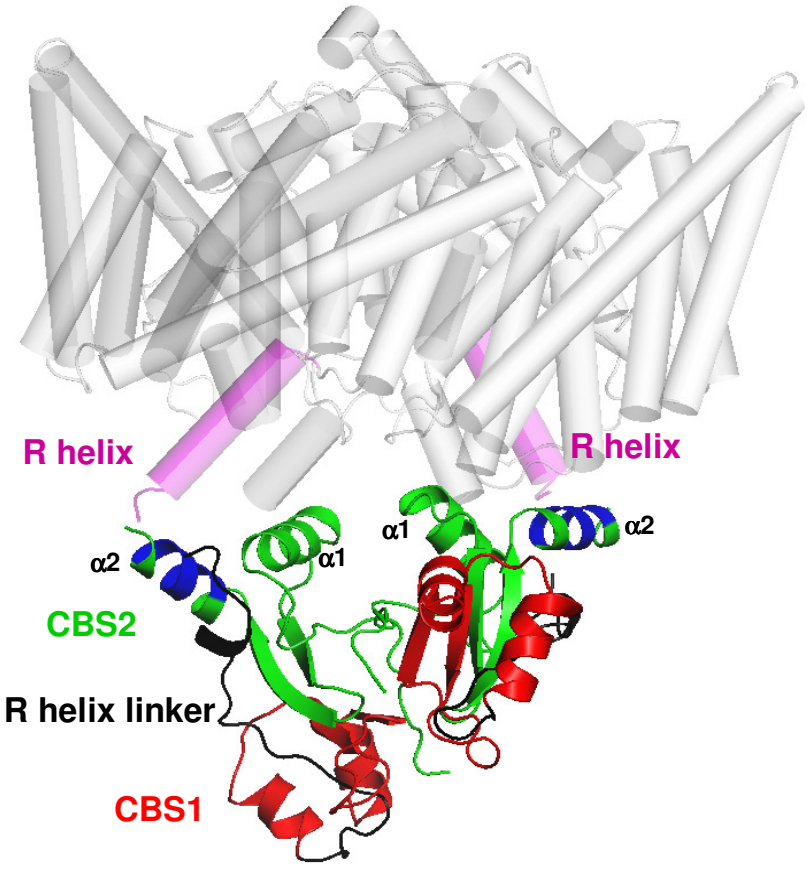

Figure 9: Ribbon diagram of CLH-3b C-terminus homology model. To provide context for the C-terminus structure, it is shown manually docked to the CLC-ec1 intramembrane region (gray and magenta; Protein Data Bank accession code 1OTS; (Dutzler et al., 2003). The R-helix of the intramembrane domain is shown in magenta and the cytoplasmic R-helix linker is shown in black. Each monomer of the cytoplasmic C-terminus dimer contains one CBS1 (red) and one CBS2 (green) domain. The six amino acid splice variation of CBS2 is shown in blue. The region (amino acids 616-782) between CBS1 and CBS2 is not modeled. Also not modeled are the first nine amino acids of the R helix linker.

Two observations are readily available, that lead to hypotheses. First, α2 may be interacting with the amino acids N-terminal of CBS1, known as the R Helix linker. The strongest predicted interaction of the R helix linker is at F559 interacting with A836 of α2 in CLH-3b (Figure 10A). The splice variation may be altering the conformation of the R helix linker, which then alters the conformation of the R helix, either by direct connection or further interactions.

Second, α2 may be interacting with α1, which in turn forms the monomer-monomer interface. An alteration of the monomer-monomer interface could lead to global changes in CLH-3a vs. CLH-3b structure, which could affect channel gating. While the model does predict an interaction of α1 with α2, splice variation of α2 is not predicted to change interactions at the monomer-monomer interface. Thus, this interaction was not pursued in further detail.

Predicting difference in structure between CLH-3a and CLH-3b: length of α-helix 2

Figure 11A shows a histogram of the predicted number of helical amino acids, of the nine, for WT CLH-3a and WT CLH-3b. Figure 11B shows a similar histogram for CLH-3b A836D, CLH-3b L835DA836D, and CLH-3b L835KA836K. The median number of helical amino acids, represented by the x-axis value at the peak of the histogram, is the most commonly found number of helical amino acids. This value is 5 for CLH-3a, 7 for CLH-3b, and 8 for all the CLH-3b mutants CLH-3b A836D, CLH-3b L835DA836D, and CLH-3b L835KA836K. This indicates that mutants expected to

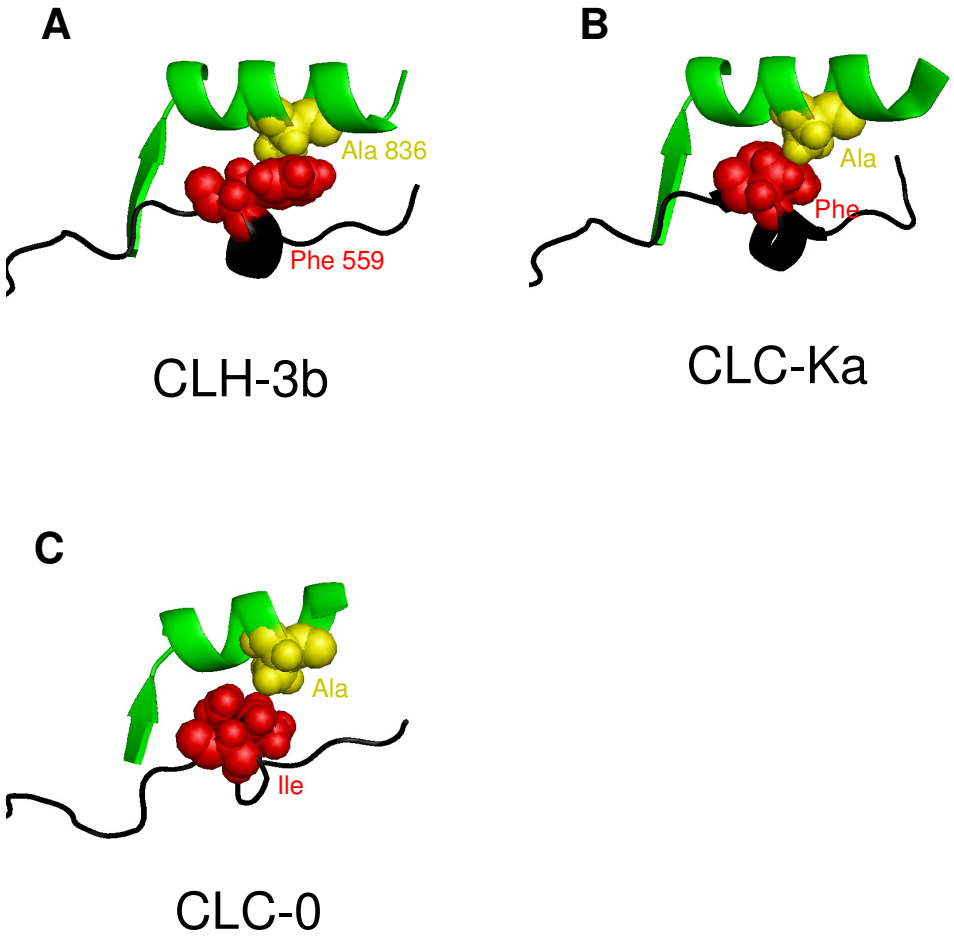

Figure 10: The CLH-3b F559 of the R helix linker (black) postulated interface with A836 of α2 (green) is conserved in crystal structures of CLC-0 and CLC-Ka. A. CLH-3b F559(red) is predicted to interface with CLH-3b A836 (yellow). B. The CLC-Ka homolog of CLH-3b F559, also a Phenylalanine (red), interfaces with an Alanine (yellow) homologous to CLH-3b A836. C. The CLC-0 homolog of CLH-3b F559, a similarly hydrophobic and bulky Isoleucine (red) interfaces with an Alanine (yellow) homologous to CLH-3b A836.

A

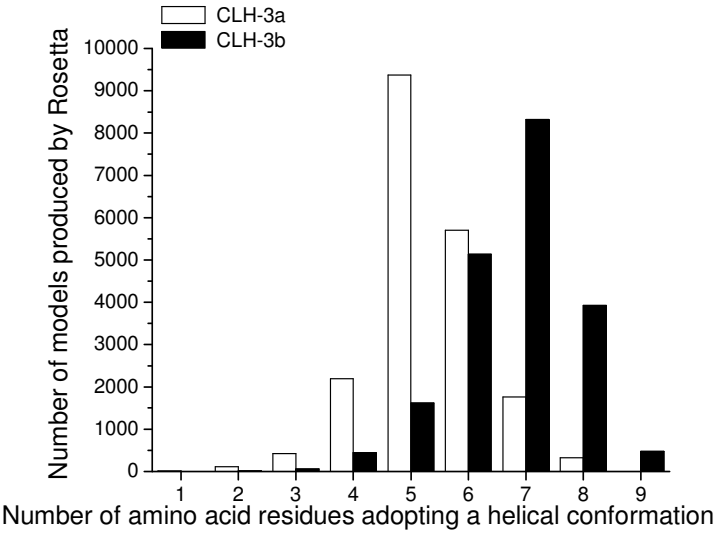

CLH-3a:	V	C	F	L	I	S	R	K	K
CLH-3b:	L	R	L	A	I	E	Y	L	Q

B

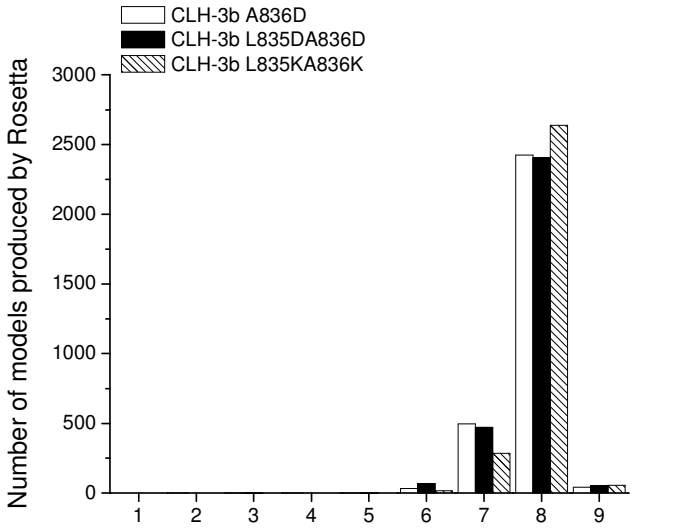

CLH-3bA836D:	L	R	L	D	I	E	Y	L	Q
CLH-3bL835DA836D:	L	R	D	D	I	E	Y	L	Q
CLH-3bL835KA836K:	L	R	K	K	I	E	Y	L	Q

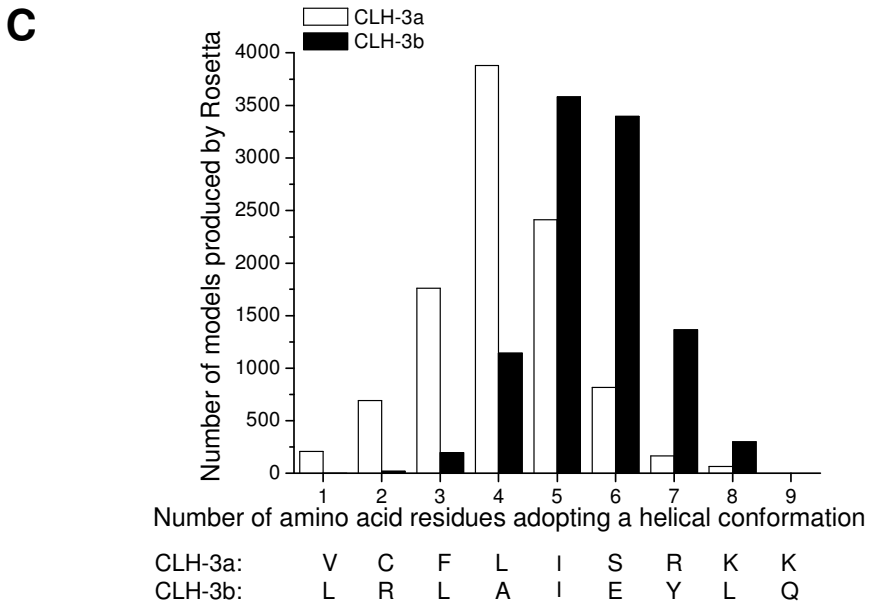

Figure 11: Rosetta modeling of amino acids comprising the splice variation of CBS2 in CLH-3a, CLH-3b and three mutants. Sequence of the nine amino acids modeled are shown at the bottom of the graph. The graph shows the number of amino acids adopting a helical conformation and the number of Rosetta models that predicted that structure. The peak of the histogram corresponds to the median number of amino acids of the splice variation that are predicted to adopt a helical conformation. Either the cytoplasmic monomer or just CBS2 was held in a fixed conformation and included in predictions to provide a structural context. A. CLH-3b is predicted to be 2 amino acids longer than CLH-3a using the cytoplasmic monomer as a structural context. Among the 20,000 models generated, the median number of helical amino acids in CLH-3a and CLH-3b are five and seven. B. CLH-3b A836D, CLH-3b L835DA836D and CLH-3b L835KA836K all have a median of 8 amino acids predicted to be helical, which is comparable or longer than that of WT CLH-3b. 3,000 models totally were generated. C. CLH-3b is predicted to be 2 amino acids longer than CLH-3a using CBS2 alone as a structural context. Among the 10,000 models totally generated, the median number of helical amino acids in CLH-3a and CLH-3b are four and six.

disrupt the postulated interactions between A836 and F559 are not expected to shorten the helix.

Initially, such calculations were done using only CBS2 as a structural context (Figure 11C). Rosetta predicts the median number of amino acids predicted to adopt a helical conformation is 4 for CLH-3a and 5-6 for CLH-3b, which is one amino acid shorter than the predictions using the entire cytoplasmic monomer.

Predicted effects of mutation of the splice variation on CBS domain stability

Stability of a protein is measured as the overall potential energy of folding the protein. The effect of a mutation on protein stability is measured by the change in potential energy from WT to a mutant, referred to as $\Delta\Delta G_{mutation}$. Table 2 shows these values for mutating each of the splice variation amino acids of CLH-3b (shown horizontally) to all other amino acids (shown vertically). A negative value for $\Delta\Delta G$ indicates that a mutant is predicted to be more stable than WT, while a positive value indicates that a mutant is predicted to be less stable than WT.

Figure 12A shows a plot of the values in Table 2. The original amino acid of the mutation is shown by a given symbol, while the resulting amino acid of the mutation is shown along the horizontal axis. The first observation is that the most destabilizing predicted mutations result in energy changes of 15-60 kcal/mole. These values arise from L883Y and mutation of A836 to the bulky amino acids: Phenylalanine (F), Histidine (H), Tryptophan, (W), or Tyrosine (Y). These mutations disrupt and form van der Waals

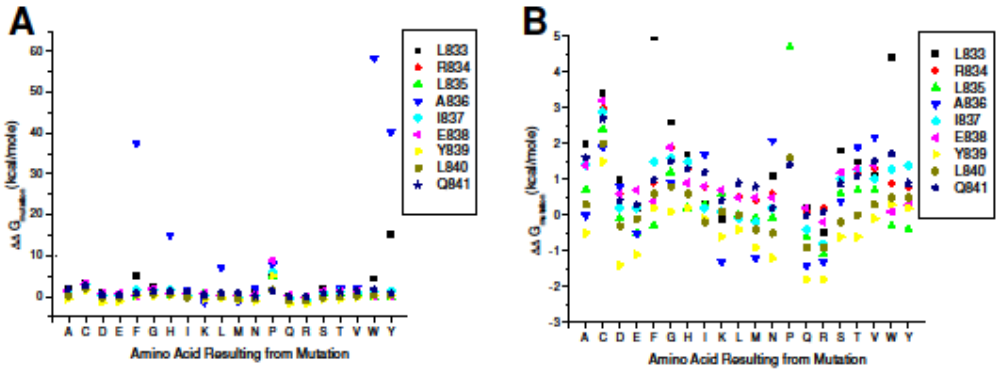

Figure 12: Predictions of change in stability of CLH-3b due to mutation of the CBS2 splice variation. A. Plot of change in predicted stability ($\Delta\Delta G_{mutation}$) due to mutation of each amino acid of the splice variation. Each series corresponds to an amino acid of the splice variation, from CLH-3b L833 to CLH-3b Q841. B. Same data plot highlighting $\Delta\Delta G_{mutation}$ values closer to the expected range.

	Splice variation amino acid								
Mutate To	L	R	L	A	I	E	Y	L	Q
A	2	1.4	0.7	0	1.4	1.4	-0.5	0.3	1.6
C	3.4	3	2.4	1.9	2.9	3.2	1.5	2	2.7
D	1	0.6	-0.1	0.8	0.2	0.6	-1.4	-0.3	0.4
E	0.2	0.2	-0.5	-0.5	0.2	0.7	-1.1	-0.1	0.3
F	5	0.9	-0.3	**37.6**	1.5	0.4	0.2	0.6	1
G	2.6	1.9	1.2	0.9	1.6	1.9	0.1	0.8	1.5
H	1.7	1.3	0.2	**15.1**	1.5	0.9	0.2	0.6	1.3
I	0.3	0.8	0.3	1.7	0.2	0.8	-0.1	-0.2	1.2
K	-0.1	0.6	0.6	-1.3	0.1	0.7	-0.6	0.1	0.4
L	0	0.5	0	7.25	-0.1	0.5	-0.4	0	0.9
M	-0.4	0.4	-0.1	-1.2	-0.2	0.5	-0.9	-0.4	0.8
N	1.1	0.6	-0.1	2.1	0.2	0.5	-1.2	-0.5	0.2
P	5.3	8.3	4.7	7.9	6	8.9	5.1	1.6	1.4
Q	0.2	0.1	-0.6	-1.4	-0.4	0.2	-1.8	-0.9	0
R	-0.5	0.2	-1.1	-1.3	-0.8	-0.2	-1.8	-0.9	0.1
S	1.8	1.2	0.6	0.4	1	1.2	-0.6	-0.2	0.9
T	1.5	1.2	0.7	1.9	1.3	1.3	-0.6	0	1.1
V	1.1	1.3	0.7	2.2	1	1.4	-0.1	0.3	1.5
W	4.4	0.9	-0.3	**58.4**	1.3	0.1	0.3	0.5	1.7
Y	**15.3**	0.8	-0.4	**40.4**	1.4	0.3	0.2	0.5	0.9

Table 2: Value of the predicted change in stability, $\Delta\Delta G_{mutation}$ due to mutation of each amino acid of the splice variation (from L833 to Q841) to all other amino acids. Negative values indicate predicted stabilization, while positive values indicate predicted destabilization. Bold indicates values greater than 15 kcal/mole.

(hydrophobic) interactions, which typically have energies of < 1 kcal/mol, as mentioned earlier. This raises doubt to the accuracy of the values predicted above ~10 kcal/mole.

The same plot is shown in Figure 12B, expanded to show the lower magnitude energy changes. This graph shows mutation of Y839 usually stabilizes the protein, as indicated by a negative $\Delta\Delta G_{mutation}$. Mutation of E838 has little effect on protein stability, which concords with its predicted facing of the cytoplasm in the homology model. Mutation of amino acids in the splice variation to proline is predicted to have a high destabilizing effect, which can be expected since prolines tend to introduce kinks in protein structure. Nonetheless, this analysis does not clearly suggest any amino acids that may be more likely to be important for maintaining proper structure.

Additionally, the effect on stability was calculated for mutating the entire CLH-3b splice variations, LRLAEIYLQ, to the sequence of CLH-3a, LRLAIEYLQ. This resulted in a $\Delta\Delta G_{mutation}$ of 10.9, indicating that CLH-3a is predicted to be less stable than CLH-3b.

Discussion

CBS domain quaternary structure in CLCs

CBS domain secondary structure is highly conserved and consists of two α-helices and three β-strands arranged as β1-α1-β2-β3-α2. CBS motifs are typically present in proteins as two or, as in CLCs, four copies. Pairs of CBS motifs associate to form a dimeric structure known as a Bateman module or domain (e.g., Adams et al., 2004; Kemp, 2004; Rudolph et al., 2007). The monomer-monomer interface between two CBS

motifs occurs at β-sheets formed by β-strands 2 and 3 (e.g., Hattori et al., 2007; Markovic et al., 2007; Meyer et al., 2007; Meyer et al., 2006; Miller et al., 2004; Rudolph et al., 2007; Zhang et al., 1999).

CBS dimers also interact to form oligomeric structures. The interface between Bateman domains is formed by the α-helices of CBS motifs in a head-to-tail or head-to-head arrangement (e.g., Hattori et al., 2007; Miller et al., 2004; Rudolph et al., 2007; Townley and Shapiro, 2007). Meyer and Dutzler (Meyer et al., 2006) postulated a head-to-tail interaction between Bateman domains of the ClC-0 cytoplasmic C-termini (i.e., CBS1 of one Bateman domain interacts with CBS2 of the second domain). However, X-ray crystallography studies on dimers of ClC-5 and CLC-Ka cytoplasmic C-termini revealed a novel interface formed by the CBS2 motifs of each C-terminal monomer (Markovic et al., 2007; Meyer et al., 2007). This "tail-to-tail" arrangement of Bateman domains is shown in the CLH-3b homology model in Figure 9.

Homology model

A central question in the CLC field is how the structure of the cytoplasmic region regulates channel or transporter function. Dutzler et al. (Dutzler et al., 2002) have suggested that the direct connection between the R-helix and the large cytoplasmic C-terminus of eukaryotic CLCs could play a critical regulatory role. The R Helix is connected to the cytoplasmic CBS domains via the R helix linker. The proximity of CBS2 to the R Helix linker concurs with the larger effect on channel gating of mutation of CBS2, as compared to CBS1 (Estevez et al., 2004).

Despite significant differences in primary sequence, the R-helix linkers of ClC-0, CLC-5 and CLC-Ka have similar and well-ordered crystal structures, except for the first approximately 10 residues (Markovic and Dutzler, 2007; Meyer et al., 2007; Meyer and Dutzler, 2006). α2 of CBS2 lies close to the R-helix linker in crystal structures of CLC-0, CLC-5 and CLC-Ka (Markovic and Dutzler, 2007; Meyer et al., 2007; Meyer and Dutzler, 2006). Thus, the R Helix linker may transmit conformational changes from α2 of CBS2 to the R Helix, and ultimately the channel gate.

Our homology model suggests that F559 of the R helix linker could interact with A836 of α2, and this interaction could be altered due to splice variation. Figure 10 shows that this potential A836-F559 interaction is conserved in crystal structures of CLC-0 and CLC-Ka, which are both in the same subfamily of CLCs as the ortholog of CLH-3b, CLC-2. Analysis of sequences reveals that F559 is conserved as a bulky hydrophobic amino acid, specifically Phenylalanine, Isoleucine or Valine, in each family member of human CLCs. A836, too, is conserved in members of each CLC channel type (CLC-0 to –2, -Ka and -Kb), but not in CLC transporters.

Predicting difference in structure between CLH-3a and CLH-3b: length of α-helix 2

Modeling methods also suggested that the splice variation is expected to form part of α2, and also include uncoiled amino acids C-terminal of α2. Comparing the predicted structure of the splice variants, α2 of CLH-3a is predicted to be 1-2 amino acids (half a turn) shorter than α2 of CLH-3b. This uncoiling of α2 in CLH-3a may lead to disruptions

of interactions with the R Helix linker, which in turn can affect conformation at the channel gate.

Similar helix length calculations were done for mutations expected to disrupt the postulated A836-F559 interaction, which are CLH-3b A836D, CLH-3b L835DA836D, and CLH-3b L835KA836K. The double mutants were chosen because of the possibility of L835 being involved in the putative interaction. All these mutants show a predicted median helix length of 8 amino acids (Figure 11), comparable to the 7 amino acid predicted median helix length of CLH-3b. This suggests that uncoiling of the α2 helix via splice variation and disruption of the possible A836-F559 interaction could be separate contributors to the difference in gating between CLH-3a and CLH-3b. One or both of these structural elements may be necessary for the difference in channel gating. Determining mutations that preserve this A836-F559 interaction, yet are still expected to shorten the helix length could provide interesting insights. Experimental data, which will be discussed in chapter III, however, is the ultimate determinant of which structural differences between the splice variants regulate channel gating.

One should note that, when predicting helix length, we observed a longer helix length prediction when the entire cytoplasmic monomer is used as a structural context, as opposed to just CBS2 (Figure 11A and 11C). This observation implies that inclusion of the rest of the monomer, i.e. the R helix linker and CBS1, is predicted to impact the helix length. This concurs with the hypothesized interaction between α2 and the R helix linker. Specifically, if there was an interaction, it is possible that the R-Helix linker structure can affect the coiling of α2.

Predicted effects of mutation of the splice variation on CBS domain stability

Theoretical calculations were performed predicting the effect of mutations to the splice variation on stability of the CBS domain complex. Mutating A836 to bulky amino acids, such as Phenylalanine, Histidine, Tryptophan, or Tyrosine, led to unreasonably high predictions of destabilizing energy values. These values, above 15 kcal/mole, are over ten fold greater than typical energy values for hydrophobic interactions. Such non-physiologically high predicted energy values can arise from extreme proximity of atoms or clashes. This rise in energy is due to repulsion of atoms, as predicted by the Lennard-Jones function (Lennard-Jones, 1924).

Of importance, these energy calculations in Rosetta require the backbone to be in a fixed position, which can lead to the clashes upon mutation and result in the unduly high predicted energies. Thus, there are two indirect inferences from these predictions. First, the backbone conformation may need to change to avoid clashes when A836 is mutated to a bulky hydrophobic amino acid. Second, A836 is likely forming a tightly packed interface with other residues. The second inference is consistent with the predicted A836-F559 interface from analysis of the homology model. These predictions also provide reasons to test the physiological effects of mutating A836.

The entire CLH-3b splice variations, LRLAIEYLQ, was found to be more stable than that of CLH-3a, VCFLISRKK, with $\Delta\Delta G$ between them of 10.9 kcal/mole. The implications of such a calculation, however, should be interpreted with caution. This is because such calculations are prone to error when predicting stability changes for multiple simultaneous mutations at adjacent positions. This possible error results from

the fact that Rosetta must calculate the new structure at the sites of mutations. With adjacent mutations, Rosetta does not have as complete a structure of the region surrounding the point of mutation, and as such, cannot calculate as accurate a new structure.

Several further prediction and experiments are useful for a more accurate assessment of the effects of mutations on protein stability. First, similar energy calculations should be done while permitting local backbone movement. Such a procedure would involve homology modeling or *de novo* building around the site of mutation and would be much more computationally expensive. Second, to reduce calculations errors, one should start with a structure where the side chains have been minimized by Rosetta as opposed to what we used, Modeller and SCWRL.

Third, "mutant cycle analysis" (Gleitsman et al., 2009; Schreiber and Fersht, 1995) using electrophysiology and/or stability calculations can test for the predicted interaction. Specifically, if two residues interface, mutating both residues simultaneously should have a non-additive effect on function or stability. Given that CLH-3b gating tends to be discrete, this method may not be as useful by assaying function. Using predictions of stability this method could easily be used to computationally test for the predicted A836-F559 interface. These calculations, however, are somewhat redundant with analysis of the model for the purpose of predicting interfaces. Nonetheless, such calculations on A836 and F559 could aid in choosing residues to mutate to in order to disrupt or recreate the predicted interface**.** Ultimately, the meaning of all these

predictions of effects of mutations on stability can be put into perspective with electrophysiological studies of mutants.

Closing Remarks

In conclusion, our modeling allows us hypothesize that **the differences in channel gating between CLH-3a and CLH-3b are mediated via possible interactions of the splice variation with the R-Helix linker**. In particular, this interaction is hypothesized to occur between A836 of the splice variation and F559 of the R Helix linker. Our modeling also suggests that the CBS domains of CLH-3a may be less stable than those of CLH-3b. These possibilities will be explored via electrophysiology and mutagenesis, described in chapter III.

CHAPTER III

UNIQUE GATING PROPERTIES OF *C. ELEGANS* CLC ANION CHANNEL SPLICE VARIANTS ARE DETERMINED BY ALTERED CBS DOMAIN CONFORMATION AND THE R-HELIX LINKER

Summary

All eukaryotic and some prokaryotic CLC anion channels and transporters have extensive cytoplasmic C-termini containing two cystathionine-β-synthase (CBS) domains. CBS domain secondary structure is highly conserved and consists of two α-helices and three β-strands arranged as β1-α1-β2-β3-α2. Mutations in CLC CBS domains give rise to muscle and bone disease and alter CLC gating. However, the precise functional roles of CBS domains and the structural bases by which they regulate CLC function are poorly understood. CLH-3a and CLH-3b are *C. elegans* CLC anion channel splice variants with strikingly different biophysical properties. Splice variation occurs at cytoplasmic N- and C-termini and includes several amino acids that form α2 of the second CBS domain (CBS2). We demonstrate that interchanging α2 between CLH-3a and CLH-3b interchanges their gating properties. The R-helix of CLC proteins forms part of the ion conducting pore and selectivity filter and is connected to the cytoplasmic C-terminus via a short stretch of cytoplasmic amino acids termed the R-helix linker. C-terminus conformation changes could cause R-helix structural rearrangements via this

linker. Crystal structures of cytoplasmic domains of three CLC proteins suggest that α2 of CBS2 interacts with the R-helix linker. We found that mutating predicted α2 and R-helix linker interacting amino acids in CLH-3b was sufficient to give rise to CLH-3a-like gating. We postulate that the R-helix linker via its interaction with CBS2 provides a pathway by which cytoplasmic C-terminus conformational changes induce conformational changes in membrane domains that in turn modulate CLC function.

Introduction

The structural bases by which the cytoplasmic C-terminus controls CLC gating and activity are poorly understood. We have exploited the distinct functional differences of the splice variants CLH-3a and CLH-3b to address this question. The discrete sequence differences due to splice variation and the clear functional differences make the channels an excellent model system for structure-function studies (see chapter I). Moreover, previous studies show mutations in CLH-3a or CLH-3b did not yield novel or intermediate gating (He et al., 2006; Denton et al., 2006). To summarize gating differences, CLH-3a has a more negative activation voltage, a slower opening kinetics, is sensitive to depolarized holding potentials, and has increased sensitivity to pH and Cl^- (Figure 3). Work in our lab over the past several years has set a foundation for detailed structure function analysis of CLCs, using the model system of CLH-3a and CLH-3b.

The *C. elegans* gene knockout project generated a worm strain, ok768, containing a *clh-3* deletion mutation. This mutation removes the 101 amino acid splice insert unique

to CLH-3b and an additional 64 upstream amino acids shared by both channels (Figure 2 and 13). Eleven of these amino acids are located at the end of CBS1 (Figure 13). The

Figure 13. Sequence of predicted intracellular N- and C-termini of CLH-3a and CLH-3b. Intramembrane domains have identical sequence and are omitted for clarity. Double vertical lines indicate start of intramembrane sequence, which ends at residues 613 for CLH-3a and 542 for CLH-3b. Splice variations in CLH-3a and CLH-3b are highlighted in yellow and green, respectively. Location of CBS domains were predicted using the domain recognition programs PFAM (Finn *et al.*, 2006), InterProScan (Zdobnov et al., 2001) and MyHits (Pagni *et al.*, 2004) and are outlined with boxes.

mutant channel exhibits voltage-dependent gating and pH and Cl^- sensitivity that resemble CLH-3a (Denton et al., 2006). This mutant also virtually abolishes channel sensitivity to cell swelling. Thus, these sets of deleted amino acids induce CLH-3a like gating in CLH-3b and regulate volume sensitivity of CLH-3b.

Deletion of the 101 amino acids (amino acids 668-768), alone, did not affect sensitivity to depolarized voltages, pH or Cl^-. Deletion of the 101 amino acids, however, did shift the activation voltage to ~-65mV and slowed current activation kinetics (He et al., 2006), as seen in CLH-3a and in CLH-3b phosphorylated by GCK-3 (Denton et al., 2005). Recent studies have identified GCK-3 phosphorylation sites within these 101 amino acids (Falin et al., 2009).

Deletion of the 11 CBS1 amino acids alone, CLH-3bΔ604-614, in the mutant worm strain induced CLH-3a like gating. Specifically, gating refers to CLH-3a like activation voltage, kinetics, and sensitivity to pH, Cl^-, and depolarizing holding potentials. Deletion of the remaining 53 of the 64 amino acids largely retained CLH-3b like gating (He et al., 2006). Thus, it was hypothesized that CBS domain configuration regulated difference in gating between CLH-3a and CLH-3b. Nonetheless, these 11 amino acids in CBS1 are identical in the channels, so some other sequence difference must also be contributing to the difference in gating.

Major differences in CLH-3a and CLH-3b sequence (Figure 2 and 13) are an N terminal addition in CLH-3a, a 160 C-Terminal extension in CLH-3b, and the insertion of 101 aforementioned amino acids. The last nine amino acids of CLH-3a, including part of CBS2, are also alternatively spliced compared to their CLH-3b homologs. Neither deleting the 71 amino acids in CLH-3a, nor adding them onto the N-terminus of CLH-3b, affected gating of either channel. As mentioned, the 101 amino acids do not regulate gating differences between CLH-3a and CLH-3b. Deletion of the C-terminal extension, plus the preceding 9 spliced amino acids (CLH-3b Δ833-1001) did induce CLH-3a like

gating in CLH-3b. Thus, gating difference between CLH-3a in CLH-3b were known to be regulated through CBS1, the 9 amino acids splice variation that includes the C-terminus of CBS2, and/or the 160 amino acid extension.

The fact that deleting non-spliced amino acids of CBS1 affected gating led us to hypothesize that proper overall CBS domain configuration is essential for normal channel gating. I proceeded to test this hypothesis by making mutations in CBS2 of CLH-3b, as well as both CBS domains of CLH-3a. This hypothesis concords with the known interaction of CBS1 with CBS2, shown in CLC cytoplasmic region crystal structures (Markovic and Dutzler, 2007; Meyer et al., 2007; Meyer and Dutzler, 2006), as well the importance of CBS domains in regulating channel gating (Bennetts et al., 2007; Yusef et al., 2006; Lin et al., 2006; Wu et al., 2006; Estevez et al., 2004; Denton et al., 2006; He et al., 2006; Bennetts et al., 2005).

In this study, we make use of our homology model (Figure 9) and mutagenesis to further characterize the role of C-terminus splice variation in regulating CLH-3b gating. This nine amino acid splice variation of CLH-3a and CLH-3b includes the second α-helix (α2) of the second CBS domain (CBS2) (Figure 11A). Our results show that interchanging α2 between the two channels interchanges their gating properties.

Homology modeling (chapter II) suggests that α2 may interact with a short stretch of amino acids, termed the R-helix linker, which connects the membrane helix R to the intracellular C-terminus (Figures 9 and 10A). Dutzler and colleagues (Dutzler et al., 2002) have first suggested that the R-helix could provide a pathway by which conformational changes in intracellular domains regulate channel/transporter function

(Figure 7). Consistent with this model, we found that mutating predicted interacting amino acids in α2 and the R-helix linker of CLH-3b was sufficient to give rise to CLH-3a-like gating. Our studies provide novel insights into the role of CBS domains, the R-helix linker and cytoplasmic C-terminus conformational changes in regulating CLC gating properties.

Material And Methods

Transfection and Whole Cell Patch clamp Recording

HEK293 (human embryonic kidney) cells were cultured in 35 mm diameter tissue culture plates in "complete MEM media", which consisted of Eagle's minimal essential medium (MEM; Gibco, Gaithersburg, MD) containing 10% fetal bovine serum (Hyclone Laboratories, Inc., Logan, UT), non-essential amino acids, sodium pyruvate, 50 U/ml penicillin and 50 μg/ml streptomycin. Cells were plated at 200K-500K cells/dish. One to three days later, after reaching 50-70% confluency, cells were transfected using FuGENE 6 (Roche Diagnostics Corporation, Indianapolis, IN) with 1 μg GFP and 1-8 μg of channel cDNAs ligated into pcDNA3.1. Typically, 5μg channel DNA was used, with the following exceptions: 3bΔ842-1001 (8 μg), CLH-3b834-1001 (3μg) cotransfected with CLH-3b Δ834-1001 (4ug), CLH-3a + YLQ (8μg), CLH-3bΔ661-1001 cotransfected with CLH-3b 661-1001 (3 μg each), CLH-3b H552D (1μg), and CLH-3b A836K (1-2 μg). A ratio of 3 μL FuGENE to 1μg DNA was used for transfection.

Mutagenesis

Channel point mutants were generated using a QuikChange Site-Directed Mutagenesis Kit (Stratagene, La Jolla, CA). Stratagene's QuikChange II XL site-directed mutagenesis kit was necessary for mutations to the R Helix linker of CLH-3b (amino acids 544 to 562). Carbamicine plates were made at 100 mg/mL. All point mutation primers were designed using Stratagene's online automatic primer design program.

Deletion mutagenesis was done using PCR fusion based strategies, except for CLH-3aΔ792-808. Specifically, fragments (designated AB and CD) of the channel encoding DNA on either end of the deletion were amplified. For each fragment, primers on the side of the deletion contained short stretches of DNA that pair with the other side of the deletion. The two PCR fragment products (AB and CD) were used as a template for a third PCR, containing primers spanning the whole insert (designated AD). Then, the insert was ligated into the PC DNA 3.1+ vector. Positive ligations were identified using DNA sequencing or restriction enzyme based PCR screens.

CLH-3aΔ792-808 was made using the Stratagene's QuickChange Site-Directed Mutagenesis Kit (Stratagene, La Jolla, CA). There are only three amino acids, RKK, remaining in CLH-3aΔ792-808 after the point of deletion. Thus, the mutant was made by substituting the first four amino acids of the deletion with RKK, followed by a stop codon. The following table shows primers used for the three deletions mutants.

Split channels were made by introducing stop codons with the Stratagene kit for the first half and by performing PCR over the second half. Restriction enzymes sites

were incorporated into the PCR primers for the second half, and these were used to ligate into the vector DNA. Positive ligations were identified using a PCR screen.

Mutant	Sequence
CLH-3bΔ822-838 AB	F:GTTAAGCTTGGTACCGCATGGGTATTGGTACAAAAATATTATC R:GCACTTTTCCAGATTGTAAATATTTTTTCGTCACGTATGCACG
CLH-3bΔ822-838 CD	F:TATTTACAATCTGGAAAAGTGC R:CTAGACTCGAGCGGCCGCTCAGAATTTTTCGTCATGAACG
CLH-3bΔ822-838 AD	F:GCTTGGTACCGCATGGGTATTGGTACAAAAATATTATC R:CGTTCATGACGAAAAATTCTGAGCGGCCGCTCG
CLH-3aΔ792-808	F:TCTCACTTCTTGGTCTAAATCGTGCATACGTGACGAAAAAACGGAAAAAGTAGGGCGTTGTCGCATTAAAAGAG
CLH-3aΔ675-685 AB	F:GGCTTATCGAAATTAATACGACTCACTATAGGGAGACCCAA R: CGGGCTTTTGTTCCAATTTGAGACGAACCGACAAGAGCTA
CLH-3aΔ675-685 CD	F:TCTCAAATTGGAACAAAAGC R:GGGTTAGGGATAGGCTTACC
CLH-3aΔ675-685 AD	F:CGAAATTAATACGACTCACTATAGG R:ATGGCTTACCTTCGAACCG

Table 3: Primers used for deletion mutants. Forward (F) and reverse (R) listed, 5' to 3'.

All mutants were confirmed by DNA sequencing.

All channel plasmids were grown via transformation in Stable 2 E. Coli. 5-10 pg DNA were transformed into 100 μL stable 2 and heat shocked at 42 deg C for 25 seconds. Subsequently, they were placed on ice for ~2 minutes, and then 900 uL S.O.C. medium was added. This 1mL mixture was incubated for 90 minutes at 30 deg C,

shaking at 225 RPM. After that, 900 uL of the mixture was added to 40-50 mL Terrific Broth with 100mg/mL Carbamicine, and grown for 26-40 hours at 30 degrees. Qiagen MIDI preps were used to isolate plasmid DNA.

GFP was grown via transformation into DH5α *E. coli*. 0.5uL DNA was transformed into 50 uL DH5a and heat shocked at 42 deg C for 45 seconds. Subsequently, the transformation was placed on ice for ~2 minutes, and 900 uL S.OC. medium was added. This mixture was plated on 50mg Carbamicine/mL LB plates and grown overnight for ~ 16 hrs at 37 deg C. The next day, one colony was picked and grown in 40-50 mL LB with NaCl. DNA was purified using a Qiagen MIDI prep.

Voltage clamp electrophysiology preparation

All experiments were performed on at least two independently transfected groups of cells. Following transfection, cells were incubated at 37ºC for 24-30 hours. Cover slips were coated with poly-L-lysine for at least 25 minutes, and then the poly-L-lysine was rinsed off three times with sterilized water. Approximately 2 h prior to patch clamp experiments, cells were detached from growth plates by exposure to 0.25% trypsin containing 1 mM EDTA (Gibco) for 45 sec. Detached cells were suspended in complete MEM media, centrifuged, resuspended in fresh media, and then plated onto the poly-L-lysine coated cover slips. Approximately 1 hour after plating, 2 mL complete MEM media was pippetted onto the cells, and the cells incubated with media for at least one hour. Plated cover slips were placed in a bath chamber mounted onto the stage of an

inverted microscope. Cells were visualized by fluorescence and differential interference contrast microscopy.

Transfected cells were identified by GFP fluorescence and patch clamped using a bath solution that contained 90 mM NMDG-Cl, 5 mM $MgSO_4$, 1 mM $CaCl_2$, 12 mM Hepes free acid, 8 mM Tris, 5 mM glucose, 80 mM sucrose and 2 mM glutamine and was titrated to pH 7.4 with Hepes free acid and Tris (297-303 mOsm), and a pipette solution containing 116 mM NMDG-Cl, 2 mM $MgSO_4$, 20 mM Hepes titrated to pH 7.0 with CsOH, 6 mM CsOH, 1 mM EGTA titrated to pH 8.3-8.5 with CsOH, 2 mM ATP, 0.5 mM GTP, and 10 mM sucrose (pH 7.2, 274-280 mOsm). Low pH bath solution contained 90 mM NMDG-Cl, 5 mM $MgSO_4$, 1 mM $CaCl_2$, 5 mM glucose, 80 mM sucrose and 2 mM glutamine and was titrated to pH 5.9 using Hepes free acid, (297-303 mOsm). Low Cl bath solution contained 10 mM NMDG-Cl, 80mM NMDG-Gluconate, 5 mM $MgSO_4$, 1 mM $CaCl_2$, 5 mM glucose, 80 mM sucrose and 2 mM glutamine and was titrated to pH 7.4 using Hepes free acid (297-303 mOsm).

Patch electrodes with resistances of 3-7 MΩ were pulled from 1.5 mm outer diameter silanized borosilicate microhematocrit tubes. Whole cell currents were measured with an Axopatch 200B (Axon Instruments, Foster City, CA) patch clamp amplifier. Electrical connections to the patch clamp amplifier were made using Ag/AgCl wires and 3 M KCl/agar bridges. Data acquisition and analysis were performed using pClamp 10 software (Axon Instruments).

Voltage Clamp Protocols and Data Analysis

Whole cell currents were evoked by stepping membrane voltage for 1 sec between -120 mV and +100 mV in 20 mV increments from a holding potential of 0 mV. Test pulses were followed by a 1 sec interval at 0 mV. Current-to-voltage relationships were constructed from mean current values recorded over the last 25 msec of each test pulse. For pre-depolarization studies, cells were held at holding voltages of -20 mV to 60 mV for 3 sec and then stepped to -120 mV for 3 sec to activate channels. Peak hyperpolarization induced current amplitude was measured over a 100 msec interval. Pseudo-steady-state current was measured over the last 20 msec of the –120 mV test pulse.

Each trace was taken for at least two trials. If the current magnitude was not consistent between these trials, the data from the traces were discarded. Cell size was monitored with a DIC camera, and data recording was stopped on a given cell if it displayed swelling or shrinkage. Only single isolated cells were patched.

Channel activation voltages were estimated from current-to-voltage relationships. A line was drawn by linear regression analysis of currents measured between 20 mV and 100 mV. A second line was drawn by linear regression analysis of currents measured between the first voltage at which inward current was detected and a second voltage 20 mV more negative. The intercept of these two lines is defined as the activation voltage.

Statistical Analysis

Data are presented as means ± S.E. Statistical significance was determined using Student's two-tailed *t* test for unpaired means. When comparing three or more groups, statistical significance was determined by one-way analysis of variance with a Tukey post-hoc test. P values of ≤ 0.05 were taken to indicate statistical significance.

Results

Large deletion mutations in CLH-3b CBS domains give rise to CLH-3a-like gating

Figure 13 shows the sequence of the predicted intracellular domains of CLH-3a and CLH-3b. The membrane-associated domains of the two channels are identical (Denton et al., 2004) and have been omitted from the figure for clarity. Splice variation occurs in cytoplasmic regions of the channels and includes a 71 amino acid extension of the CLH-3a N-terminus, a 101 amino acid insert located between CBS1 and CBS2 in CLH-3b and a 160 amino acid extension of the CLH-3b C-terminus. In addition, eight of the last nine C-terminal amino acids of CLH-3a are distinct from those in the same region of CLH-3b. Six of these nine amino acids are predicted to be located at the end of CBS2.

Studies using *C. elegans* deletion mutants (He et al., 2006) have demonstrated that disruption of CLH-3b CBS1 domain structure gives rise to channels with CLH-3a functional properties. In addition, deletion of the last 169 amino acids of CLH-3b, which includes part of CBS2 (Figure 13), yields channels that have gating properties identical to those of CLH-3a. To determine whether disruption of CBS2 structure *per se* was responsible for this effect, we deleted the last seventeen amino acids (residues 822-838)

of CBS2 in CLH-3b. Figure 14 shows the characteristics of wild type CLH-3a and CLH-3b and the mutant channel CLH-3bΔ822-838. Both CLH-3a and CLH-3b show strong inward rectification and activation at hyperpolarized voltages (Figure 14A). However, CLH-3a activation requires much stronger hyperpolarization. Mean activation voltages were -54 mV for CLH-3a and -27 mV for CLH-3b (Figure 14B). Deletion of the last seventeen amino acids of CBS2 in CLH-3b induced a hyperpolarizing shift in activation voltage (Figures 14A-B). The mean activation voltage of CLH-3bΔ822-838 was ~-52 mV and was not significantly ($P>0.6$) different from that of CLH-3a.

CLC channels are activated by extracellular acidification (Jentsch et al., 2002). Reduction of bath pH to 5.9 activates CLH-3a and CLH-3b ~3.2- and ~1.6-fold, respectively. Deletion of amino acids 822-838 significantly ($P<0.001$) increased the pH sensitivity of CLH-3b resulting in a ~4.4-fold activation by reducing bath pH to 5.9 (Figure 14C).

CLH-3a shows unique sensitivity to depolarized holding voltages termed pre-depolarization induced potentiation (He et al., 2006; Denton et al., 2006; Denton et al., 2004). As shown in Figures 14D-E, increasing the degree of holding potential depolarization increases the extent of or "potentiates" hyperpolarization induced current activation. Currents potentiated by pre-depolarization also undergo slow, partial inactivation (Figures 14D and F). Wild type CLH-3b is insensitive to depolarized holding voltages (Figures 14 D-F). However, the deletion mutation in CBS2 induced sensitivity to pre-depolarization that resembled that of CLH-3a (Figures 14D-F). Taken together, data in Figure 14 and our previous studies (Denton et al., 2006; He et al., 2006)

demonstrate that disruption of either CBS1 or CBS2 structure in CLH-3b gives rise to channels with CLH-3a-like biophysical properties.

In contrast to CLH-3b, deletion of the last 11 amino acids of CBS1 or the last 17 amino acids of CBS2 in CLH-3a had no effect on voltage and pH sensitivity (Figures 15A-B) or the response to depolarized holding potentials (Figure 15C-D). These data demonstrate that the unique gating properties of CLH-3a are insensitive to disruption of CBS domain conformation.

The C-terminal extension does not regulate gating differences of splice variants

Our previous studies showed that gating differences between CLH-3a and CLH-3b are regulated by CBS domains or the C-terminal 160 amino acid extension of CLH-3b. In this study, a split channel was made coexpressing CLH-3bΔ833-1001 (CLH-3b truncated at the start of the nine amino acid splice variation) and the remaining C-terminus, CLH-3b 833-1001. Preliminary data on this coexpression had gating resembling CLH-3a, no different from the published data of CLH-3bΔ833-1001(He et al., 2006). Because there was no effect of coexpressing the plasmids, as compared to the plasmid for the N-terminal region alone, this experiment was inconclusive and not pursued further.

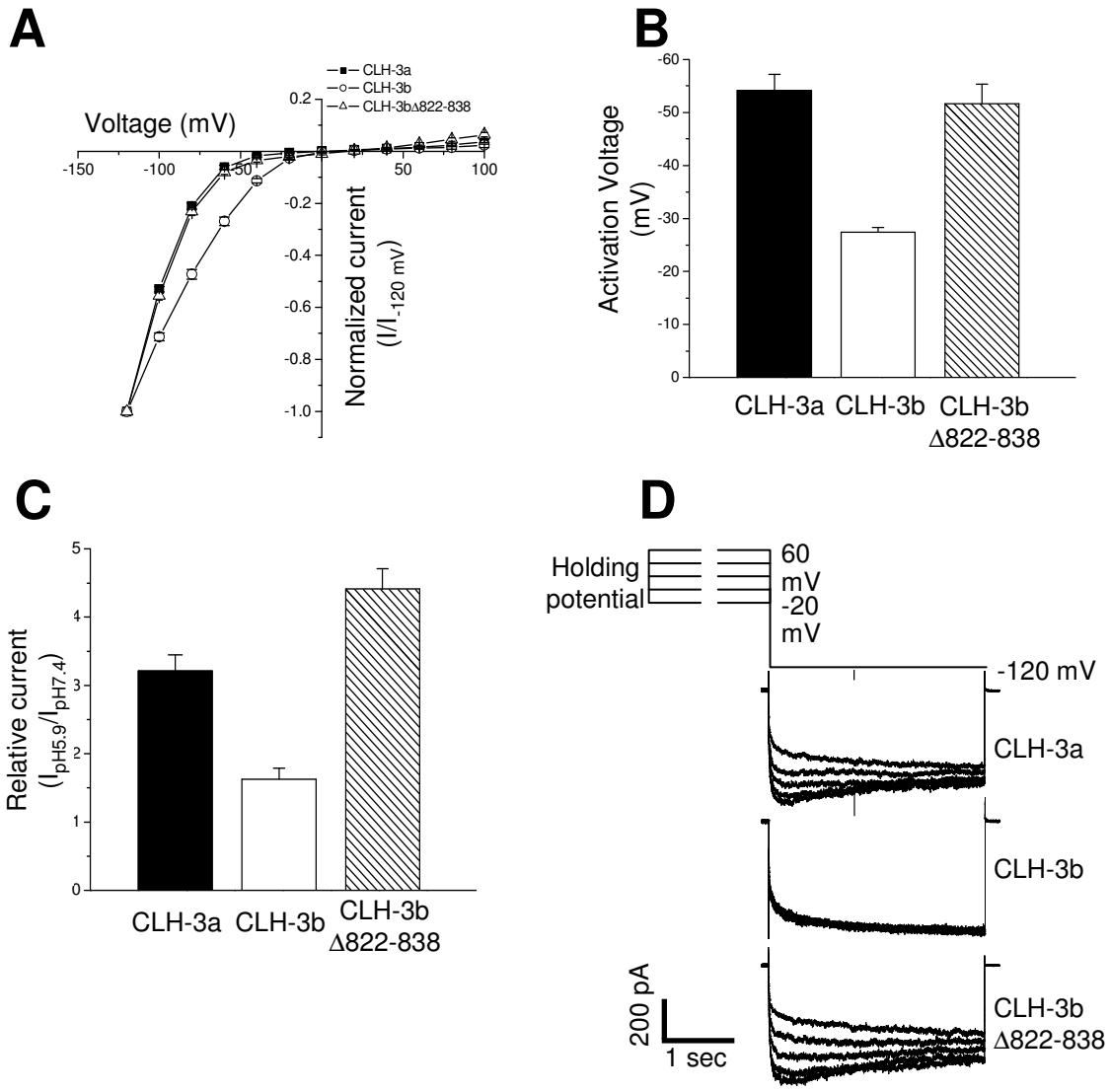

Figure 14. CLH-3b CBS domain deletion mutations give rise to CLH-3a-like gating. Current-to-voltage relationships, activation voltages and activation by bath acidification are shown in A, B and C, respectively. Effects of depolarized holding potentials are shown in D, E and F. D. Representative current traces showing hyperpolarization induced current activation in cells held at depolarized holding potentials. Cells were held at voltages of -20 to 60 mV for 3 sec before currents were activated by stepping to -120 mV. E. Current activation by depolarized holding potentials. Peak current amplitudes are normalized to that measured following a holding potential of –20 mV (I_{-20} mV holding potential). F. Effect of holding potential on current inactivation. Mean pseudo-steady-state current ($I_{steady\ state}$) was measured over the last 20 msec of the –120 mV test pulse and normalized to peak current (I_{peak}) amplitude. Values in A, B, C, E and F are means ± S.E. (n=5-12).

Figure 14, cont.

E

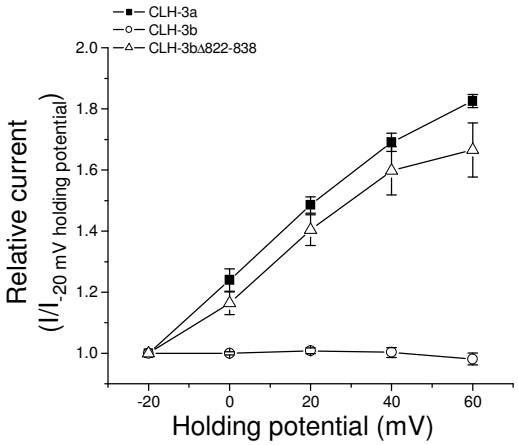

F

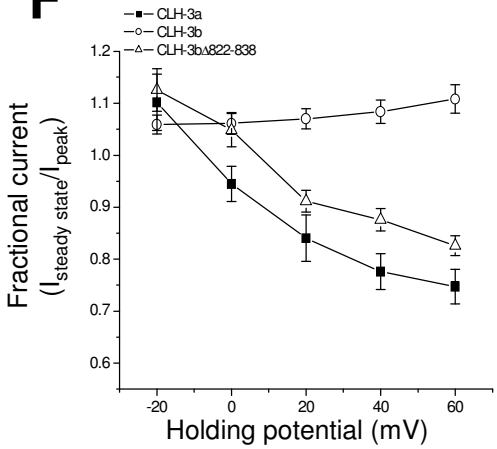

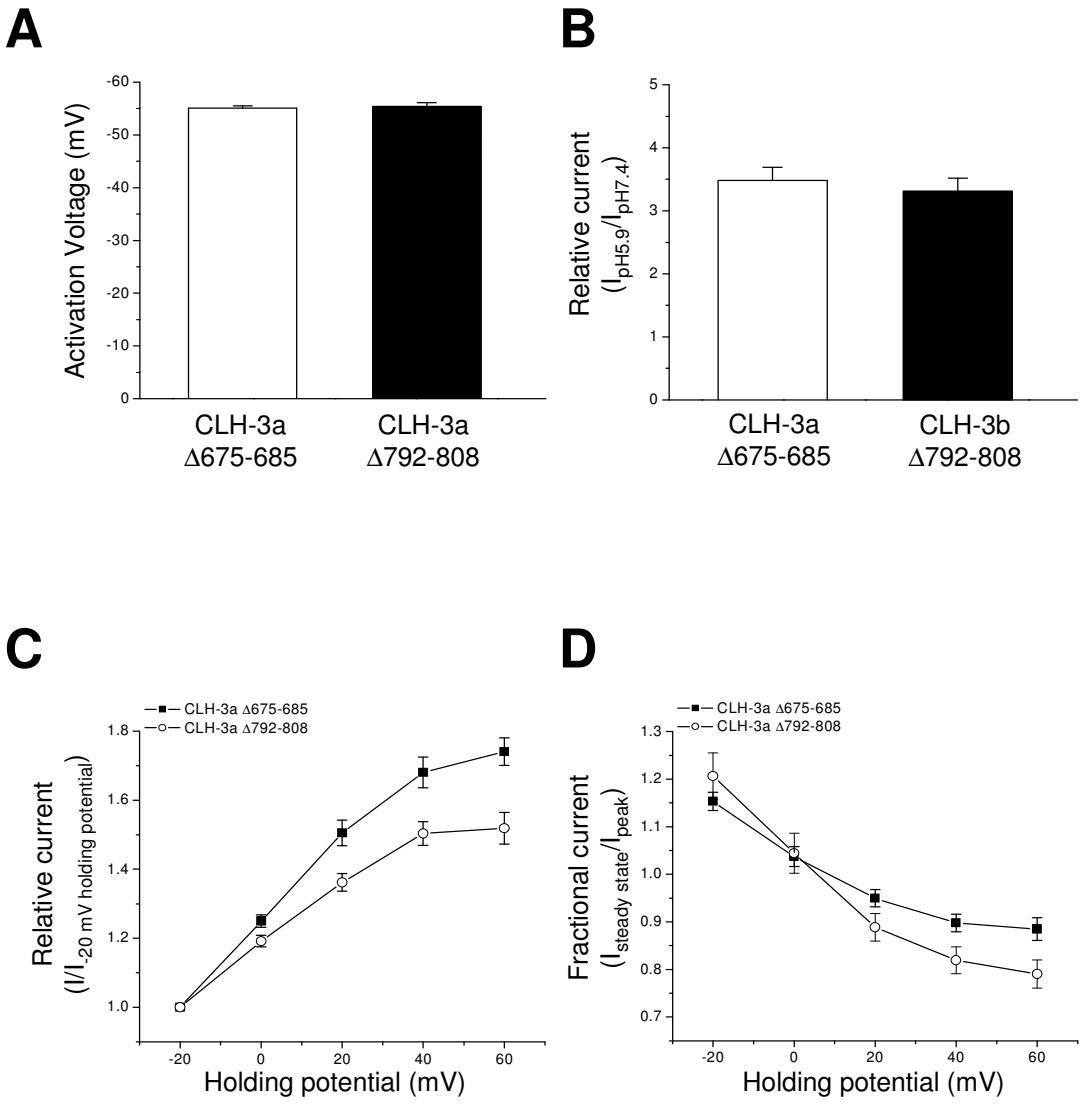

Figure 15. CLH-3a gating is unaffected by large deletion mutations in CBS1 or CBS2. A. Activation voltage. B. Activation by bath acidification. C. Current activation by depolarized holding potentials. D. Effect of holding potential on current inactivation. Data in C and D were acquired as described in Figure 14 legend. Values are means ± S.E. (n=4-12).

Next CLH-3bΔ842-1001, which had this 160 amino acid extension deleted, was created, and gating was assessed. CLH-3bΔ842-1001's sensitivity to depolarizing holding voltages clearly mimicked that of CLH-3b (data not shown). External pH of 5.9 magnified current by a factor of 2.42 $\pm$ 0.21 and external [Cl^-] of 12 mM decreased current to 0.86 $\pm$ 0.026 of the original value. These data were significantly less than the pH and Cl^- sensitivity of CLH-3a ($P<0.05$), and CLH-3bΔ842-1001's activation voltage (-40.9 $\pm$ 0.27) was also significantly less negative than that of CLH-3a ($P<0.01$). This demonstrates that the 160 amino acid C-terminal extension, which follows 3 amino acids C-terminal of the predicted CBS2 in CLH-3b, does not mediate gating differences between CLH-3a and CLH-3b.

Splice variation of CBS2 determines CLH-3a and CLH-3b gating characteristics

The primary sequence of CBS domains in diverse proteins is variable, but the motif has a highly conserved secondary structure consisting of an N-terminal β-strand (β1) followed by an α-helix (α1), two β-strands (β2 and β3) and an α-helix (α2) (Bateman, 1997; Ignoul and Eggermont, 2005). As shown recently by Dutzler and coworkers (Markovic and Dutzler, 2007; Meyer et al., 2007), CBS1 and CBS2 domains play an important role in determining the overall homodimeric structure of the cytoplasmic regions of CLC proteins. Large deletions in either CBS1 or CBS2 are expected to dramatically disrupt C-terminus conformation and function. Our deletion mutation studies (Figures 14-15) as well as previous work (Denton et al., 2006; He et al.,

2006) demonstrate that overall CBS domain architecture plays a critical role in determining CLH-3b but not CLH-3a functional properties.

As shown in Figure 13, CBS2 domains of CLH-3a and CLH-3b predicted using the domain recognition programs PFAM (Finn et al., 2006), InterProScan (Zdobnov and Apweiler, 2001) and MyHits (Pagni et al., 2004) are alternatively spliced at the last six amino acids. This region forms part of α2. The sequences of the six splice variant amino acids in CLH-3a and CLH-3b are VCFLIS and LRLAIE, respectively.

We postulated that splice variation of α2 may be a critical determinant of channel biophysical properties. To test this hypothesis, we interchanged the six alternatively spliced amino acids between the channels. CLH-3b+VCFLIS exhibited a hyperpolarized activation voltage (Figure 16A), increased pH sensitivity (Figure 16B) and sensitivity to depolarized holding potentials (Figures 16C-D). Replacement of the last six amino acids in CBS2 of CLH-3a with the analogous amino acids in CLH-3b (CLH-3a+LRLAIE) had little effect on activation voltage or pH sensitivity (data not shown).

The response of CLH-3a+LRLAIE to pre-depolarization was variable between cells. Of the 15 cells that were patch clamped from two separate transfections, we found that two cells showed a strong response to pre-depolarization resembling that of wild type CLH-3a, seven cells showed no response and six cells exhibited a weak response (data not shown). This variability suggested to us that additional spliced amino acids may contribute to channel gating properties. Additionally, our modeling results (Figure 11) showed that the first 5 spliced amino acids in CLH-3a are predicted to be helical, while in CLH-3b the a2 helix is predict to extend to include seven spliced amino acids.

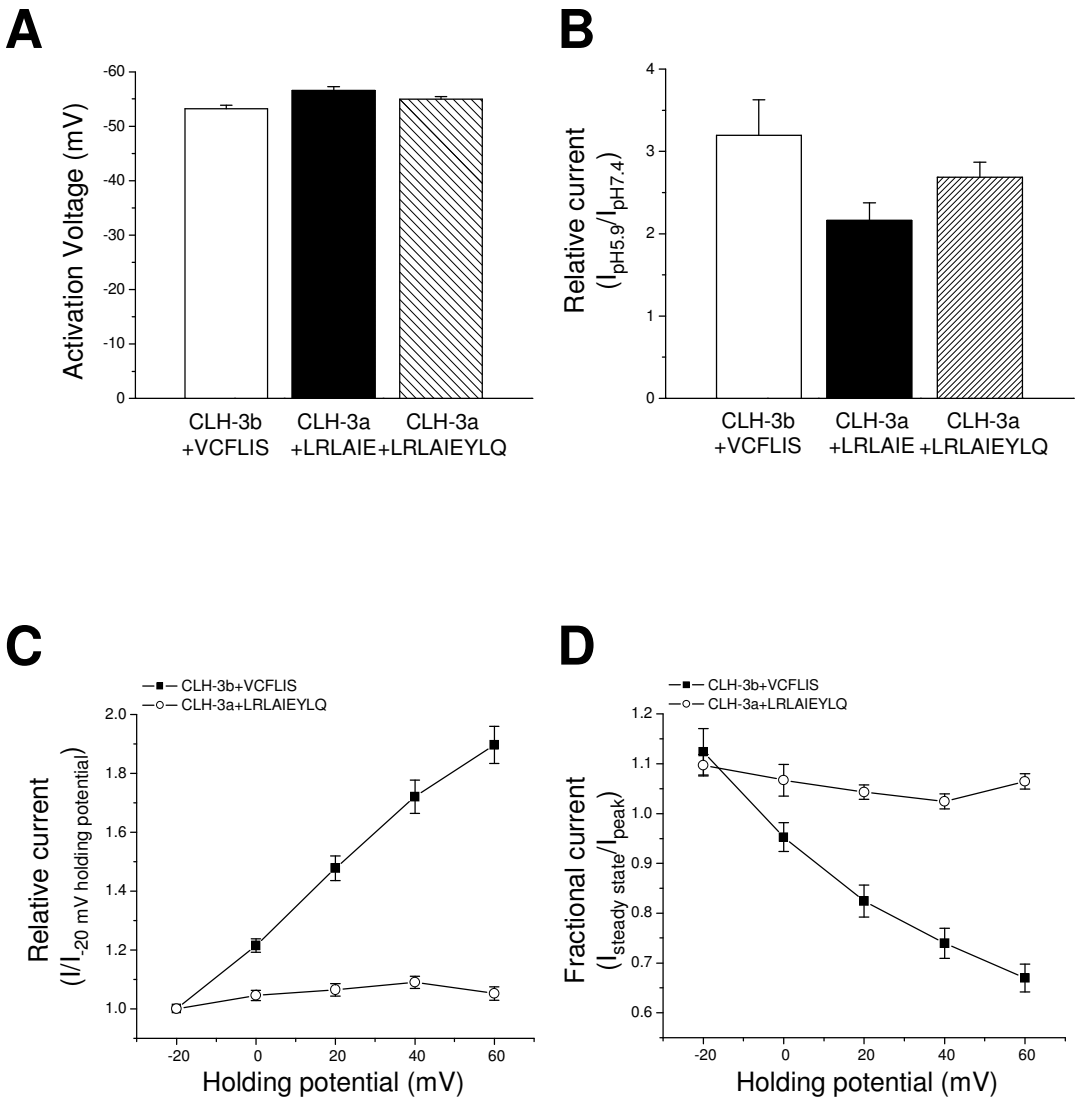

Figure 16. Interchanging alternatively spliced amino acids in CBS2 interchanges channel functional properties. A. Activation voltage. B. Activation by bath acidification. C. Current activation by depolarized holding potentials. D. Effect of holding potential on current inactivation. Data in C and D were acquired as described in Figure 14 legend. Values are means ± S.E. (n=5-11).

Given the possible differences in α2 length and the variable response of CLH-3a+LRLAIE to depolarizing voltages, we interchanged the last nine amino acids of CLH-3a with the analogous amino acids of CLH-3b. The activation voltage of CLH-3a+LRLAIEYLQ remained hyperpolarized and pH sensitivity was similar to that of wild type CLH-3a (Figures 16A-B). However, in contrast to CLH-3a+LRLAIE, none of the currents recorded from CLH-3a+LRLAIEYLQ expressing cells (10 cells in six separate transfections) showed sensitivity to depolarized holding potentials (Figures 16 C-D).

To determine whether the last three amino acids of CLH-3a (i.e., RKK) independently regulate channel properties, we exchanged them with the analogous amino acids of CLH-3b (i.e., YLQ). Replacing RKK with YLQ (i.e., CLH-3a+YLQ) had no significant effect on pH sensitivity or activation voltage ($P>0.7$) or sensitivity to depolarized voltages (data not shown). Similarly, CLH-3b+RKK showed pH sensitivity similar to that of wild type CLH-3b and was insensitive to pre-depolarization (data not shown). However, the activation voltage for CLH-3b+RKK was similar to that of CLH-3a (see Figure 14B) and significantly ($P<0.0001$) hyperpolarized compared to CLH-3b with a mean ± S.E. value of -51 ± 1 mV (n=13).

The R-helix linker plays a critical role in determining CLH-3a and CLH-3b gating properties

Data in Figure 16 demonstrate that splice variation of α2 of CBS2 plays a major role in determining the gating characteristics of CLH-3a and CLH-3b. Differences in the primary and secondary structure of α2 could alter local interactions within the channel

that give rise to unique gating properties. Our homology models of the cytoplasmic C-termini of CLH-3a and CLH-3b (Figure 9) have provided insights into such interactions.

The 20 amino acid R-helix linker connects the C-terminus of the R-helix of CLH-3a and CLH-3b to the N-terminus of CBS1 (Figure 17A). The R-helix forms part of the channel pore and selectivity filter. Cytoplasmic domains may modulate the conformation of the R-helix and thus channel properties (Dutzler et al., 2002).

Crystal structures of ClC-0, CLC-Ka and ClC-5 cytoplasmic C-termini (Markovic et al., 2007; Meyer et al., 2007; Meyer et al., 2006) indicate that part of the cytoplasmic R-helix linker lies close to and may therefore interact with α2 of CBS2 (Figure 9). This suggested that the linker could play an important role in mediating the differences in CLH-3a and CLH-3b gating induced by α2 splice variation.

As discussed in Chapter II, the homology models indicated that F559 in the R-helix linker of CLH-3b lies very close to A836 in α2 of CBS2 (Figure 17B). The orientation of the homologous phenylalanine in CLH-3a, F630, could be altered due to the presence of a bulkier leucine residue, L806, at the corresponding position in α2. To test whether F559 plays a role in regulating channel properties, we mutated it to aspartate (F559D). As shown in Figures 7A-D, this mutation gave rise to CLH-3a-like voltage and pH sensitivity and sensitivity to depolarized holding potentials. In contrast, mutation of F630 to aspartate in CLH-3a had no effect on channel properties (data not shown).

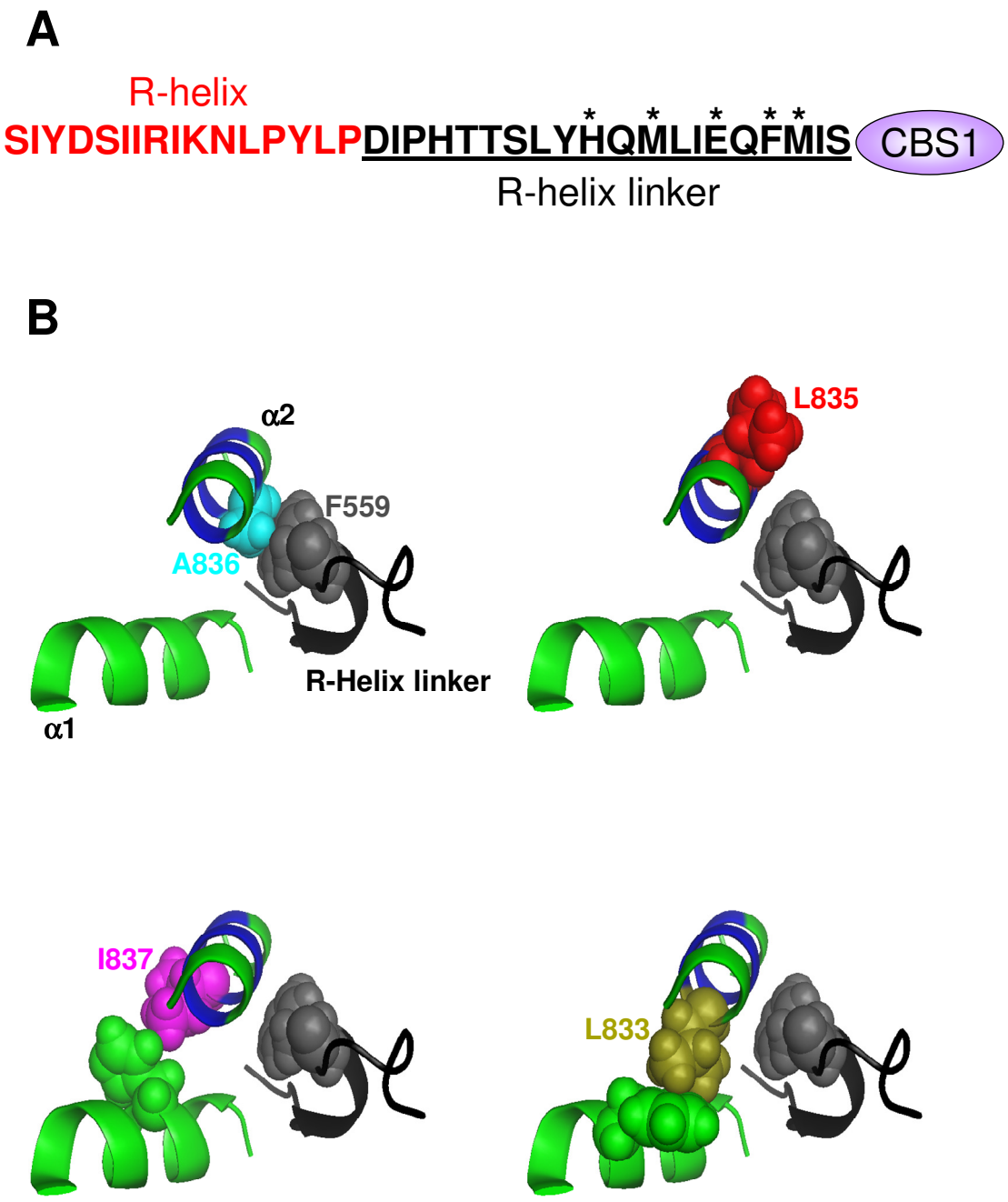

Figure 17. Depictions of mutated amino acids. A. Sequence of the R-helix and R-helix linker in CLH-3b. Asterisks denote mutated amino acids in the R-helix linker. B. Ribbon diagrams showing the relationship of mutated amino acids in α2 of CBS2 to F559 in the R-helix linker and α1.

To determine whether the channel gating was uniquely sensitive to mutation of F559, we also performed charge addition or charge swapping mutations to the neighboring amino acids H552, M554, E557, or M560 (see Figure 17A). None of these amino acids were predicted to have strong interactions with α2. Consistent with this prediction, mutation of M554 or E557 to lysine or H552 or M560 to aspartate had no effect on CLH-3b gating (Figure 18A-D).

We then mutated A836 to aspartate, phenylalanine, and lysine. The A836D mutant gave rise to a small hyperpolarizing shift in activation voltage and potentiation behavior that was considerably less than that observed with wild type CLH-3a (data not shown). The A836F mutant gave rise to pH sensitivity (preliminary data, n=3), activation voltage, and potentiation that resembled those of CLH-3b (data not shown). We therefore mutated A836 to a large and positively charged amino acid, lysine. The A836K mutant exhibited voltage and pH sensitivity nearly identical to those of CLH-3a (Figure 19A-D).

To summarize, F559D and A836K both induce CLH-3a like gating and are predicted to interface. Thus, we constructed the double mutant CLH-3b F559D / A836K. If F559 and A836 interact, this mutant may reconstitute the interaction with a salt bridge. The double mutant CLH-3b F559D / A836K had pH sensitivity, activation voltage, and sensitivity to depolarized holding potentials closely resembling that of CLH-3a (data not shown), which is similar to gating of CLH-3b F559D or CLH-3b A836K. Because of the absence of an effect, no conclusions could be drawn.

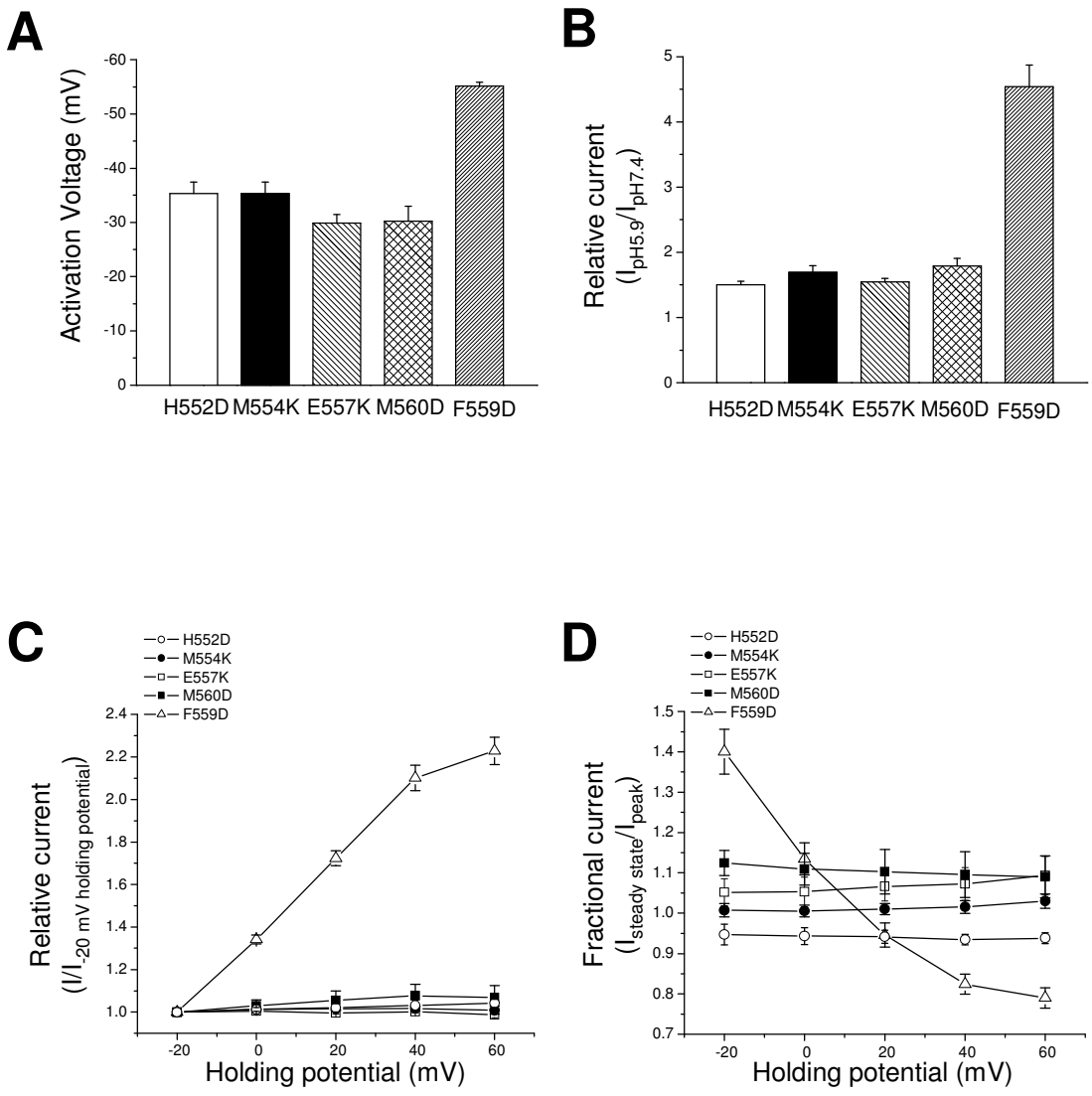

Figure 18. A single point mutation in the R-helix linker gives rise to CLH-3a-like gating. (A) Activation voltage. (B) Activation by bath acidification. (C) Current activation by depolarized holding potentials. (D) Effect of holding potential on current inactivation. Data in (C) and (D) were acquired as described in Figure 14 legend. Values are means ± S.E. (n=5-12). Wild type CLH-3a and CLH-3b gating are shown in Figure 14.

We also mutated amino acids immediately adjacent to A836. Mutation of L835 to lysine (L835K) had no effect on the voltage or pH sensitivity of CLH-3b while mutating I837 to lysine (I837K) gave rise to CLH-3a-like behavior (Figure 19A-D). Both amino acids are predicted to face away from the R-helix linker (Figure 17B). Crystal structures of various tandem CBS domain containing proteins indicate that that α1 and α2 lie close together and may physically interact (e.g. Meyer et al., 2006; (Miller et al., 2004; Markovic and Dutzler, 2007; Meyer et al., 2007; Zhang et al., 1999). We examined the CLH-3b homology model to assess the relationship of α2 amino acids to α1 in CBS2. As shown in Figure 17B, L835 faces away from α1 while I837 faces towards it and could interact with amino acids on this helix. This suggests that the I837K mutation may disrupt putative α1-α2 interactions. To test this possibility, we mutated L833, which also lies close to α1 (Figure 17B), to glutamate (L833E). The L833E mutant exhibited CLH-3a-like behavior (Figures 19A-D). Data shown in Figures 14-16 and 18-19, and our previous findings (Denton et al., 2006; He et al., 2006) indicate that mutations that disrupt CBS domain structure and/or putative interactions of CBS2 with the R-helix linker give rise to gating characteristics resembling those of CLH-3a.

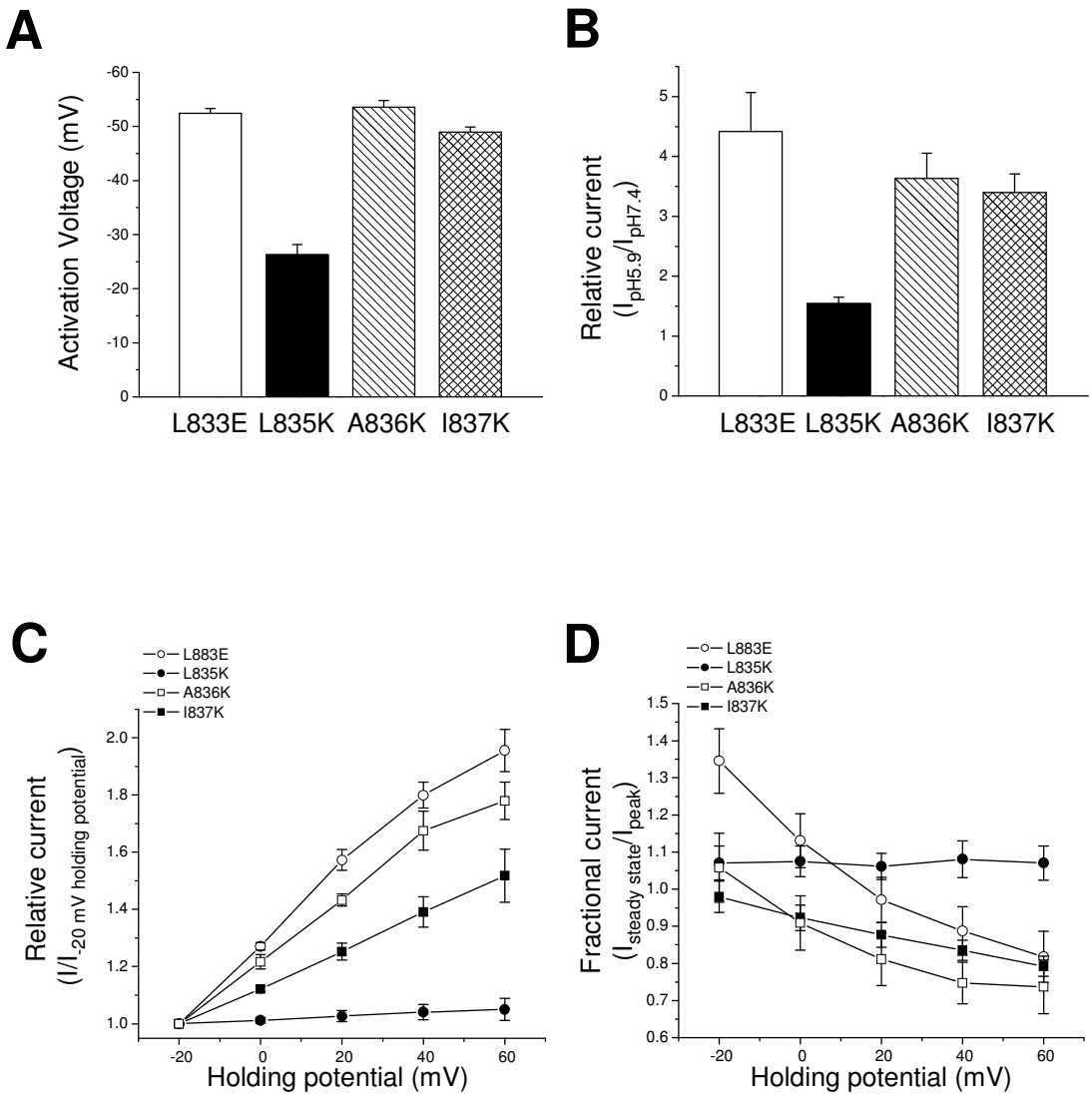

Figure 19. Mutation of amino acids in α2 of CBS2 predicted to interact with F559 in the R-helix linker or α1 amino acids give rise to CLH-3a-like gating. A. Activation voltage. B. Activation by bath acidification. C. Current activation by depolarized holding potentials. D. Effect of holding potential on current inactivation. Data in C and D were acquired as described in Figure 14 legend. Values are means ± S.E. (n=5-8).

Discussion

The CBS domain is a highly conserved motif found in diverse proteins including channels, transporters, kinases and metabolic enzymes of archeabacteria, eubacteria and eukaryotes (Bateman, 1997; Ignoul et al., 2005). Mutations in CBS domains cause diverse inherited diseases such as cardiomyopathy, homocystinuria, retinitis pigmentosa, osteopetrosis, and myotonia (e.g., (Pusch, 2002; Ignoul and Eggermont, 2005; Sasaki et al., 1999)). The precise function of CBS domains, however, is poorly understood (Ignoul et al., 2005).

CBS domains have been crystallized in a variety of proteins (e.g., (Hattori et al., 2007; Zhang et al., 1999; Rudolph et al., 2007; Miller et al., 2004)) including CLCs (Markovic et al., 2007; Meyer et al., 2007; Meyer et al., 2006). CBS domains are typically present in groups of two or four. The two CBS domains, CBS1 and CBS2, may dimerize with another CBS domain pair, to form quaternary structure groups of four CBS domains. CBS1 and CBS2 always interface at the β strands β_2 and β_3. In the two crystallized CLC CBS domain dimers, the cytoplasmic CBS domain pairs interact at CBS2, as shown in the CLH-3b homology model (Figure 9).

Large deletion mutations in either CBS1 or CBS2 are expected to dramatically disrupt CBS domain tertiary structure and this in turn likely disrupts oligomerization. For instance, deletion of the last 17 amino acids of CBS2, which encompass α2 and β3, would be expected to disrupt pairing of CBS1 and CBS2 occurring at the β strands. Our results demonstrate that disruption of CLH-3b CBS domain structure (Figure 2 and (Denton et al., 2006; He et al., 2006)) gives rise to channels with CLH-3a-like

biophysical properties while disruption of CLH-3a CBS structure has little effect on channel gating (Figure 15). These findings indicate 1) that the overall CBS domain architecture of CLH-3b plays a critical role in determining the functional properties of the channel and 2) that CLH-3a gating appears to be largely insensitive to changes in CBS domain conformation.

The C-terminal end of CBS2 is alternatively spliced in CLH-3a and CLH-3b (Figure 13). This spliced region forms the second α-helix domain, α2. Splice variation is predicted to alter secondary structure and result in α2 in CLH-3b being longer than that of CLH-3a (Figure 11). Consistent with this, we found that insertion of the last six amino acids of the CLH-3a CBS2 domain (i.e., VCFLIS) into CLH-3b CBS2 gives rise to CLH-3a-like voltage- and pH-sensitivity (Figure 16). Inserting the analogous six amino acids of CLH-3b (i.e., LRLAIE) into CLH-3a had little effect on activation voltage or pH sensitivity and had an inconsistent effect on sensitivity to depolarized holding potentials. However, when the nine alternatively spliced amino acids comprising the longer α2 of CLH-3b (i.e., LRLAIEYLQ) were inserted into CLH-3a, the mutant channels were fully insensitive to depolarized voltages (Figures 16C-D).

Given that large scale disruption of CBS structure by deletion mutations has no effect on CLH-3a gating, we suggest that splice variation of α2 in CBS2 of this channel disrupts critical interactions between CBS domains and other regions within the C-terminus. The absence of these interactions gives rise to the gating characteristics of CLH-3a. In contrast, both the primary sequence and predicted altered secondary structure of CLH-3b α2 mediate important functional interactions. Disruption of these

interactions by mutation of either CBS1 or CBS2 gives rise to channels with CLH-3a-like properties.

It is important to note that the CLH-3a+LRLAIEYLQ chimeric channel did not fully recapitulate CLH-3b gating. Activation voltage and pH sensitivity of this chimera resembled those of wild type CLH-3a (Figures 16A-B). These results indicate that other cytoplasmic domains unique to CLH-3b play a role in determining these gating characteristics. Our previous studies have shown that deletion of the 101 amino acid linker domain between CBS1 and CBS2 in CLH-3b (Figure 1) gives rise to channels with a strongly hyperpolarized activation voltage (He et al., 2006). In addition, deletion of the 160 amino acids immediately C-terminal to LRLAIEYLQ (Figure 13), as in the mutant CLH-3bΔ842-1001, increases pH sensitivity and hyperpolarizes channel activation voltage.

The molecular mechanisms by which cytoplasmic structures and intracellular signaling events regulate CLC channel/transporter function are poorly understood. Dutzler and colleagues have suggested that the membrane-associated R-helix may play an important role in this regulation (Dutzler et al., 2002). By virtue of its direct connection to the large cytoplasmic C-terminus, the R-helix may provide a pathway by which conformational changes in intracellular domains induce rearrangements of the pore that in turn alter channel/transporter activity.

As discussed in chapter II, a short cytoplasmic linker connects the R-helix to CBS1. This R-helix linker lies close to α2 of CBS2 in crystal structures of ClC-0, ClC-5 and CLC-Ka (Markovic et al., 2007; Meyer et al., 2006; Meyer et al., 2007). Our

homology models of CLH-3a and CLH-3b suggested that potential interactions between α2 amino acids and an R-helix linker phenylalanine residue that could be altered by splice variation. Consistent with this, we found that mutation of CLH-3b F559 to aspartate or mutation of a predicted interacting alanine residue in α2, A836, gave rise to channels with gating properties fully recapitulating those of CLH-3a (Figures 18-19). In contrast, mutation of the analogous R-helix linker phenylalanine residue in CLH-3a had no effect on channel activity.

It should not be overlooked that mutating the predicted interfacing alanine to aspartate, A836D, only partially induced CLH-3a like gating, and A836F did not affect gating. The absence of effect of the phenylalanine is consistent with the hydrophobic nature predicted for the putative interface between the R-Helix linker and α2. However, it is not supported by the predictions on protein stability that suggest A836F may lead to steric repulsions and change of backbone conformation (Chapter II). Nonetheless, such calculations need further refinement before comparison with experimental data.

There are two hypotheses for why CLH-3b A836D had an incomplete effect on channel gating. First, both bulk and charge may be necessary to break the predicted A836-F559 interface. That is, A836D may only be weakening or altering the predicted interface. Second, there may be other interactions, in conjunction with the proposed α2-R Helix linker interface, that are necessary for CBS domains to regulate gating. This hypothesis is consistent with the need for proper overall CBS domain configuration to maintain CLH-3b like gating. The hypothesis is also consistent with the data from CLH-3a+ LRLAIEYLQ, which shows a need for the entire CLH-3b helix to reconstitute CLH-

3b like gating in CLH-3a. This hypothesis would also be strengthened if CLH-3a+LRLAIE A836D gave rise to gating completely resembling that of CLH-3a. Regardless of other interactions, mutating both sides of the predicted R Helix linker - α2 interface did create gating more closely resembling CLH-3a, while mutating several nearby amino acids did not. These data strengthen the proposition that the interface is specific to A836 and F559.

Our data are consistent with a physical interaction between amino acid residues in α2 of CBS2 and the R-helix linker, as observed in crystal structures (Markovic et al., 2007; Meyer et al., 2006; Meyer et al., 2007) and our model. This interaction could be important for determining the conformation of the R-helix and other associated regions that control channel gating. We propose that splice variation of α2 in CLH-3a may be disrupting its ability to interact with the R-helix linker, giving rise to the channel's unique gating characteristics. Mutation of CBS1, CBS2 or the R-helix linker of CLH-3b could also disrupt this interaction, giving rise to CLH-3a-like voltage- and pH sensitivity.

Closing Remarks

In summary, our studies provide unique insights into the functional roles of CLC CBS domains and the R-helix linker in regulating channel properties. Our results clearly demonstrate a role of CBS2 splice variation in regulating CLH-3a and CLH-3b channel gating. We postulate that the R-helix linker via its interaction with CBS2 provides a pathway by which C-terminus conformational changes can modulate the conformation of

the R-helix and associated structures and lead to changes in channel function. Measuring solvent accessibility of the channel gate can provide a quick assessment of whether the channel gate conformation changes in response to the mutations studied. Ultimately, structural and biochemical studies will be needed to directly test for the postulated interaction and to determine the role played by the R-helix linker in mediating the regulation of CLC channels and transporters by intracellular signaling events such as phosphorylation (e.g., (Falin et al., 2009; Denton et al., 2005) and ATP binding (e.g., (De Angeli et al., 2009; Zifarelli and Pusch, 2009b).

CHAPTER IV

CYSTEINE ACCESSIBILITY, AN ASSESSMENT OF EXTRACELLULAR CONFORMATION, IS SIMILAR FOR CLH-3a AND THE R-HELIX LINKER MUTANT WITH CLH-3a LIKE GATING

Summary

Experiments assessing solvent accessibility of extracellular cysteine residues can be used to understand protein conformational changes near an introduced cysteine that result from mutations. In the method, Methyl ThioSulfonate (MTS) reagents are applied extracellularly and function is assayed. A different functional response to MTS reagents indicates a different solvent accessibility, and thus conformation, of the extracellular cysteines in a protein. Using this method, we found MTSET inhibits channel function in a similar manner for CLH-3a and the R-Helix linker mutant with similar gating, CLH-3b F559D. This inhibition is drastically faster than MTSET inhibition of CLH-3b. All channels studied had a cysteine introduced at the channel gate. These finding are consistent with the conformation at the channel gate being similar for CLH-3a and CLH-3b F559D, but different for CLH-3b.

Introduction

Cysteine accessibility experiments can detect presence of conformational changes

Assessing "accessibility" of a residue can be used to detect conformational changes at the residue. A residue is considered accessible to solvent, or a solute, if the extracellular solvent or solute molecules contact the residue. The accessibility of a residue can change if the protein conformation near the residue changes.

Methyl Thiosulfonate (MTS) reagents are commonly used as the solute molecule to detect changes in accessibility of cysteine residues. This is because the MTS reagents react with accessible cysteines and this reaction can alter channel function. The Substituted Cysteine Accessibility Method (SCAM) (Karlin and Akabas, 1998) involves applying extracellular MTS reagents and assessing change in protein function. Often cysteines are engineered at points of interest and native cysteines are mutated to alanine. We use a MTS reagent called MTSET to detect change in accessibility of a cysteine placed at the glutamate gate of CLH-3a, CLH-3b, or mutant channels. This allows us to detect change in conformation of the glutamate gate in response to the mutations.

SCAM typically involves mutating native cysteines & quantitative functional assays

Extracellular MTS reagents can covalently and irreversibly bind to solvent accessible SH groups, found in cysteines, by the following reaction:

The chemical modification of the cysteine would likely change channel function if the cysteine is at a functionally important part of the protein. In cysteine accessibility experiments, MTS reagents react with all solvent accessible cysteine reagents on the side of the membrane the reagent is applied. Thus, native cysteines are typically mutated, although information on conformational changes can be inferred even without such mutations.

SCAM experiments are often done on ion channels because of the easy and quantitative functional assay available, i.e. electrophysiology. Functional response to MTS reagents could be a change in current magnitude or change in the rate of change of current magnitude in response to a MTS reagent. A change in function due to MTS reagents can be due to a change in accessibility of cysteines, as well as a change in one or more of at least three other factors: dissociation rate of the cysteine SH group, steric constraints on binding of MTS reagents to cysteines, and the electric field around the cysteine residue (Karlin and Akabas, 1998). Dissociation of the SH group can prevent disulfide bond formation between MTS reagents and cysteines. Steric constraints could prevent or slow MTS reagents binding to cysteines, even if the cysteine is accessible to solvent. Electric field near the cysteine residue can impact the binding of charged MTS reagents to cysteines.

A plethora of available MTS reagents allows for using accessibility to infer many different structural properties of a protein**.** MTS reagents can be used to determine the size of solvent pockets in a channel, assess changes in structure due to activation, locate channel gates and selectivity filters, and map electrostatic potential (Karlin and Akabas,

1998). MTS reagents with R groups of known and extended length, or flexible R groups, can be particularly useful for assessing channel size or measuring distances between residues. One such study has been done to assess voltage-dependent conformational changes in the *Shaker* K^+ channel (Darman et al., 2006). Similar studies have been done with non-sulfhydryl long-chain pharmacological compounds that bind channels (Blaustein et al., 2000). Studies of this nature, however, are still few and limited.

Previous studies show CLH-3b deletion mutants have gating and inhibition by MTSET resembling CLH-3a

Experiments done in our lab use the reagent MTSET to assess change in extracellular conformation. Native cysteines are maintained and another cysteine is introduced at the glutamate gate. Native cysteines are maintained because CLH-3b with all eleven cysteines mutated to alanine (CLH-3b 11CA) has current magnitudes too small for accurate analysis, although the kinetics looked similar by eye inspection. The functional assay we use is the change in rate of current inhibition, i.e. time constant for inhibition, in response to MTSET.

Previous work in our lab by He et al. identified deletion mutations that introduced CLH-3a like gating in CLH-3b and also induced CLH-3a like response to MTSET. These mutants are CLH-3b Δ833-1001, which deletes the last six amino acids of CBS2 and the C-terminal tail, and CLH-3b Δ604-614, which deletes the last 11 amino acids of CBS1 (He et al., 2006). CLH-3a and CLH-3b have similar time constants (tau ~ 25 sec) for inhibition by MTSET (He et al., 2006). However, when a cysteine is introduced at

the channel gate (CLH-3b E167C and CLH-3a E238C), only the time constant for CLH-3b drastically increases (tau ~150 sec) (He et al., 2006). The CLH-3b deletion mutants which also have a mutated glutamate gate have a time constant of inhibition similar to CLH-3a E238C (He et al., 2006). This observation lends support to the hypothesis that the extracellular conformation of CLH-3a is similar to that of the CLH-3b deletion mutants with gating resembling CLH-3a.

Is the extracellular conformation of CLH-3b F559D similar to that of CLH-3a?

We identified a point mutation, F559D, in the R-Helix linker of CLH-3b that creates gating resembling CLH-3a (Figure 18). Similar to previous studies, **we tested the hypothesis that CLH-3b F559D / E167C, the R-Helix linker and glutamate gate mutant, has an extracellular conformation different from that CLH-3b E167C.** We also attempted to test the same hypothesis for the same two plasmids with all the native cysteines mutated to alanine: CLH-3b F559D / E167C 11CA and CLH-3b E167C 11CA.

Methods

MTSET preparation

1 mM MTSET ([2-(Trimethylammonium)ethyl] methanethiosulfonate bromide) working solutions were used. 40 uL stocks at 40mM were made in water and stored at –80 deg C. 37.5 uL of stocks were dissolved in 15 mL of bath solution immediately before experiments. MTSET solution was used for up to 1.5 hrs after preparation.

Electrophysiology

Cells were transfected with 5-8ug of plasmids, as described in methods for chapter III. Whole cell electrophysiology was used to assess channel currents, using solutions described in methods of chapter III.

The following protocol was used for an MTSET recording after achieving whole cell configuration. First, with normal bath solution, we ran at least one minute of voltage steps to –100 mV, with each step lasting one second in duration. Current was observed, but not recorded. If the current stabilized, and there were no signs of cell swelling or shrinkage, normal bath solution was perfused while continuing to monitor response to –100 mV steps. Once current magnitude stabilized with perfusion, recording in response to the –100mV voltage steps was initiated, while continuing perfusion. Five seconds after the start of recording, we changed the perfusion to normal bath supplemented with 1 mM MTSET. Perfusion with MTSET supplemented bath solution alone was continued for twenty seconds, after which perfusion was stopped and recording continued until current magnitude stabilized. Periodically through the recording, the seal was checked. If the seal dropped below 1G ohm or if the cell started to swell or shrink, the recording was stopped. Once MTSET was applied to a dish of cells, no new cells were patched.

Analysis

Current magnitude within a single trace was independent of time. Current magnitude was averaged over 100msec for each trace. The averages were plotted against

time from application of MTSET, and fit with a single exponential function using Origin 7.0. The time constant of the exponential function was reported.

Results

To determine whether the CLH-3b F559D R-Helix linker mutation alters the conformation of CLH-3b extracellular domains, we mutated the glutamate residue that functions as the fast gate to cysteine (i.e., CLH-3b E167C). Consistent with our previous observations (He et al., 2006), this mutation gave rise to constitutively active channels that are no longer sensitive to voltage.

Exposure of the CLH-3b E167C mutant to 1 mM MTSET inhibited whole cell current amplitude in a manner similar to our previous report (He et al., 2006). The mean ± S.E. time constant for inhibition was 283 ± 34 sec (n=6). An additional mutation of F559 to aspartate (CLH-3b E167C F559D) reduced the inhibition time constant nearly 7-fold to a mean ± S.E. value of 41 ± 6.6 sec (n=5) (Figure 20). The striking difference in rates of MTSET inhibition for E167C and the E167C/F559D double mutant is remarkably similar to the difference observed between CLH-3a and CLH-3b (He et al., 2006). These data demonstrate that mutation of a single amino acid in the R-helix linker, F559, to aspartate converts CLH-3b extracellular cysteine reactivity to those resembling CLH-3a.

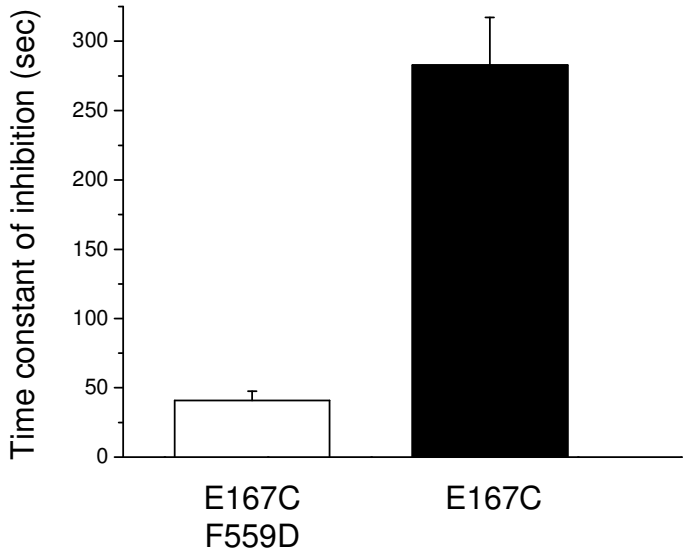

Figure 20: An R Helix linker mutant that has CLH-3a like gating also has CLH-3a like time constants for MTSET inhibition. Effect of 1mM MTSET on CLH-3b E167C and CLH-3b E167C / F559D (n=5-6).

Discussion

The SCAM method was invented in 1992 (Akabas et al., 1994; Akabas et al., 1992) by Akabas and colleagues, who provide a comprehensive review (Karlin and Akabas, 1998) of the method and its applications. Cysteine accessibility studies in CLCs have largely focused on the channel pore. Using the method, Chen and colleagues have determined the positive charge nature of the pore (Zhang et al., 2006; Zhang et al., 2010). They have also explored the effects of oxidation and reduction in CLC-0 (Li et al., 2005).

Cysteine accessibility studies have also provided evidence for the conservation of the intracellular pore region structure (Engh and Maduke, 2005) and fast gate location (Lin and Chen, 2003) between prokaryotic and eukaryotic CLCs. Our lab has previously used cysteine accessibility studies to provide support for intracellular mutations changing the conformation at the CLH-3b channel gate (He et al., 2006).

Our current results show that an R-helix linker mutation, F559D dramatically speeds up the rate of inhibition by MTSET of CLH-3b E167C, in a manner similar to the faster inhibition seen in CLH-3a (Figure 20). This suggests that F559D changes the extracellular conformation of the channel, and the data is consistent with the new conformation being similar to that seen in CLH-3a.

Unlike many cysteine accessibility studies, we retained native CLH-3b cysteines in these experiments due to the extremely small currents of the cysteine-less channel. Thus, the effect of MTSET could be due to inhibition at any of CLH-3b's extracellular cysteines. More information about conformation changes at only the glutamate gate could be gained from CLH-3b E167 10CA, which has only 10 of the 11 cysteines replaced with alanines and has normal current magnitudes. If experimental methods could be modified to produce larger currents for the CLH-3b 11CA E167C mutant, this would provide the ideal mutant for assessing conformation changes at just the channel gate.

Further similar cysteine accessibility experiments can be quite insightful. Using the mutants CLH-3b + VCFLIS E167C and CLH-3a + LRLAIEYLQ E238C, we could test if the conformation change due to splice variation could be similar to the change due

to mutation of the R Helix linker. The mutant CLH-3b + RKK demonstrated CLH-3b like gating in all manners except activation voltage (chapter III). Thus similar cysteine accessibility studies on CLH-3b+RKK can compare conformational changes that regulate activation voltage with those that regulate other gating properties. Our current, and such future, cysteine accessibility experiments, however, provide information on only the existence of conformational changes, not their nature.

Cysteine accessibility experiments have great potential for measuring residue distances and provide a more detailed assessment of conformational changes due to mutations. Specifically, one would use MTS compounds with long R group chains, and one sulfyhydrl group at each end of the chain to crosslink cysteines in the channel. Crosslinking would only occur if the length of the MTS compound was comparable to the distance between the cysteines. Thus, a combination of MTS compounds with R groups of various lengths can be used to measure distances between cysteines. Flexible long chain MTS compounds (Darman et al., 2006) could provide a tool that can provide a more efficient tool that detects whether cysteines are at a certain length or closer. While sulfhydryl reagents have great promise for measuring distances, such methods can be time consuming and have yet to become established procedures.

Biochemical methods, such as EPR, FRET, and crystallography provide a more direct assessment of conformational changes. Given the minimal functional effect of removing native CLH-3b cysteines, EPR could prove very useful. Such future studies are discussed in Chapter V.

Closing remarks

Our results show that the time constant for MTSET inhibition, like channel gating, is similar in CLH-3b F559D and CLH-3a, but different from that of CLH-3b. This data is consistent with the F559D R Helix linker mutant having an extracellular conformation similar to that CLH-3a. While these findings are very interesting, future biochemical experiments are needed to make definitive conclusions regarding changes in protein structure due to mutations.

CHAPTER V

CONCLUSION

Background and Summary

CLC chloride channels mediate a variety of essential cellular functions and mutations in CLCs give rise to muscle, kidney, and bone diseases (Jentsch, 2008). Some of these mutations are in the large intracellular tail of CLCs, including in the Cystathionie-β-Synthase domains (Lin et al., 2006; Lloyd et al., 1997). Thus, a central question in the field is how the intracellular portion of CLCs regulate channel function.

We have made used of the *clh-3* encoded *C. elegans* splice variants to address this question. Initial studies began in our lab using *C. elegans* because of the ease of studying osmotic stress (Strange, 2007) and performing RNAi in these nematodes (Mellouli et al., 2002), which identified the gene underlying a swelling-activated current. This gene, *clh-3,* encodes the splice variants CLH-3a and CLH-3b (He et al., 2006); (Denton et al., 2004) which have unique properties that make them ideal for structure-function studies. These properties are the localized differences in sequence (Denton et al., 2004) inherent with splice variants and the clear and discrete gating differences between CLH-3a and CLH-3b (He et al., 2006). Discreteness means that mutations to the

cytoplasmic portion of CLH-3a and CLH-3b generally give rise to channels with gating resembling one of the two splice variants (He et al., 2006). This discreteness may be due to gating differences between CLH-3a and CLH-3b originating from a small localized region of the channel.

Indeed, my studies have identified this small region to be nine consecutive amino acids near the C-terminus of the last CBS domain (CBS2). Specifically, interchanging these amino acids between CLH-3a and CLH-3b interchanges the channel gating. I have advanced the understanding of mechanisms for this modulation by utilizing homology modeling, model driven mutagenesis, and electrophysiology.

Our models show that these nine amino acids include part of the last alpha helix (α2) of CBS2, and predict that this alpha helix is 1-2 amino acids longer in CLH-3b than in CLH-3a. Using the model, I have predicted a possible interaction between A836 of α2 and F559 of the R Helix linker in CLH-3b.

Mutagenesis and electrophysiology reveal that mutation of either of these amino acids, A836K or F559D, converts gating of CLH-3b to that of CLH-3a. This demonstrates that α2 and the R helix linker both modulate channel gating and that they could interface, as predicted. There is only one other study (Martinez and Maduke, 2008) demonstrating that the R Helix linker regulates gating, and our study is the first that predicts the R helix linkers interface with functionally important regions of CBS domains. In short, this study presents a novel mechanisms by which CBS domains could regulate CLC gating. Future studies would be very beneficial for conclusively demonstrating this suggested role of the R Helix linker.

Future Directions

Conservation of the predicted R Helix linker – α2 interface

Interestingly, there is significant conservation of our proposed interaction between F559 in the R Helix linker and A836 in α2. F559 is conserved as a bulky hydrophobic amino acid in each family member of human CLCs, and A836 is conserved in CLC channels, but not transporters. Thus, one could hypothesize that there may be a mechanism shared among CLC channels where the R Helix linker may play a critical role in communicating information about the conformation of cytoplasmic C-terminus to intramembrane and extracellular regions. To test this, one would separately mutate to lysine or aspartate homologs of A836 and F559 in various CLCs. If these two mutations had similar effects on gating, there may be an interaction between the homologs of A836 and F559 that regulates channel gating.

Within CLH-3b, F559 may regulate gating changes due to cytoplasmic events besides α2 splice variation. Such events include phosphorylation via GCK-3 of the intracellular 101 amino acid regulatory domain (Figure 2), which mediates CLH-3b's volume sensitivity (Falin et al., 2009; Denton et al., 2005). If F559 mediated phosphorylation's effect on gating, F559D would likely alter sensitivity to cell swelling or GCK-3 phosphorylation (see introduction). Both these experiments regarding conservation could provide support for a role of the R helix linker's in transmitting various cytoplasmic conformational changes to the channel gate.

Is there a biochemical interaction between α2 and the R helix linker?

An essential follow up is to conclusively test for the predicted F559 - A836 interaction. The seemingly easiest approach is to mutate F559 and A836 to Cysteine, record gating, crosslink via oxidation, and rerecord gating. If the cysteine mutations changes gating and oxidation restores WT gating, one would conclude there is a physiological interaction. However, given that F559A and A836F have WT gating (unpublished preliminary data), F559C and A836C may also have WT gating. In that case, such experiments would be inconclusive.

As such, biochemical methods are needed. For instance, CLH-3b F559C/A836C could be split between the two CBS domains, oxidized to induce crosslinking, and run on a denaturing western. With that split location, the CBS1-CBS2 non-covalent interactions (Markovic and Dutzler, 2007; Meyer et al., 2007; Meyer and Dutzler, 2006) could maintain the overall cytoplasmic structure. The denaturing conditions would later disrupt the CBS1-CBS2 interaction, but not the predicted F559C-A836C disulfide bridge. Thus, if the residues interface, the full-length molecular weight would be detected. Instead of a western, Mass Spectrometry, Gel Filtration or Analytical Ultracentrifugation could be used to measure molecular weights.

In another approach, mass spectrometry could detect an interface. When Mass Spectrometry is used for sequencing proteins, the protein is digested into fragments whose composition can be determined (Hunt et al., 1986). Using a similar approach, if a fragment from the digested crosslinked cysteine mutant (CLH-3b F559C/A836C) contains both A836 and F559, then the residues interface.

As a control, each mentioned experiment should be performed on WT CLH-3b or CLH-3b with cysteines introduced at other known interaction sites in different monomers. A likely such interaction site is the monomer-monomer interface in α1 of CBS2 (Markovic and Dutzler, 2007), which is a leucine in CLC-Ka and the CLH-3b model.

Electron paramagnetic resonance can assess structural changes due to mutations

Electron paramagnetic resonance (EPR) can be used, not only to detect interactions, but also measure distances between residues (Klug and Feix, 2008), thereby elucidating structural information. Such structural information could identify whether the putative F559 – A836 interaction was altered by mutations, but not disrupted. Proteins with two strategically engineering cysteines would be tagged with sulfyhydryl compounds that contain one excitable unpaired electron. The two unpaired electrons, one per tag, can influence each other's excitation in a distance dependent manner, leading to distance measurements between the tagged cysteines (Klug and Feix, 2008).

I would measure distance in WT CLH-3b, WT CLH-3a, and CLH-3b F559D cytoplasmic regions. Two approaches are possible: engineering one cysteine per monomer of the homodimer or engineering two cysteines within one monomer and coexpressing with excess amounts of a cysteine-less monomer. The second method would allow more direct measurement of distances of our interest. However, I would consider it less favorable since it would entail synthesis of high amounts of protein and analysis could be complicated by the possibility of a four-cysteine complex.

Strategic placement of the cysteine residues is critical. Using one cysteine per monomer, I would engineer cysteines in four general locations: the outer surface of CBS1 (α1 or α2) and CBS2 α2, and the R Helix linker near F559 and near the ends of its rigid portion. Using cysteines in only monomer, I would engineer cysteines nearby to F559 and at either α2 of CBS2, another rigid part of the R Helix linker, or residues spread throughout the cytoplasmic region.

Do cytoplasmic mutations affect the conformation of the R helix?

An important question in the field is whether cytoplasmic CLC mutations affect the conformation of the R Helix, not just the R Helix linker. Such experiments would require synthesizing full length CLCs, which include the membrane region. Thus, using EPR and X-ray Crystallography to address this question would be challenging.

Computational studies involving docking the cytoplasmic and membrane regions may allow us to predict whether the R Helix interacts non-covalently with the R Helix linker or CBS2. If there is a predicted interface, then model-driven mutations and functional assays may shed light on the possibility of the R Helix transmitting functional information from the cytoplasmic region to the gate. Such models, however, must be interpreted with caution.

Cysteine accessibility experiments, such as those we used to assess extracellular conformational changes, could theoretically be used. The R helix, however, is exposed to the intracellular region, and as such would require membrane permeable sulfhydryl reagents or use of inside-out patch, which has been published in CLC-0 (Pusch et al.,

1997; Zifarelli et al., 2008), CLC-1 (Liantonio et al., 2003), a likely ortholog of CLC-2 (Ugarte et al., 2005), CLC-5 (Zifarelli and Pusch, 2009b), and renal Cl^- channels (Nissant et al., 2006; Lourdel et al., 2003), but not in the low conductance CLH-3b. CLC-0 to 2, as such, may make better model systems where the function altering R Helix linker mutation, F559D, is semi-conserved. Nonetheless, cysteine accessibility experiments have not been carried out with inside out-patch in CLCs, likely due to the low current magnitude nature of inside-out patch. The membrane permeable reagents may prove useful; however kinetics of inhibition cannot be accurately observed with these reagents.

Thus, it remains challenging and important to address whether cytoplasmic mutations, such as splice variation or R helix linker mutations, affect conformation of the R Helix. Such studies would be greatly enhanced by structural studies on full length protein or fast acting membrane permeable sulfhydryl reagents.

Closing Remarks

My studies have made significant headway into understanding how Cystathionine-β-Synthase domains regulate CLC channel gating. In particular, my studies demonstrate that interchanging α2 of CBS2 in the splice variants interchanges their gating properties. Moreover, mutation of predicted interacting residues in α2 and the R Helix linker also induces CLH-3a like gating in CLH-3b. This is the first study to provide support for a possible role of the R Helix linker in CBS domain regulation of channel gating. A role of the R Helix linker, which connects the R Helix to CBS

domains, is consistent with the hypothesized importance of the pore-forming R Helix in modulation of channel gating (Meyer and Dutzler, 2006; Dutzler et al., 2002). By extension, my studies suggest novel and valuable insights into mechanisms by which CBS domains could regulate gating and lead to muscle, kidney, and bone disorders of CLC channel function.

BIBLIOGRAPHY

Accardi,A. and Miller,C. (2004). Secondary active transport mediated by a prokaryotic homologue of ClC Cl- channels. Nature *427*, 803-807.

Akabas,M.H., Kaufmann,C., Archdeacon,P., and Karlin,A. (1994). Identification of acetylcholine receptor channel-lining residues in the entire M2 segment of the alpha subunit. Neuron *13*, 919-927.

Akabas,M.H., Stauffer,D.A., Xu,M., and Karlin,A. (1992). Acetylcholine receptor channel structure probed in cysteine-substitution mutants. Science *258*, 307-310.

Altschul,S.F., Madden,T.L., Schaffer,A.A., Zhang,J., Zhang,Z., Miller,W., and Lipman,D.J. (1997). Gapped BLAST and PSI-BLAST: a new generation of protein database search programs. Nucleic Acids Res. *25*, 3389-3402.

Barlassina,C., Dal Fiume,C., Lanzani,C., Manunta,P., Guffanti,G., Ruello,A., Bianchi,G., Del Vecchio,L., Macciardi,F., and Cusi,D. (2007). Common genetic variants and haplotypes in renal CLCNKA gene are associated to salt-sensitive hypertension. Hum. Mol. Genet. *16*, 1630-1638.

Bateman,A. (1997). The structure of a domain common to archaebacteria and the homocystinuria disease protein. Trends Biochem. Sci. *22*, 12-13.

Bateman,A. and Kickhoefer,V. (2003). The TROVE module: a common element in Telomerase, Ro and Vault ribonucleoproteins. BMC. Bioinformatics. *4*, 49.

Bennetts,B., Parker,M.W., and Cromer,B.A. (2007). Inhibition of skeletal muscle ClC-1 chloride channels by low intracellular pH and ATP. J. Biol. Chem. *282*, 32780-32791.

Bennetts,B., Roberts,M.L., Bretag,A.H., and Rychkov,G.Y. (2001). Temperature dependence of human muscle ClC-1 chloride channel. J. Physiol *535*, 83-93.

Bennetts,B., Rychkov,G.Y., Ng,H.L., Morton,C.J., Stapleton,D., Parker,M.W., and Cromer,B.A. (2005). Cytoplasmic ATP-sensing domains regulate gating of skeletal muscle ClC-1 chloride channels. J Biol. Chem. *280*, 32452-32458.

Bisset,D., Corry,B., and Chung,S.H. (2005). The fast gating mechanism in ClC-0 channels. Biophys. J. *89*, 179-186.

Blaustein,R.O., Cole,P.A., Williams,C., and Miller,C. (2000). Tethered blockers as molecular 'tape measures' for a voltage-gated K+ channel. Nat. Struct. Biol. *7*, 309-311.

Bonneau,R., Strauss,C.E., Rohl,C.A., Chivian,D., Bradley,P., Malmstrom,L., Robertson,T., and Baker,D. (2002). De novo prediction of three-dimensional structures for major protein families. J Mol. Biol. *322*, 65-78.

Bradley,P., Chivian,D., Meiler,J., Misura,K.M., Rohl,C.A., Schief,W.R., Wedemeyer,W.J., Schueler-Furman,O., Murphy,P., Schonbrun,J., Strauss,C.E., and Baker,D. (2003). Rosetta predictions in CASP5: successes, failures, and prospects for complete automation. Proteins *53 Suppl 6*, 457-468.

Brakemeier,S., Si,H., Gollasch,M., Hoffler,D., Buhl,M., Kohler,R., Hoyer,J., and Eichler,I. (2004). Dent's disease: identification of a novel mutation in the renal chloride channel CLCN5. Clin. Nephrol. *62*, 387-390.

Brandt,S. and Jentsch,T.J. (1995). ClC-6 and ClC-7 are two novel broadly expressed members of the CLC chloride channel family. FEBS Lett. *377*, 15-20.

Bykova,E.A., Zhang,X.D., Chen,T.Y., and Zheng,J. (2006). Large movement in the C terminus of CLC-0 chloride channel during slow gating. Nat. Struct. Mol. Biol. *13*, 1115-1119.

Canutescu,A.A., Shelenkov,A.A., and Dunbrack,R.L., Jr. (2003). A graph-theory algorithm for rapid protein side-chain prediction. Protein Sci. *12*, 2001-2014.

Carr,G., Simmons,N., and Sayer,J. (2003). A role for CBS domain 2 in trafficking of chloride channel CLC-5. Biochem. Biophys. Res. Commun. *310*, 600-605.

Chen,T.Y. (1998). Extracellular zinc ion inhibits ClC-0 chloride channels by facilitating slow gating. J. Gen. Physiol *112*, 715-726.

Christensen,E.I., Devuyst,O., Dom,G., Nielsen,R., Van der,S.P., Verroust,P., Leruth,M., Guggino,W.B., and Courtoy,P.J. (2003). Loss of chloride channel ClC-5 impairs endocytosis by defective trafficking of megalin and cubilin in kidney proximal tubules. Proc. Natl. Acad. Sci. U. S. A *100*, 8472-8477.

Cox,J.P., Yamamoto,K., Christie,P.T., Wooding,C., Feest,T., Flinter,F.A., Goodyer,P.R., Leumann,E., Neuhaus,T., Reid,C., Williams,P.F., Wrong,O., and Thakker,R.V. (1999). Renal chloride channel, CLCN5, mutations in Dent's disease. J. Bone Miner. Res. *14*, 1536-1542.

Dan,I., Watanabe,N.M., and Kusumi,A. (2001). The Ste20 group kinases as regulators of MAP kinase cascades. Trends Cell Biol. *11*, 220-230.

Darman,R.B., Ivy,A.A., Ketty,V., and Blaustein,R.O. (2006). Constraints on voltage sensor movement in the shaker K+ channel. J. Gen. Physiol *128*, 687-699.

Davis,M.W., Somerville,D., Lee,R.Y., Lockery,S., Avery,L., and Fambrough,D.M. (1995). Mutations in the Caenorhabditis elegans Na,K-ATPase alpha-subunit gene, eat-6, disrupt excitable cell function. J. Neurosci. *15*, 8408-8418.

Day,P., Sharff,A., Parra,L., Cleasby,A., Williams,M., Horer,S., Nar,H., Redemann,N., Tickle,I., and Yon,J. (2007). Structure of a CBS-domain pair from the regulatory gamma1 subunit of human AMPK in complex with AMP and ZMP. Acta Crystallogr. D. Biol. Crystallogr. *63*, 587-596.

De Angeli,A., Moran,O., Wege,S., Filleur,S., Ephritikhine,G., Thomine,S., Barbier-Brygoo,H., and Gambale,F. (2009). ATP binding to the C terminus of the Arabidopsis thaliana nitrate/proton antiporter, AtCLCa, regulates nitrate transport into plant vacuoles. J. Biol. Chem. *284*, 26526-26532.

de Diego,C., Gamez,J., Plassart-Schiess,E., Lasa,A., Del Rio,E., Cervera,C., Baiget,M., Gallano,P., and Fontaine,B. (1999). Novel mutations in the muscle chloride channel CLCN1 gene causing myotonia congenita in Spanish families. J Neurol. *246*, 825-829.

de Santiago,J.A., Nehrke,K., and Arreola,J. (2005). Quantitative analysis of the voltage-dependent gating of mouse parotid ClC-2 chloride channel. J. Gen. Physiol *126*, 591-603.

Denton,J., Nehrke,K., Rutledge,E., Morrison,R., and Strange,K. (2004). Alternative splicing of N- and C-termini of a C. elegans ClC channel alters gating and sensitivity to external Cl- and H+. J. Physiol *555*, 97-114.

Denton,J., Nehrke,K., Yin,X., Beld,A.M., and Strange,K. (2006). Altered gating and regulation of a carboxy-terminal ClC channel mutant expressed in the Caenorhabditis elegans oocyte. Am. J. Physiol Cell Physiol *290*, C1109-C1118.

Denton,J., Nehrke,K., Yin,X., Morrison,R., and Strange,K. (2005). GCK-3, a newly identified Ste20 kinase, binds to and regulates the activity of a cell cycle-dependent ClC anion channel. J. Gen. Physiol *125*, 113-125.

Dill,K.A. (1990). Dominant forces in protein folding. Biochemistry *29*, 7133-7155.

Dong,E., Smith,J., Heinze,S., Alexander,N., and Meiler,J. (2008). BCL::Align-sequence alignment and fold recognition with a custom scoring function online. Gene *422*, 41-46.

Dowd,B.F. and Forbush,B. (2003). PASK (proline-alanine-rich STE20-related kinase), a regulatory kinase of the Na-K-Cl cotransporter (NKCC1). J. Biol. Chem. *278*, 27347-27353.

Dudley,N.R. and Goldstein,B. (2005). RNA interference in Caenorhabditis elegans. Methods Mol. Biol. *309*, 29-38.

Dutzler,R., Campbell,E.B., Cadene,M., Chait,B.T., and MacKinnon,R. (2002). X-ray structure of a ClC chloride channel at 3.0 A reveals the molecular basis of anion selectivity. Nature *415*, 287-294.

Dutzler,R., Campbell,E.B., and MacKinnon,R. (2003). Gating the selectivity filter in ClC chloride channels. Science *300*, 108-112.

Engh,A.M. and Maduke,M. (2005). Cysteine accessibility in ClC-0 supports conservation of the ClC intracellular vestibule. J. Gen. Physiol *125*, 601-617.

Estevez,R., Pusch,M., Ferrer-Costa,C., Orozco,M., and Jentsch,T.J. (2004). Functional and structural conservation of CBS domains from CLC chloride channels. J Physiol *557*, 363-378.

Estevez,R., Schroeder,B.C., Accardi,A., Jentsch,T.J., and Pusch,M. (2003). Conservation of chloride channel structure revealed by an inhibitor binding site in ClC-1. Neuron *38*, 47-59.

Fahlke,C. (2001). Ion permeation and selectivity in ClC-type chloride channels. Am. J. Physiol Renal Physiol *280*, F748-F757.

Falin,R.A., Morrison,R., Ham,A.J., and Strange,K. (2009). Identification of regulatory phosphorylation sites in a cell volume- and Ste20 kinase-dependent ClC anion channel. J. Gen. Physiol *133*, 29-42.

Finn,R.D., Mistry,J., Schuster-Bockler,B., Griffiths-Jones,S., Hollich,V., Lassmann,T., Moxon,S., Marshall,M., Khanna,A., Durbin,R., Eddy,S.R., Sonnhammer,E.L.L., and Bateman,A. (2006). Pfam: clans, web tools and services. Nucl. Acids Res. *34*, D247-D251.

Fong,P., Rehfeldt,A., and Jentsch,T.J. (1998). Determinants of slow gating in ClC-0, the voltage-gated chloride channel of Torpedo marmorata. Am. J. Physiol *274*, C966-C973.

Gagnon,K.B., England,R., and Delpire,E. (2006). Volume sensitivity of cation-Cl- cotransporters is modulated by the interaction of two kinases: Ste20-related proline-alanine-rich kinase and WNK4. Am. J. Physiol Cell Physiol *290*, C134-C142.

Gleitsman,K.R., Shanata,J.A., Frazier,S.J., Lester,H.A., and Dougherty,D.A. (2009). Long-range coupling in an allosteric receptor revealed by mutant cycle analysis. Biophys. J. *96*, 3168-3178.

Goodman,M.B., Hall,D.H., Avery,L., and Lockery,S.R. (1998). Active currents regulate sensitivity and dynamic range in C. elegans neurons. Neuron *20*, 763-772.

Grand,T., Mordasini,D., L'Hoste,S., Pennaforte,T., Genete,M., Biyeyeme,M.J., Vargas-Poussou,R., Blanchard,A., Teulon,J., and Lourdel,S. (2009). Novel CLCN5 mutations in patients with Dent's disease result in altered ion currents or impaired exchanger processing. Kidney Int. *76*, 999-1005.

Greenstein,D. (2005). Control of oocyte meiotic maturation and fertilization. WormBook. 1-12.

Hara-Chikuma,M., Wang,Y., Guggino,S.E., Guggino,W.B., and Verkman,A.S. (2005). Impaired acidification in early endosomes of ClC-5 deficient proximal tubule. Biochem. Biophys. Res. Commun. *329*, 941-946.

Hartzell,C., Qu,Z., Putzier,I., Artinian,L., Chien,L.T., and Cui,Y. (2005). Looking chloride channels straight in the eye: bestrophins, lipofuscinosis, and retinal degeneration. Physiology. (Bethesda.) *20*, 292-302.

Hattori,M., Tanaka,Y., Fukai,S., Ishitani,R., and Nureki,O. (2007). Crystal structure of the MgtE Mg2+ transporter. Nature *448*, 1072-1075.

He,L., Denton,J., Nehrke,K., and Strange,K. (2006). Carboxy terminus splice variation alters ClC channel gating and extracellular cysteine reactivity. Biophys. J. *90*, 3570-3581.

Hebeisen,S., Biela,A., Giese,B., Muller-Newen,G., Hidalgo,P., and Fahlke,C. (2004). The role of the carboxyl terminus in ClC chloride channel function. J Biol. Chem. *279*, 13140-13147.

Henikoff,S. and Henikoff,J.G. (1992). Amino acid substitution matrices from protein blocks. Proc. Natl. Acad. Sci. U. S. A *89*, 10915-10919.

Hryciw,D.H., Rychkov,G.Y., Hughes,B.P., and Bretag,A.H. (1998). Relevance of the D13 region to the function of the skeletal muscle chloride channel, ClC-1. J. Biol. Chem. *273*, 4304-4307.

Hunt,D.F., Yates,J.R., III, Shabanowitz,J., Winston,S., and Hauer,C.R. (1986). Protein sequencing by tandem mass spectrometry. Proc. Natl. Acad. Sci. U. S. A *83*, 6233-6237.

Igarashi,T., Gunther,W., Sekine,T., Inatomi,J., Shiraga,H., Takahashi,S., Suzuki,J., Tsuru,N., Yanagihara,T., Shimazu,M., Jentsch,T.J., and Thakker,R.V. (1998). Functional characterization of renal chloride channel, CLCN5, mutations associated with Dent'sJapan disease. Kidney Int. *54*, 1850-1856.

Ignoul,S. and Eggermont,J. (2005). CBS domains: structure, function, and pathology in human proteins. Am J Physiol Cell Physiol *289*, C1369-C1378.

Janosik,M., Kery,V., Gaustadnes,M., Maclean,K.N., and Kraus,J.P. (2001). Regulation of Human Cystathionine-Beta-Synthase by S-Adenosyl-L-methionine: Evidence for Two Catalytically Active Conformations Involving an Autoinhibitory Domain in the C-Terminal Region. Biochemistry *40*, 10625-10633.

Jeck,N., Konrad,M., Peters,M., Weber,S., Bonzel,K.E., and Seyberth,H.W. (2000). Mutations in the chloride channel gene, CLCNKB, leading to a mixed Bartter-Gitelman phenotype. Pediatr. Res. *48*, 754-758.

Jentsch,T.J. (2008). CLC chloride channels and transporters: from genes to protein structure, pathology and physiology. Crit Rev. Biochem. Mol. Biol. *43*, 3-36.

Jentsch,T.J., Gunther,W., Pusch,M., and Schwappach,B. (1995). Properties of voltage-gated chloride channels of the ClC gene family. J. Physiol *482*, 19S-25S.

Jentsch,T.J., Stein,V., Weinreich,F., and Zdebik,A.A. (2002). Molecular structure and physiological function of chloride channels. Physiol Rev. *82*, 503-568.

Jhee,K.H., McPhie,P., and Miles,E.W. (2000). Domain Architecture of the Heme-Independent Yeast Cystathionine-Beta-Synthase Provides Insights into Mechanisms of Catalysis and Regulation. Biochemistry *39*, 10548-10556.

Jin,X., Townley,R., and Shapiro,L. (2007). Structural Insight into AMPK Regulation: ADP Comes into Play. Structure *15*, 1285-1295.

Jones,D.T. (1999). Protein secondary structure prediction based on position-specific scoring matrices. J Mol. Biol. *292*, 195-202.

Karlin,A. and Akabas,M.H. (1998). Substituted-cysteine accessibility method. Methods Enzymol. *293*, 123-145.

Karplus,K., Barrett,C., and Hughey,R. (1998). Hidden Markov models for detecting remote protein homologies. Bioinformatics *14*, 846-856.

Kaufmann,K.W., Lemmon,G.H., Deluca,S.L., Sheehan,J.H., and Meiler,J. (2010). Practically useful: what the Rosetta protein modeling suite can do for you. Biochemistry *49*, 2987-2998.

Kawakami,S. and Hashida,M. (2007). Targeted delivery systems of small interfering RNA by systemic administration. Drug Metab Pharmacokinet. *22*, 142-151.

Kennan,A., Aherne,A., Palfi,A., Humphries,M., McKee,A., Stitt,A., Simpson,D.A., Demtroder,K., Orntoft,T., Ayuso,C., Kenna,P.F., Farrar,G.J., and Humphries,P. (2002). Identification of an IMPDH1 mutation in autosomal dominant retinitis pigmentosa

(RP10) revealed following comparative microarray analysis of transcripts derived from retinas of wild-type and Rho(-/-) mice. Hum. Mol. Genet. *11*, 547-557.

Klug,C.S. and Feix,J.B. (2008). Methods and applications of site-directed spin labeling EPR spectroscopy. Methods Cell Biol. *84*, 617-658.

Koch,M.C., Steinmeyer,K., Lorenz,C., Ricker,K., Wolf,F., Otto,M., Zoll,B., Lehmann-Horn,F., Grzeschik,K.H., and Jentsch,T.J. (1992). The skeletal muscle chloride channel in dominant and recessive human myotonia. Science *257*, 797-800.

Konrad,M., Vollmer,M., Lemmink,H.H., van den Heuvel,L.P., Jeck,N., Vargas-Poussou,R., Lakings,A., Ruf,R., Deschenes,G., Antignac,C., Guay-Woodford,L., Knoers,N.V., Seyberth,H.W., Feldmann,D., and Hildebrandt,F. (2000). Mutations in the chloride channel gene CLCNKB as a cause of classic Bartter syndrome. J. Am. Soc. Nephrol. *11*, 1449-1459.

Kornak,U., Kasper,D., Bosl,M.R., Kaiser,E., Schweizer,M., Schulz,A., Friedrich,W., Delling,G., and Jentsch,T.J. (2001). Loss of the ClC-7 chloride channel leads to osteopetrosis in mice and man. Cell *104*, 205-215.

Kortemme,T. and Baker,D. (2002). A simple physical model for binding energy hot spots in protein-protein complexes. Proc. Natl. Acad. Sci. U. S. A *99*, 14116-14121.

Laskowski,R.A., MacArthur,M.W., Moss,D.S., and Thornton,J.M. (1993). PROCHECK: a program to check the stereochemical quality of protein structures. Journal of Applied Crystallography *26*, 283-291.

Lee,R.Y., Lobel,L., Hengartner,M., Horvitz,H.R., and Avery,L. (1997). Mutations in the alpha1 subunit of an L-type voltage-activated Ca2+ channel cause myotonia in Caenorhabditis elegans. EMBO J. *16*, 6066-6076.

Lennard-Jones, JE. On the Determination of Molecular Fields. Proceeds of the Royal Society of London 106[738], 463-477. 1924.
Ref Type: Generic

Li,Y., Yu,W.P., Lin,C.W., and Chen,T.Y. (2005). Oxidation and reduction control of the inactivation gating of Torpedo ClC-0 chloride channels. Biophys. J. *88*, 3936-3945.

Liantonio,A., De Luca,A., Pierno,S., Didonna,M.P., Loiodice,F., Fracchiolla,G., Tortorella,P., Antonio,L., Bonerba,E., Traverso,S., Elia,L., Picollo,A., Pusch,M., and Camerino,D.C. (2003). Structural requisites of 2-(p-chlorophenoxy)propionic acid analogues for activity on native rat skeletal muscle chloride conductance and on heterologously expressed CLC-1. Br. J. Pharmacol. *139*, 1255-1264.

Lieberman,J., Song,E., Lee,S.K., and Shankar,P. (2003). Interfering with disease: opportunities and roadblocks to harnessing RNA interference. Trends Mol. Med. *9*, 397-403.

Lin,C.W. and Chen,T.Y. (2003). Probing the pore of ClC-0 by substituted cysteine accessibility method using methane thiosulfonate reagents. J. Gen. Physiol *122*, 147-159.

Lin,M.J., You,T.H., Pan,H., and Hsiao,K.M. (2006). Functional characterization of CLCN1 mutations in Taiwanese patients with myotonia congenita via heterologous expression. Biochem. Biophys. Res. Commun. *351*, 1043-1047.

Lloyd,S.E., Gunther,W., Pearce,S.H., Thomson,A., Bianchi,M.L., Bosio,M., Craig,I.W., Fisher,S.E., Scheinman,S.J., Wrong,O., Jentsch,T.J., and Thakker,R.V. (1997). Characterisation of renal chloride channel, CLCN5, mutations in hypercalciuric nephrolithiasis (kidney stones) disorders. Hum. Mol. Genet. *6*, 1233-1239.

Lloyd,S.E., Pearce,S.H., Fisher,S.E., Steinmeyer,K., Schwappach,B., Scheinman,S.J., Harding,B., Bolino,A., Devoto,M., Goodyer,P., Rigden,S.P., Wrong,O., Jentsch,T.J., Craig,I.W., and Thakker,R.V. (1996). A common molecular basis for three inherited kidney stone diseases. Nature *379*, 445-449.

Lockery,S.R., Goodman,M.B., and Faumont,S. (2009). First report of action potentials in a C. elegans neuron is premature. Nat. Neurosci. *12*, 365-366.

Lossin,C. and George,A.L., Jr. (2008). Myotonia congenita. Adv. Genet. *63*, 25-55.

Lourdel,S., Paulais,M., Marvao,P., Nissant,A., and Teulon,J. (2003). A chloride channel at the basolateral membrane of the distal-convoluted tubule: a candidate ClC-K channel. J. Gen. Physiol *121*, 287-300.

Lu,G. and Moriyama,E.N. (2004). Vector NTI, a balanced all-in-one sequence analysis suite. Brief. Bioinform. *5*, 378-388.

Ludewig,U., Pusch,M., and Jentsch,T.J. (1996). Two physically distinct pores in the dimeric ClC-0 chloride channel. Nature *383*, 340-343.

Ludewig,U., Pusch,M., and Jentsch,T.J. (1997). Independent gating of single pores in CLC-0 chloride channels. Biophys. J. *73*, 789-797.

Macias,M.J., Teijido,O., Zifarelli,G., Martin,P., Ramirez-Espain,X., Zorzano,A., Palacin,M., Pusch,M., and Estevez,R. (2007). Myotonia-related mutations in the distal C-terminus of ClC-1 and ClC-0 chloride channels affect the structure of a poly-proline helix. Biochem. J. *403*, 79-87.

Maeno,E., Ishizaki,Y., Kanaseki,T., Hazama,A., and Okada,Y. (2000). Normotonic cell shrinkage because of disordered volume regulation is an early prerequisite to apoptosis. Proc. Natl. Acad. Sci. U. S. A *97*, 9487-9492.

Mahmood,N.A., Biemans-Oldehinkel,E., and Poolman,B. (2009). Engineering of ion sensing by the cystathionine beta-synthase module of the ABC transporter OpuA. J. Biol. Chem. *284*, 14368-14376.

Markovic,S. and Dutzler,R. (2007). The structure of the cytoplasmic domain of the chloride channel ClC-Ka reveals a conserved interaction interface. Structure. *15*, 715-725.

Martinez,G.Q. and Maduke,M. (2008). A cytoplasmic domain mutation in ClC-Kb affects long-distance communication across the membrane. PLoS. One. *3*, e2746.

Matsumura,Y., Uchida,S., Kondo,Y., Miyazaki,H., Ko,S.B., Hayama,A., Morimoto,T., Liu,W., Arisawa,M., Sasaki,S., and Marumo,F. (1999). Overt nephrogenic diabetes insipidus in mice lacking the CLC-K1 chloride channel. Nat. Genet. *21*, 95-98.

McGuffin,L.J., Bryson,K., and Jones,D.T. (2000). The PSIPRED protein structure prediction server. Bioinformatics. *16*, 404-405.

Meiler,J. and Baker,D. (2003). Coupled prediction of protein secondary and tertiary structure. Proc. Natl. Acad. Sci. U. S. A *100*, 12105-12110.

Mellem,J.E., Brockie,P.J., Madsen,D.M., and Maricq,A.V. (2008). Action potentials contribute to neuronal signaling in C. elegans. Nat. Neurosci. *11*, 865-867.

Mellouli,L., Karray-Rebai,I., and Bejar,S. (2002). Construction of alpha-amylase-producing strains not subject to carbon catabolite repression. FEMS Microbiol. Lett. *206*, 157-162.

Meyer,S. and Dutzler,R. (2006). Crystal structure of the cytoplasmic domain of the chloride channel ClC-0. Structure. *14*, 299-307.

Meyer,S., Savaresi,S., Forster,I.C., and Dutzler,R. (2007). Nucleotide recognition by the cytoplasmic domain of the human chloride transporter ClC-5. Nat. Struct. Mol. Biol. *14*, 60-67.

Miller,C. (1982). Open-state substructure of single chloride channels from Torpedo electroplax. Philos. Trans. R. Soc. Lond B Biol. Sci *299*, 401-411.

Miller,M.D., Schwarzenbacher,R., von Delft,F., Abdubek,P., Ambing,E., Biorac,T., Brinen,L.S., Canaves,J.M., Cambell,J., Chiu,H.J., Dai,X., Deacon,A.M., DiDonato,M., Elsliger,M.A., Eshagi,S., Floyd,R., Godzik,A., Grittini,C., Grzechnik,S.K., Hampton,E.,

Jaroszewski,L., Karlak,C., Klock,H.E., Koesema,E., Kovarik,J.S., Kreusch,A., Kuhn,P., Lesley,S.A., Levin,I., McMullan,D., McPhillips,T.M., Morse,A., Moy,K., Ouyang,J., Page,R., Quijano,K., Robb,A., Spraggon,G., Stevens,R.C., van den,B.H., Velasquez,J., Vincent,J., Wang,X., West,B., Wolf,G., Xu,Q., Hodgson,K.O., Wooley,J., and Wilson,I.A. (2004). Crystal structure of a tandem cystathionine-beta-synthase (CBS) domain protein (TM0935) from Thermotoga maritima at 1.87 A resolution. Proteins *57*, 213-217.

Mitchison,J.M. (2003). Growth during the cell cycle. Int. Rev. Cytol. *226*, 165-258.

Nehrke,K., Begenisich,T., Pilato,J., and Melvin,J.E. (2000). Into ion channel and transporter function. Caenorhabditis elegans ClC-type chloride channels: novel variants and functional expression. Am. J. Physiol Cell Physiol *279*, C2052-C2066.

Nissant,A., Paulais,M., Lachheb,S., Lourdel,S., and Teulon,J. (2006). Similar chloride channels in the connecting tubule and cortical collecting duct of the mouse kidney. Am. J. Physiol Renal Physiol *290*, F1421-F1429.

Oliveira,S.M., Ehtisham,J., Redwood,C.S., Ostman-Smith,I., Blair,E.M., and Watkins,H. (2003). Mutation analysis of AMP-activated protein kinase subunits in inherited cardiomyopathies: implications for kinase function and disease pathogenesis. J Mol. Cell Cardiol. *35*, 1251-1255.

Pagni,M., Ioannidis,V., Cerutti,L., Zahn-Zabal,M., Jongeneel,C.V., and Falquet,L. (2004). MyHits: a new interactive resource for protein annotation and domain identification. Nucl. Acids Res. *32*, W332-W335.

Pangrazio,A., Pusch,M., Caldana,E., Frattini,A., Lanino,E., Tamhankar,P.M., Phadke,S., Lopez,A.G., Orchard,P., Mihci,E., Abinun,M., Wright,M., Vettenranta,K., Bariae,I., Melis,D., Tezcan,I., Baumann,C., Locatelli,F., Zecca,M., Horwitz,E., Mansour,L.S., Van Roij,M., Vezzoni,P., Villa,A., and Sobacchi,C. (2010). Molecular and clinical heterogeneity in CLCN7-dependent osteopetrosis: report of 20 novel mutations. Hum. Mutat. *31*, E1071-E1080.

Pena-Munzenmayer,G., Catalan,M., Cornejo,I., Figueroa,C.D., Melvin,J.E., Niemeyer,M.I., Cid,L.P., and Sepulveda,F.V. (2005). Basolateral localization of native ClC-2 chloride channels in absorptive intestinal epithelial cells and basolateral sorting encoded by a CBS-2 domain di-leucine motif. J Cell Sci *118*, 4243-4252.

Petalcorin,M.I., Oka,T., Koga,M., Ogura,K., Wada,Y., Ohshima,Y., and Futai,M. (1999). Disruption of clh-1, a chloride channel gene, results in a wider body of Caenorhabditis elegans. J. Mol. Biol. *294*, 347-355.

Picollo,A. and Pusch,M. (2005). Chloride/proton antiporter activity of mammalian CLC proteins ClC-4 and ClC-5. Nature *436*, 420-423.

Plans,V., Rickheit,G., and Jentsch,T.J. (2009). Physiological roles of CLC Cl(-)/H (+) exchangers in renal proximal tubules. Pflugers Arch. *458*, 23-37.

Pombo,C.M., Force,T., Kyriakis,J., Nogueira,E., Fidalgo,M., and Zalvide,J. (2007). The GCK II and III subfamilies of the STE20 group kinases. Front Biosci. *12*, 850-859.

Ponder,J.W. and Case,D.A. (2003). Force fields for protein simulations. Adv. Protein Chem *66*, 27-85.

Pugalenthi,G., Shameer,K., Srinivasan,N., and Sowdhamini,R. (2006). HARMONY: a server for the assessment of protein structures. Nucleic Acids Res. *34*, W231-W234.

Pusch,M. (2002). Myotonia caused by mutations in the muscle chloride channel gene CLCN1. Hum. Mutat. *19*, 423-434.

Pusch,M., Ludewig,U., and Jentsch,T.J. (1997). Temperature dependence of fast and slow gating relaxations of ClC-0 chloride channels. J. Gen. Physiol *109*, 105-116.

Pusch,M., Ludewig,U., Rehfeldt,A., and Jentsch,T.J. (1995). Gating of the voltage-dependent chloride channel CIC-0 by the permeant anion. Nature *373*, 527-531.

Quevillon,E., Silventoinen,V., Pillai,S., Harte,N., Mulder,N., Apweiler,R., and Lopez,R. (2005). InterProScan: protein domains identifier. Nucleic Acids Res. *33*, W116-W120.

R.M.Schwartz and M.O.Dayhoff. Matrices for detecting distant relationships. Atlas of Protein Sequence and Structure , 353-358. 1978. Natl. Biomed. Res. Found., Washington, DC.
Ref Type: Generic

Rohl,C.A., Strauss,C.E., Chivian,D., and Baker,D. (2004). Modeling structurally variable regions in homologous proteins with rosetta. Proteins *55*, 656-677.

Rudolph,M.J., Amodeo,G.A., Iram,S.H., Hong,S.P., Pirino,G., Carlson,M., and Tong,L. (2007). Structure of the Bateman2 domain of yeast Snf4: dimeric association and relevance for AMP binding. Structure. *15*, 65-74.

Rutledge,E., Bianchi,L., Christensen,M., Boehmer,C., Morrison,R., Broslat,A., Beld,A.M., George,A.L., Greenstein,D., and Strange,K. (2001). CLH-3, a ClC-2 anion channel ortholog activated during meiotic maturation in C. elegans oocytes. Curr. Biol. *11*, 161-170.

Rutledge,E., Denton,J., and Strange,K. (2002). Cell cycle- and swelling-induced activation of a Caenorhabditis elegans ClC channel is mediated by CeGLC-7alpha/beta phosphatases. J. Cell Biol. *158*, 435-444.

Rychkov,G.Y., Pusch,M., Astill,D.S., Roberts,M.L., Jentsch,T.J., and Bretag,A.H. (1996). Concentration and pH dependence of skeletal muscle chloride channel ClC-1. J. Physiol *497 (Pt 2)*, 423-435.

Sali,A. and Blundell,T.L. (1993). Comparative Protein Modelling by Satisfaction of Spatial Restraints. Journal of Molecular Biology *234*, 779-815.

Sasaki,R., Ichiyasu,H., Ito,N., Ikeda,T., Takano,H., Ikeuchi,T., Kuzuhara,S., Uchino,M., Tsuji,S., and Uyama,E. (1999). Novel chloride channel gene mutations in two unrelated Japanese families with Becker's autosomal recessive generalized myotonia. Neuromuscul. Disord. *9*, 587-592.

Sasaki,S., Uchida,S., Kawasaki,M., Adachi,S., and Marumo,F. (1994). ClC family in the kidney. Jpn. J. Physiol *44 Suppl 2*, S3-S8.

Schmidt-Rose,T. and Jentsch,T.J. (1997). Reconstitution of functional voltage-gated chloride channels from complementary fragments of CLC-1. J Biol. Chem. *272*, 20515-20521.

Schreiber,G. and Fersht,A.R. (1995). Energetics of protein-protein interactions: analysis of the barnase-barstar interface by single mutations and double mutant cycles. J. Mol. Biol. *248*, 478-486.

Schriever,A.M., Friedrich,T., Pusch,M., and Jentsch,T.J. (1999). CLC chloride channels in Caenorhabditis elegans. J. Biol. Chem. *274*, 34238-34244.

Schultz,J., Milpetz,F., Bork,P., and Ponting,C.P. (1998). SMART, a simple modular architecture research tool: identification of signaling domains. Proc. Natl. Acad. Sci. U. S. A *95*, 5857-5864.

Scott,J.W., Hawley,S.A., Green,K.A., Anis,M., Stewart,G., Scullion,G.A., Norman,D.G., and Hardie,D.G. (2004). CBS domains form energy-sensing modules whose binding of adenosine ligands is disrupted by disease mutations. J Clin. Invest *113*, 274-284.

Shan,X. and Kruger,W.D. (1998). Correction of disease-causing CBS mutations in yeast. Nat. Genet. *19*, 91-93.

Simon,D.B., Bindra,R.S., Mansfield,T.A., Nelson-Williams,C., Mendonca,E., Stone,R., Schurman,S., Nayir,A., Alpay,H., Bakkaloglu,A., Rodriguez-Soriano,J., Morales,J.M., Sanjad,S.A., Taylor,C.M., Pilz,D., Brem,A., Trachtman,H., Griswold,W., Richard,G.A., John,E., and Lifton,R.P. (1997). Mutations in the chloride channel gene, CLCNKB, cause Bartter's syndrome type III. Nat. Genet. *17*, 171-178.

Simons,K.T., Kooperberg,C., Huang,E., and Baker,D. (1997a). Assembly of protein tertiary structures from fragments with similar local sequences using simulated annealing and Bayesian scoring functions. J. Mol. Biol. *268*, 209-225.

Simons,K.T., Kooperberg,C., Huang,E., and Baker,D. (1997b). Assembly of protein tertiary structures from fragments with similar local sequences using simulated annealing and bayesian scoring functions. Journal of Molecular Biology *268*, 209-225.

Steinmeyer,K., Schwappach,B., Bens,M., Vandewalle,A., and Jentsch,T.J. (1995). Cloning and functional expression of rat CLC-5, a chloride channel related to kidney disease. J. Biol. Chem. *270*, 31172-31177.

Steinmeyer,K., Ortland,C., and Jentsch,T.J. (1991). Primary structure and functional expression of a developmentally regulated skeletal muscle chloride channel. Nature *354*, 301-304.

Stobrawa,S.M., Breiderhoff,T., Takamori,S., Engel,D., Schweizer,M., Zdebik,A.A., Bosl,M.R., Ruether,K., Jahn,H., Draguhn,A., Jahn,R., and Jentsch,T.J. (2001). Disruption of ClC-3, a chloride channel expressed on synaptic vesicles, leads to a loss of the hippocampus. Neuron *29*, 185-196.

Strange,K. (2007). Revisiting the Krogh Principle in the post-genome era: Caenorhabditis elegans as a model system for integrative physiology research. J. Exp. Biol. *210*, 1622-1631.

Suzuki,M., Morita,T., and Iwamoto,T. (2006). Diversity of Cl(-) channels. Cell Mol. Life Sci. *63*, 12-24.

Tanaka,Y., Hattori,M., Fukai,S., Ishitania,R., and Nureki,O. (2007). Crystallization and preliminary X-ray diffraction analysis of the cytosolic domain of the Mg2+ transporter MgtE. Acta Crystallogr. Sect. F. Struct. Biol. Cryst. Commun. *63*, 678-681.

Thiemann,A., Grunder,S., Pusch,M., and Jentsch,T.J. (1992). A chloride channel widely expressed in epithelial and non-epithelial cells. Nature *356*, 57-60.

Ticku,M.K. (1983). Benzodiazepine-GABA receptor-ionophore complex. Current concepts. Neuropharmacology *22*, 1459-1470.

Timmons,L., Tabara,H., Mello,C.C., and Fire,A.Z. (2003). Inducible systemic RNA silencing in Caenorhabditis elegans. Mol. Biol. Cell *14*, 2972-2983.

Tosetto,E., Ceol,M., Mezzabotta,F., Ammenti,A., Peruzzi,L., Caruso,M.R., Barbano,G., Vezzoli,G., Colussi,G., Vergine,G., Giordano,M., Glorioso,N., Degortes,S., Soldati,L., Sayer,J., D'Angelo,A., and Anglani,F. (2009). Novel mutations of the CLCN5 gene

including a complex allele and A 5' UTR mutation in Dent disease 1. Clin. Genet. *76*, 413-416.

Townley,R. and Shapiro,L. (2007). Crystal structures of the adenylate sensor from fission yeast AMP-activated protein kinase. Science *315*, 1726-1729.

Traverso,S., Elia,L., and Pusch,M. (2003). Gating competence of constitutively open CLC-0 mutants revealed by the interaction with a small organic Inhibitor. J Gen. Physiol *122*, 295-306.

Traverso,S., Zifarelli,G., Aiello,R., and Pusch,M. (2006). Proton sensing of CLC-0 mutant E166D. J. Gen. Physiol *127*, 51-65.

Uchida,S. (2000). Physiological role of CLC-K1 chloride channel in the kidney. Nephrol. Dial. Transplant. *15 Suppl 6*, 14-15.

Ugarte,G., Delgado,R., O'Day,P.M., Farjah,F., Cid,L.P., Vergara,C., and Bacigalupo,J. (2005). Putative ClC-2 chloride channel mediates inward rectification in Drosophila retinal photoreceptors. J. Membr. Biol. *207*, 151-160.

Vriend,G. (1990). WHAT IF: a molecular modeling and drug design program. J. Mol. Graph. *8*, 52-6, 29.

Waldegger,S. and Jentsch,T.J. (2000). From tonus to tonicity: physiology of CLC chloride channels. J. Am. Soc. Nephrol. *11*, 1331-1339.

Wang,X.Q., Deriy,L.V., Foss,S., Huang,P., Lamb,F.S., Kaetzel,M.A., Bindokas,V., Marks,J.D., and Nelson,D.J. (2006). CLC-3 channels modulate excitatory synaptic transmission in hippocampal neurons. Neuron *52*, 321-333.

Wolf,K., Meier-Meitinger,M., Bergler,T., Castrop,H., Vitzthum,H., Riegger,G.A., Kurtz,A., and Kramer,B.K. (2003). Parallel down-regulation of chloride channel CLC-K1 and barttin mRNA in the thin ascending limb of the rat nephron by furosemide. Pflugers Arch. *446*, 665-671.

Woods,R. and Case,D. (2005). The Amber biomolecular simulation programs. J. Computat. Chem *26*, 1668-1688.

Wu,W., Rychkov,G.Y., Hughes,B.P., and Bretag,A.H. (2006). Functional complementation of truncated human skeletal-muscle chloride channel (hClC-1) using carboxyl tail fragments. Biochem. J. *395*, 89-97.

Yamamoto,K., Cox,J.P., Friedrich,T., Christie,P.T., Bald,M., Houtman,P.N., Lapsley,M.J., Patzer,L., Tsimaratos,M., Van'T Hoff,W.G., Yamaoka,K., Jentsch,T.J., and

Thakker,R.V. (2000). Characterization of renal chloride channel (CLCN5) mutations in Dent's disease. J. Am. Soc. Nephrol. *11*, 1460-1468.

Yusef,Y.R., Zuniga,L., Catalan,M., Niemeyer,M.I., Cid,L.P., and Sepulveda,F.V. (2006). Removal of gating in voltage-dependent ClC-2 chloride channel by point mutations affecting the pore and C-terminus CBS-2 domain. J Physiol *572*, 173-181.

Zdobnov,E.M. and Apweiler,R. (2001). InterProScan - an integration platform for the signature-recognition methods in InterPro. Bioinformatics *17*, 847-848.

Zhang,R., Evans,G., Rotella,F.J., Westbrook,E.M., Beno,D., Huberman,E., Joachimiak,A., and Collart,F.R. (1999). Characteristics and Crystal Structure of Bacterial Inosine-5'-monophosphate Dehydrogenase. Biochemistry *38*, 4691-4700.

Zhang,X.D., Li,Y., Yu,W.P., and Chen,T.Y. (2006). Roles of K149, G352, and H401 in the channel functions of ClC-0: testing the predictions from theoretical calculations. J. Gen. Physiol *127*, 435-447.

Zhang,X.D., Yu,W.P., and Chen,T.Y. (2010). Accessibility of the CLC-0 pore to charged methanethiosulfonate reagents. Biophys. J. *98*, 377-385.

Zhao,Q., Wei,Q., He,A., Jia,R., and Xiao,Y. (2009). CLC-7: a potential therapeutic target for the treatment of osteoporosis and neurodegeneration. Biochem. Biophys. Res. Commun. *384*, 277-279.

Zifarelli,G., Murgia,A.R., Soliani,P., and Pusch,M. (2008). Intracellular proton regulation of ClC-0. J. Gen. Physiol *132*, 185-198.

Zifarelli,G. and Pusch,M. (2007). CLC chloride channels and transporters: a biophysical and physiological perspective. Rev. Physiol Biochem. Pharmacol. *158*, 23-76.

Zifarelli,G. and Pusch,M. (2009a). Conversion of the 2 Cl(-)/1 H+ antiporter ClC-5 in a NO3(-)/H+ antiporter by a single point mutation. EMBO J. *28*, 175-182.

Zifarelli,G. and Pusch,M. (2009b). Intracellular regulation of human ClC-5 by adenine nucleotides. EMBO Rep. *10*, 1111-1116.

Zuniga,L., Niemeyer,M.I., Varela,D., Catalan,M., Cid,L.P., and Sepulveda,F.V. (2004). The voltage-dependent ClC-2 chloride channel has a dual gating mechanism. J. Physiol *555*, 671-682.